DOI 10.12905/0380.sydowia75-2023-313 Published online 14 June 2023

Fungal Systematics and Evolution: FUSE 9

Renée Lebeuf[1,2], Jacques Landry[2], Joseph F. Ammirati[3], Arne Aronsen[4], Taimy Cantillo[5], Robinson Castillo[6], Mike Anderson Corazon-Guivin[7], Gladstone Alves da Silva[8], Alden C. Dirks[9], Rosanne A. Healy[10], Quincy Marvin Holzapfel[11], Marian Jagers[12], Abdul Nasir Khalid[13], Yves Lamoureux[2,14], Hugo Madrid[15], Arooj Naseer[13], Jorinde Nuytinck[11,16], Fritz Oehl[17], André Paul[1,2], Viviane Monique Santos[8], Garrett Taylor[18], Adela Vallejos-Tapullima[7], Michał Gorczak[19,20,21], Danny Haelewaters[16,22,*] & Irmgard Krisai-Greilhuber[23]

[1] Saint-Casimir, QC GOA 3L0, Canada
[2] Mycoquébec, Québec, QC G1Y 1N7, Canada
[3] Department of Biology, University of Washington, Seattle, Washington 98195, USA
[4] 3135 Torød, Norway
[5] Departamento de Ciências Biológicas, Universidade Estadual de Feira de Santana, 44036-900 Feira de Santana, Brazil
[6] Facultad de Ciencias, Universidad Mayor, Huechuraba, Chile
[7] Laboratorio de Biología y Genética Molecular, Universidad Nacional de San Martín, Jr. Amorarca 315, Morales, Peru
[8] Departamento de Micologia, Centro de Biociências, Universidade Federal de Pernambuco, Cidade Universitária, 50740-600 Recife, Brazil
[9] Department of Ecology and Evolutionary Biology, University of Michigan, Ann Arbor, Michigan 48109, USA
[10] Department of Plant Pathology, University of Florida, Gainesville, Florida 32611, USA
[11] Naturalis Biodiversity Center, 2300 RA Leiden, The Netherlands
[12] Reelaan 13, 7522 LR Enschede, The Netherlands
[13] Department of Botany, University of the Punjab, Quaid-e-Azam Campus, 54590 Lahore, Pakistan
[14] Saint-Alphonse-Rodriguez, QC J0K 1W0, Canada
[15] Departamento de Tecnología Médica, Facultad de Ciencias de la Salud, Universidad de Tarapacá, Sede Iquique, Iquique, Chile
[16] Research Group Mycology, Department of Biology, Ghent University, 9000 Ghent, Belgium
[17] Agroscope, Competence Division for Plants and Plant Products, Ecotoxicology, 8046 Zürich, Switzerland
[18] Bradford, Pennsylvania 16701, USA
[19] Institute of Evolutionary Biology, Faculty of Biology, University of Warsaw, 02-089 Warsaw, Poland
[20] Botanic Garden, Faculty of Biology, University of Warsaw, 00-478 Warsaw, Poland
[21] Białowieża National Park, 17-230 Białowieża, Poland
[22] Faculty of Science, University of South Bohemia, 370 05 České Budějovice, Czech Republic
[23] Department of Botany and Biodiversity Research, University of Vienna, 1030 Wien, Austria

* e-mail: danny.haelewaters@gmail.com

Lebeuf R., Landry J., Ammirati J.F., Aronsen A., Cantillo T., Castillo R., Corazon-Guivin M.A., da Silva G.A., Dirks A.C., Healy R.A., Holzapfel Q.M., Jagers M., Khalid A.N., Lamoureux Y., Madrid H., Naseer A., Nuytinck J., Oehl F., Paul A., Santos V.M., Taylor G., Vallejos-Tapullima A., Gorczak M., Haelewaters D. & Krisai-Greilhuber I. (2023) Fungal Systematics and Evolution: FUSE 9. – Sydowia 75: 313–377.

In this 9th contribution to the Fungal Systematics and Evolution series published by Sydowia, the authors formally describe 12 species: *Bipolaris chusqueae* from Chile (Pleosporales); *Cortinarius anomalosimilis* and *C. brunneoviscidus* from Canada and the USA, *Inocybe nigroumbonata* from Pakistan, *Mycena amoena* from the Netherlands, *Tricholoma imbricatoides* and *T. pseudoterreum* from Canada, *T. mcneilii* and *T. robustipes* from Canada and the USA, *T. pallens* from Canada, the USA, and China (Agaricales); *Diversispora alba* from Peru (Diversisporales); and *Phaeotremella dejopia* from the USA (Tremellales). The following new country records are reported: *Camptomyces africanus* (Laboulbeniales) on *Astenus* sp. (Coleoptera, Staphylinidae) from Tanzania and *Tricholoma fulvimarginatum* (Agaricales) from Canada.

Keywords: 12 new species, 2 new records, Agaricomycetes, Cortinariaceae, Glomeromycetes, integrative taxonomy, Laboulbeniaceae, Tricholomataceae.

Materials and methods

Sample collection, isolation, and specimen examination

For the *Bipolaris* Shoemaker study, dead branches, leaves, culms, and roots of *Chusquea cumingii* (Poaceae) were collected at the El Granizo area in La Campana National Park, central Chile. Samples were placed in plastic bags and kept in a refrigerator at 4–7 °C until processed. Materials were incubated in moist chambers at 25 °C and observed periodically for a 1-month period under a stereomi-

croscope. To obtain pure cultures, conidia were transferred directly from colonies on the natural substrate to malt extract agar (MEA) plates using a sterile dissection needle. Morphological features of fungi were studied on water agar with sterilized corn leaves after 14 days at 25 °C. Semipermanent microscope slides were mounted on lactophenol cotton blue (Sigma-Aldrich, Oakville, Canada).

Basidiomata of *Cortinarius* (Pers.) Gray were collected in Canada (Québec) and in the USA (Iowa, New York), photographed *in situ*, then dried at 40 °C. The habitat, altitude, soil characteristics, and nearby trees were noted. Macro-anatomical characters were described from fresh basidiomata and from pictures, with color codes of Kornerup & Wanscher (1978). Macrochemical reactions were noted on fresh basidiomata. Micro-anatomical studies were conducted on exsiccatae with a Nikon Labophot microscope (Nelville, NY) and a Moticam 2500 digital camera (Motic, Richmond, Canada). Tissues were rehydrated in 70 % isopropanol, hand-sectioned, and observed in 3 % KOH, in Melzer's reagent for spore dextrinoidity, and in sodium dodecyl sulphate (SDS) Congo Red (1 % SDS, 1 % Congo Red) for better visualization. Microstructures were measured with an optical micrometer, and descriptions follow Brandrud et al. (1990–2014) concepts. A minimum of 20 basidiospores per basidioma, obtained from spore print or natural deposit on cortina or veil, were randomly selected and measured using the following notation: (a–)b–c(–d) [e/f/g], where 'b' and 'c' represent the 5th and 95th percentile of the measured values: 'a' and 'd' the extreme values, and 'e/f/g' the total number of spores, basidiomata, and collections, respectively. Q (minimum and maximum length/width ratio) and Q_{av} (average length/width ratio) were calculated. Collections were deposited in public fungaria abbreviated following Index Herbariorum (Thiers continuously updated) where indicated, or are otherwise kept in the private fungarium of R. Lebeuf (code HRL).

For the *Diversispora* C. Walker & A. Schüßler study, soil samples were taken between March and July 2021 in two coffee plantations in Lamas Province (San Martin State, Peru), at a depth of 0–30 cm. One sampling site was located in Paucarpata (6°26'8.82"S, 76°31'52.1"W, 502 m a.s.l.), the other in Pamashto (6°21'8.59"S, 76°32'15.66"W, 831 m a.s.l.). These sites are cultivated as traditional agroforestry systems, where coffee is grown with native forest species, without any addition of chemical fertilizers and pesticides. Mean annual temperatures are about 21–25 °C, varying between 18 and 38 °C throughout the year. Mean annual precipitation is approximately 1500 mm, with monthly rainfall between 60 and 170 mm. Soil pH (H_2O) was 7.7 in Paucarpata and 5.7 in Pamashto; available phosphor (Olsen et al. 1954) was 6.8 and 9.4 mg/kg, respectively. Bait cultures were established in the greenhouse of the Laboratorio de Biología y Genética Molecular (Universidad Nacional de San Martín, Peru) under ambient temperature conditions in cylindrical 3-l pots with 3 kg of substrate. The substrate consisted of a 1:1:2 mixture of coarse river sand, vermiculite, and collected rhizosphere soil with root fragments of coffee plants (Corazon-Guivin et al. 2022b). At bait culture establishment, the pots were first filled to 90 % with the substrate. Thereafter seeds of *Sorghum vulgare* and *Urochloa brizantha* (Poaceae) were sown together in the pot to establish the arbuscular mycorrhizal fungal (AMF) associations and reproduce spores of the new fungal species together with the native AMF communities. Finally, the seeds were covered with the remaining 10 % of the substrate. The seeds were surface-sterilized before seeding, using 0.5 % sodium hypochlorite (NAOCl). Minimum, mean, and maximum temperatures during time of cultivation were 22 °C ± 2.0 °C, 30.0 °C ± 3.0 °C, and 37.0 °C ± 2.0 °C, respectively. Relative humidity ranged from 40 to 70 %. The pots were irrigated every other day and fertilized with a Long Ashton nutrient solution every two weeks, with reduced P contents (60 % reduction, 20 µg P/ml, Hewitt 1966). The description of morphological spore characteristics and their subcellular structures are based on observations of specimens mounted in polyvinyl alcohol-lactic acid-glycerol (PVLG, Koske & Tessier 1983), Melzer's reagent, a 1:1 mixture of PVLG and Melzer's reagent (Brundrett et al. 1994), a 1:1 mixture of lactic acid and water, and water (Spain 1990). Terminology of spore structures follows Estrada et al. (2011), Oehl et al. (2011), Symanczik et al. (2018), and Błaszkowski et al. (2019) for species of Diversisporaceae. Photographs were taken with a digital camera (Leica DFC 295) mounted on a Leitz Laborlux S compound microscope, using Leica Application Suite version 4.1 software (Leica Microsystems, Bochum, Germany). Specimens mounted in PVLG and a 1:1 mixture of PVLG and Melzer's reagent were deposited at Z and ZT, the joint mycological herbarium of the University of Zurich and the Federal Institute of Technology (Zürich, Switzerland).

Collections of *Inocybe* (Fr.) Fr. were made during field studies to explore the fungal diversity associated with oak forests of Swat district, Khyber Pakhtunkhwa Province, Pakistan during 2014–2020. Basidiomata were found in a pure *Quercus* forest in

Shawar Valley. Basidiomata were collected following Lodge et al. (2014) and photographed in their natural habitats using a Nikon D70S camera. Morphological characteristics were taken from fresh specimens. Colors were designated based on the macOS mColorMeter application. Specimens were deposited in LAH. Microscopic characteristics are based on freehand sections from fresh and dried specimens mounted in 5 % (w/v) aqueous potassium hydroxide (KOH) solution. Tissues from lamellae, pileipellis, and stipitipellis were mounted in 1 % phloxine for better contrast and examined using a Meiji Techno MX4300H compound microscope (Saitama, Japan). A total of 30 basidiospores, basidia, cystidia, and hyphae were measured from each collection. For basidiospores, the abbreviation 'n/m/p' indicates n basidiospores measured from m basidiomata of p collections. Dimensions for basidiospores are given as length × width and extreme values are presented in parentheses. The range contains a minimum of 90 % of measured values. Measurements include arithmetic mean of length and width for all basidiospores measured. Q = minimum and maximum length/width ratio and Q_{av} = average length/width ratio were calculated and presented ± standard deviation.

Basidiomata of *Mycena* (Pers.) Roussel were collected in the field and in addition successfully cultured in moist chambers. In the second case nuts from the location were transferred into plastic boxes measuring 18 × 13 × 5 cm with paper towels at the bottom. Afterwards the boxes were filled with tap water (pH 7.5) and closed with transparent lids. After two days the water was cast off. The boxes were kept under diffuse daylight at a temperature of about 20 °C. The nuts were kept moist by using a plant sprayer, delicately, to prevent the growth of unwanted molds. Primordia usually appeared within a week. Fresh basidiomata were used to describe the macroscopical characteristics. Microscopic mounts of both fresh and dried tissue were examined under a Leica DM1000 light microscope and captured with a ToupTek UA510CA camera (ToupTek Photonics, Hangzhou, P.R. China). Small macroscopical details were captured through a trinocular Leica S6D with an ILCE-5000 photo camera (Sony Corporation, Tokyo, Japan). From five fresh basidiomata collected in 2019, 20 mature spores per basidioma were measured in water, using a 100× oil immersion objective. Measurements of length and width (and its ratio Q) are presented as follows: mean ± 2× standard deviation. The average value of Q per basidioma is denoted by Q_{av}. Cherocytes, acanthocysts, and basal disc cystidia were measured in water. Basidia, cystidia, and several other characteristics were measured in Congo Red with 5 % KOH. Basidia were measured without sterigmata, and basidiospores without apiculus. Melzer's reagent was used to test the basidiospores and tissues for amyloid, dextrinoid, or negative reactions.

Fresh basidiomata of *Phaeotremella* Rea were collected from dead wood in Arizona and Michigan, photographed *in situ*, dehydrated in electric dehydrators, and deposited in ARIZ and MICH (sensu Thiers continuously updated). Two *Phaeotremella* specimens were studied on loan from FLAS and MU. A specimen of *Tremella aspera* Coker was loaned by BPI (the holotype was requested but not acquired). Micromorphological characters were studied by shaving off thin sections of dried basidiomata, mounting the tissue in a drop of 5 % KOH stained with phloxine B, and pressing on the cover slip to squash the rehydrated tissue. Squash mounts were observed under an LW Scientific i4 Infinity compound microscope (Lawrenceville, GA). Photographs and measurements were taken with an AmScope MU500 microscope camera (AmScope, Irvine, CA). For each specimen, 30–45 spores, 10 basidia, and 10 hyphae were measured at 1000× magnification. Sizes are presented as (a–)b–c(–d), where 'a' and 'd' are the minimum and maximum observed values, respectively, and 'b–c' is the range consisting of the mean ± standard deviation. The following abbreviations are used in describing the sizes of microscopic characters: n/x = total number of units measured (n) divided by the number of specimens (x), av. = mean size, Q = quotient of length/width ratios, Q_{av} = mean of Q values.

Basidiomata of *Tricholoma* were collected in the province of Québec, Canada, and in New York state, USA, photographed *in situ* or in the laboratory, then dried at 40 °C. The habitat, altitude, soil characteristics, and nearby trees were noted. Macro-anatomical characters were described from fresh basidiomata and from pictures, with the color codes of Kornerup & Wanscher (1978). Micro-anatomical studies were conducted on exsiccatae with a Nikon Labophot microscope and a Moticam 2500 digital camera. Tissues were rehydrated in 70 % isopropanol, hand-sectioned, and observed in 3 % KOH and SDS Congo Red (1 % SDS, 1 % Congo Red). Microstructures were measured with the aid of an optical micrometer, and microscopic characters follow Vellinga's (1988) concepts. A minimum of 20 basidiospores per basidioma, generally obtained from spore prints, more rarely from lamellar fragments, were randomly selected and measured in 3 % KOH using the following notation: (a–)b–c(–d) [e/f/g],

where 'b' and 'c' represent the 5th and 95th percentile of the measured values: 'a' and 'd' the extreme values, and 'e/f/g' the total number of spores, basidiomata, and collections, respectively. Q (length/width ratio) of each spore (minimum and maximum values shown) and Q_{av} (average Q) were calculated. Collections were deposited in public fungaria abbreviated following Index Herbariorum (Thiers continuously updated) where indicated, or are otherwise kept in the private fungarium of R. Lebeuf (code HRL).

For the *Camptomyces* Thaxt. study, infected host specimens were sent to D. Haelewaters by Vladimir Gusarov (Natural History Museum, University of Oslo, Norway). Thalli were removed from the host at their foot and mounted on microscope slides in Amman solution (Benjamin 1971), with the help of Minuten Pins (BioQuip #1208SA) inserted manually onto wooden rods. The pin was first submerged in Hoyer's medium to make the thalli stick to the pin and prevent them from getting lost or flying away. Thalli or groups of thalli were placed in a droplet of Hoyer's on a microscope slide, oriented vertically, and allowed to settle briefly. A drop of Amman solution was placed on a coverslip that was dropped sideways onto the thalli in the Hoyer's medium. Finally, the coverslip was ringed with nail varnish. Mounted specimens were studied microscopically under 400–1000× magnification using differential interference contrast on an Olympus BX51 fluorescence microscope (Olympus, Tokyo, Japan) with a digital camera Olympus DP72. Series of photographs were focus-stacked for increased depth of field using Helicon Focus software (Helicon Soft Ltd., Kharkiv, Ukraine). Measurements in the morphological description are presented as (a–)b–c–d(–e) [n], where 'c' represents the mean, 'b' and 'd' the mean ± standard deviation, 'a' and 'e' the extreme values, and 'n' the number of structures measured. Host specimens are deposited at the Zoological Collection, Natural History Museum, University of Oslo (ZMUN, https://www.nhm.uio.no/english/collections/zoological/insect/index.html). Permanent slides are deposited at O.

DNA extraction, PCR amplification, and sequencing

For the *Bipolaris* study, genomic DNA was extracted from fungal colonies on MEA grown for 1 week at 25 °C, using the Fast DNA Kit (Bio 101, Vista, CA). Three loci were amplified: internal transcribed spacer (ITS) region and large subunit (LSU) of the nuclear ribosomal DNA (rDNA) operon, as well as the glyceraldehyde-3-phosphate dehydrogenase (*gapdh*) gene. Primer pairs used were ITS5/ITS4 for ITS (White et al. 1990), LR0R/LR5 for LSU (Vilgalys & Hester 1990, Hopple 1994), and gpd1/gpd2 for *gapdh* (Berbee et al. 1999). Amplifications were carried out following the illustra PuReTaq Ready-To-Go PCR beads protocol (VWR), with both primers at a concentration of 0.5 µM, and using 1 µl of diluted template DNA in a final reaction volume of 25 µl. The amplification program included an initial denaturation at 94 °C for 5 min, followed by 35 cycles of denaturation at 95 °C for 30 s, annealing for 1 min at 50 °C (ITS, LSU) or 52 °C (*gapdh*), and extension for 1 min at 72 °C, with final extension at 72 °C for 7 min. PCR amplification success was checked on 2 % agarose gels with GelRed fluorescent nucleotide stain (Merck Millipore, Burlington, MA). Purification of PCR products and Sanger sequencing were outsourced to Macrogen (Seoul, South Korea). Amplicons were bidirectionally sequenced and consensus sequences were obtained from forward and reverse reads using the SeqTrace software (Stucky 2012).

For the *Cortinarius* and *Tricholoma* studies, DNA extraction, PCR amplification, and sequencing were outsourced to the Canadian Centre for DNA Barcoding (https://ccdb.ca). Sequences of the ITS region were obtained as part of two recent studies aiming at sequencing major *Cortinarius* and *Tricholoma* collections from public (CMMF and QFB) and private fungaria in the province of Québec, Canada (Landry et al. 2021, 2022). For the Iowa collections of *Cortinarius*, approximately 1 cm^3 of clean tissue from dried vouchers was sampled into CTAB, and genomic DNA was extracted using a modified CTAB method (Gardes & Bruns 1993). The ITS region was amplified with the primer pair ITS1f/ITS4 (White et al. 1990). PCR products were run on a 1.5 % agarose gel with electrophoresis, and successful PCR products stained with SYBR Green 1 (Molecular Probes, Eugene, OR) were visualized with UV light. Amplicons were enzymatically cleaned with EXO (exonuclease I) and AP (antarctic phosphatase) (New England Biolabs, Ipswich, MA) (Werle et al. 1994), and Sanger sequencing was performed by GENEWIZ (South Plainfield, NJ) using the same primers. Finally, the type collection of *Tricholoma fulvimarginatum* Ovrebo & Halling was sequenced as part of this study by Molecular Solutions LLC in Portland, OR (https://molecular-solutions.com/index.html).

Intact, healthy spores of *Diversispora* were isolated from the bait culture samples and cleaned by friction on fine filter paper (Corazon-Guivin et al.

2019a, b, d). Spores were surface-sterilized (Mosse 1962) using a solution of 2 % chloramine T, 0.02 % streptomycin, and Tween 20 (2–5 drops in 25 ml final volume) for 20 min, followed by five times rinsing in milli-Q water. One independent group of 10–15 surface-sterile spores were selected under a laminar flow hood and together transferred into Eppendorf PCR tubes. Crude extract was obtained by crushing the spores with a sterile disposable fine-tipped pilon in 2.0 µl milli-Q water at 5× magnification using a stereoscope (Corazon-Guivin et al. 2022c). Direct PCR of these crude extracts was performed in an Eppendorf Mastercycler nexus (Hamburg, Germany) with Platinum *Taq* DNA Polymerase High Fidelity (Invitrogen, Carlsbad, CA) following the manufacturer's instructions and using a 0.4 µM concentration of each primer. A two-step PCR was conducted to amplify the ribosomal fragment consisting of partial small subunit (SSU), ITS, and partial LSU rDNA using the primers SSUmAf/LSUmAr and SSUmCf/LSUmBr, consecutively, following Krüger et al. (2009). PCR products from the second round of amplifications (~1500 bp) were separated electrophoretically on 1.2 % agarose gels, stained with Diamond Nucleic Acid Dye (Promega, Madison, WI) and viewed with UV illumination. The band of the expected size was excised with a scalpel and isolated with the GFX PCR DNA and Gel Band Purification Kit (Sigma-Aldrich) following the manufacturer's instructions, cloned into the pCR2.1 vector (Invitrogen), and transformed into One Shot TOP10 chemically competent *Escherichia coli* (Invitrogen). Twelve recombinant colonies (each six derived from the isotype and from the paratype) were selected by blue/white screening and the presence of inserts detected by PCR amplification with KOD DNA Polymerase (Sigma-Aldrich) using universal forward and reverse M13 vector primers. After isolation from transformed cells, plasmids were sequenced on both strands with M13F/M13R primers using the BigDye Terminator kit version 3.1 (Applied Biosystems). The products were sequenced on an ABI 3730XL DNA analyzer (Macrogen).

Genomic DNA of *Inocybe* was extracted from basidioma gills following a modified CTAB extraction method (Bruns 1995). The ITS region was amplified using the primer pair ITS1f/ITS4B (White et al. 1990, Gardes & Bruns 1993). PCR amplification was performed in 25-µl volume reactions. Visualization of PCR products was accomplished using SYBR Green and 1.5 % agarose gels with TAE buffer for gel electrophoresis. Successful amplicons were purified by enzymatic purification using Exonuclease I and Shrimp Alkaline Phosphatase enzymes (Werle et al. 1994). Purified products were sequenced by the Interdisciplinary Center for Biotechnology Research at the University of Florida (http://www.biotech.ufl.edu/). Forward and reverse sequence reads were trimmed, edited, and assembled using Sequencher version 4.1 (Gene Codes Corporation, Ann Arbor, MI). Edited sequences were submitted to GenBank (Tab. 1).

DNA was extracted from dried herbarium material or from fresh basidiomata of *Mycena* stored in cetyltrimethylammonium bromide (CTAB) buffer. After subsampling and lysis of the material with a TissueLyser (Qiagen, Hilden, Germany), the KingFisher extraction robot (Thermo Scientific, Waltham, MA) with magnetic particle separation technology was used in combination with the NucleoMag Plant kit for DNA purification (Macherey-Nagel, Düren, Germany). The internal transcribed spacer (ITS) region of the nuclear ribosomal DNA (rDNA) operon was amplified using primers ITS1f (Gardes & Bruns 1993) and ITS4 (White et al. 1990). In a final volume of 25 µl, 2.5 µl of 10× CoralLoad buffer (Qiagen), 1 µl of each 10 µM primer, 1 µl of 2.5 mM dNTPs, 1.5 µl of 2.5 mM MgCl, 0.25 µl of *Taq* polymerase (5 U/µl, Qiagen), and 1µl of DNA template were mixed. Reaction mixtures were preheated at 96 °C for 5 min, followed by 40 cycles of denaturation at 96 °C for 45 s, annealing at 45 °C for 45 s, and extension at 72 °C for 60 s, with final extension at 72 °C for 7 min. PCR amplification success was checked on an E-Gel with SYBR Safe DNA Gel Stain, 2 % (Invitrogen). Amplicons were bidirectionally sequenced using Sanger sequencing by BaseClear (Leiden, The Netherlands). Forward and reverse reads were assembled into contigs using Geneious Prime version 2021.1.1 (Tab. 1).

For the *Phaeotremella* study, DNA from dried basidiomata was extracted using the 2× CTAB extraction protocol described in James et al. (2008), excluding phenol. All PCR reactions were carried out with 5 µL of 1:20 diluted DNA template in a total volume of 12.5 µL GoTaq Green Master Mix (Promega). The internal transcribed spacer (ITS) region and large subunit (LSU) of the nuclear ribosomal DNA (rDNA) operon, as well as the eukaryotic translation elongation factor 1- gene (*tef1*) were amplified with primer pairs ITS1f and ITS4 (White et al. 1990, Gardes & Bruns 1993), LR0R and LR5 (Vilgalys & Hester 1990, Hopple 1994), and EF1-983F and EF1-1567R (Rehner & Buckley 2005), respectively. Amplicons were sent to Genewiz (South Plainfield, NJ) for Sanger sequencing. Forward and reverse sequences were assembled and manually edited with Codon Code Aligner version 10.0.1

(Centerville, MA). Sequences were deposited in NCBI GenBank (https://www.ncbi.nlm.nih.gov/genbank/) under the accession numbers provided in Tab. 1.

For the *Camptomyces* study, a modified protocol for the REPLI-g Single Cell Kit (Qiagen) was used for DNA extraction (Haelewaters et al. 2019). A Minuten Pin was submerged into glycerin to make a single, mature thallus stick to the pin and prevent it from getting lost or flying away. The thallus was removed from the host and placed in a droplet of glycerin on a microscopic slide. The thallus was then placed in a 0.2 mL PCR tube with 2 µl of phosphate-buffered saline (PBS). After adding 1.5 ml of prepared D2 buffer, the tube was incubated at 65 °C for 30 min. Subsequent steps followed the manufacturer's instructions. Amplification of the SSU and LSU regions was done using Laboulbeniomycetes-specific forward primer NSL1 (5'-GTAGTGTCCTCrCATGCTTTTGAC-3') in combination with reverse primer R (5'-TGATCCTTCTGCAGGTTCACCTACG-3') (Wrzosek 2000, Haelewaters et al. 2015) for SSU and the LR0R/LR5 primer combination for LSU (Vilgalys & Hester 1990, Hopple 1994). PCR reactions consisted of 13.3 µl of Extract-N-Amp PCR ReadyMix (Sigma-Aldrich), 2.5 µL of each 10 µM primer, 5.7 µl of H_2O, and 1 µl of template genomic DNA. The amplification reactions were run under the following thermocycler conditions: initial denaturation at 94 °C for 3 min; 35 cycles of denaturation at 94 °C for 1 min, annealing at 50 °C for 45 s, and extension at 72 °C for 90 s; with a final extension step at 72 °C for 10 min (Haelewaters et al. 2018). Successful PCR products were cleaned using the QIAquick PCR Purification Kit (Qiagen) and subsequently sequenced. Subsequently, 10-µl sequencing reactions were prepared containing the same primers and 1–3 µl of purified PCR product. Sequencing reactions were performed using the Big Dye® Terminator version 3.1 Cycle Sequencing Kit (Life Technologies, Carlsbad, CA). Generated sequences were assembled, trimmed, and edited in Sequencher version 4.10.1 (Gene Codes Corporation). Newly generated sequences were uploaded to GenBank under accession numbers MF314140 (SSU) and MF314141 (LSU).

Phylogenetic analyses

For the *Bipolaris* study, only sequences of *gapdh* were included in the phylogenetic analysis. This gene provides a higher resolution in Pleosporaceae compared to ITS and LSU (Brun et al. 2013, Madrid et al. 2014). Nonetheless, sequences of ITS and LSU were also submitted to GenBank as they represent useful markers for identification at least at the level of genus. The *gapdh* dataset included 32 strains of *Bipolaris* species and *Exserohilum rostratum* (Drechsler) K.J. Leonard & Suggs (strain CBS 320.64) as outgroup (Tab. 1). A maximum likelihood (ML) phylogenetic reconstruction was obtained in MEGA X (Kumar et al. 2018) using the best substitution model as determined by this software, i.e., K2 + G. ML bootstrap (MLBS) analysis was performed with 1000 replicates.

Sequences of the new *Cortinarius* species were supplemented with closely related sequences as found by BLAST searches in NCBI GenBank and UNITE (Abarenkov et al. 2010) and with sequences of species of selected sections in subgenus *Telamonia* as delimited in recent infrageneric classification studies (Liimatainen et al. 2020). Representative species of *Thaxterogaster* Singer section *Multiformes* were selected as outgroup. Sequences were aligned using MUSCLE version 3.7 (Edgar 2004) and corrected manually as needed. The phylogenetic tree was constructed with the help of MEGA7 (Kumar et al. 2016) with default settings. ML was inferred based on the Tamura-Nei model (Tamura & Nei 1993). ML bootstrap (MLBS) analysis was performed with 100 replicates. Initial tree(s) for the heuristic search were obtained automatically by applying Neighbor-Joining and BioNJ algorithms to a matrix of pairwise distances estimated using the Maximum Composite Likelihood (MCL) approach, and then selecting the topology with superior log likelihood value.

Newly generated AM fungal sequences (partial SSU–ITS–partial LSU) were aligned with other *Diversispora* sequences downloaded from GenBank in ClustalX2 (Larkin et al. 2007). *Acaulospora laevis* Gerd. & Trappe was included as outgroup. Prior to phylogenetic analysis, the model of nucleotide substitution was estimated using Topali version 2.5 (Milne et al. 2004), resulting in the GTR+G model. ML analyses were performed in PhyML (Guindon & Gascuel 2003), and bootstrapping was performed with 1000 replicates. Bayesian inference (BI) was performed in MrBayes version 3.1.2 (Ronquist & Huelsenbeck 2003) and included two runs over 5×10^6 generations, with a sample frequency of 500 and a burn-in value of 25 %.

ITS consensus sequences of *Inocybe* were used to query NCBI GenBank and UNITE. Representative sequences from the genus *Inocybe* were downloaded and imported into an alignment using BioEdit version 7.2.6 (Hall 1999). Sequences were aligned with MUSCLE version 5.1.0 (Edgar 2004). ML anal-

Species	ID (isolate, strain[1], status[2], voucher)	Country, substrate/host	ITS	LSU	partial SSU–ITS–partial LSU	*gapdh*	*tef1*	Reference(s)
Acaulospora laevis	isolate BEG13, T	New Zealand			FN547511			Stockinger et al. (2010)
Acaulospora laevis	isolate BEG13, T	New Zealand			FN547512			Stockinger et al. (2010)
Amparoina sp. DH-2020	HONDURAS19-F011a	Honduras	MT571522					Haelewaters et al. (2021)
Bipolaris austrostipae	BRIP 12490, T	Australia, *Austrostipa verticillata*				KX452408		Tan et al. (2016)
Bipolaris axonopodicola	BRIP 11740, T	Australia, *Axonopus fissifolius*				KX452409		Tan et al. (2016)
Bipolaris bicolor	CBS 690.96	Cuba, unknown substrate				KM042893		Manamgoda et al. (2014)
Bipolaris chloridis	CBS 242.77	Australia, *Chloris gayana*				JN600961		Manamgoda et al. (2011)
Bipolaris chusqueae	SGO 166370, T	Chile, *Chusquea cummingii*				OM912808		This study
Bipolaris clavata	BRIP 12530, T	Australia, *Dactyloctenium radulans*				KJ415422		Tan et al. (2014)
Bipolaris coffeana	BRIP 14845, T	Kenya, *Coffea arabica*				KJ415421		Tan et al. (2014)
Bipolaris cookei	MAFF 51191	Japan, *Sorghum bicolor*				KM034834		Manamgoda et al. (2014)
Bipolaris crotonis	BRIP 14838	Samoa, *Croton* sp.				KJ415420		Tan et al. (2014)
Bipolaris cynodontis	CBS 109894, T	Hungary, *Cynodon dactylon*				KM034838		Manamgoda et al. (2014)
Bipolaris cynodontis	CBS 285.51	Kenya, *Cynodon transvaalensis*				LT715772		Hernández-Restrepo et al. (2018)
Bipolaris gossypina	BRIP 14840, T	Kenya, *Gossypium* sp.				KJ415418		Tan et al. (2014)
Bipolaris heliconiae	BRIP 17186, T	Australia, *Heliconia psittacorum*				KJ415417		Tan et al. (2014)
Bipolaris heveae	CBS 241.92	Nigeria, *Hevea* sp.				KM034843		Manamgoda et al. (2014)
Bipolaris luttrellii	BRIP 14643, T	Australia, *Dactyloctenium aegyptium*				AF081402		Berbee et al. (1999)
Bipolaris maydis	CBS 137271	USA, *Zea mays*				KM034846		Berbee et al. (1999)
Bipolaris microlaenae	BRIP 15613, T	Australia, *Microlaena stipoides*				JN600974		Manamgoda et al. (2011)
Bipolaris microstegii	CBS 132550, T	USA, *Microstegium vimineum*				JX089575		Manamgoda et al. (2014)
Bipolaris oryzae	MFLUCC 100715, T	Thailand, *Oryza sativa*				JX276430		Manamgoda et al. (2012)
Bipolaris panici-miliacei	CBS 199.29, T	Japan, *Panicum miliaceum*				KM042896		Manamgoda et al. (2014)
Bipolaris peregianensis	BRIP 12790, T	Australia, *Cynodon dactylon*				JN600977		Manamgoda et al. (2011)
Bipolaris pluriseptata	BRIP 14839, T	Zambia, *Eleusine coracana*				KJ415414		Tan et al. (2014)
Bipolaris sacchari	ICMP 6227	New Zealand, *Oplismenus imbecillis*				KM034842		Manamgoda et al. (2014)
Bipolaris saccharicola	CBS 155.26, T	Unknown country and substrate				KY905686		Marin-Felix et al. (2017)
Bipolaris salviniae	IMI 228224	Brazil, *Salvinia auriculata*				KM034829		Manamgoda et al. (2014)
Bipolaris secalis	BRIP 14453, T	Argentina, *Secale cereale*				KJ415409		Tan et al. (2014)
Bipolaris sorokiniana	CBS 110.14	USA, *Hordeum* sp.				KM034822		Manamgoda et al. (2014)
Bipolaris urochloae	ATCC 58317	Australia, *Urochloa panicoides*				KM230396		Manamgoda et al. (2014)
Bipolaris variabilis	CBS 127716, T	Argentina, *Pennisetum clandestinum*				KY905688		Marin-Felix et al. (2017)
Bipolaris victoriae	CBS 327.64, T	USA, *Avena sativa*				KM034811		Manamgoda et al. (2014)
Bipolaris yamadae	CBS 202.29, T	Japan, *Panicum milliaceum*				KM034830		Manamgoda et al. (2014)
Bipolaris zeae	AR 3795	USA, *Pennisetum virgatum*				KM034816		Manamgoda et al. (2014)
Bipolaris zeicola	AR 5166	USA, *Sorghum* sp.				KM034813		Manamgoda et al. (2014)
Camptomyces africanus	D. Haelew. 1222d	Tanzania		MF314141				Blackwell et al. (2020)
Cortinarius acutispissipes	PC:1610/2065, T	France	MT934845					Liimatainen et al. (2020)
Cortinarius albomalus	H:7000816, T	Canada	MZ568645					Liimatainen & Niskanen (2021)
Cortinarius alboviolaceus	S:H. Lindström CFP432, T	Sweden	MT934857					Liimatainen et al. (2020)
Cortinarius anomalosimilis	HRL0862	Canada	KX897435					P.B. Matheny, R.A. Swenie, R. Lebeuf & A. Paul, unpubl.
Cortinarius anomalosimilis	HRL1298, T	Canada	MN751619					Landry et al. (2021)
Cortinarius anomalosimilis	ISC-F-0135059	USA	OM675981					This study
Cortinarius anomalosimilis	ISC-F-0135061	USA	OM675978					This study
Cortinarius anomalosimilis	ISC-F-0135078	USA	OM675980					This study
Cortinarius anomalosimilis	ISC-F-0135088	USA	OM675982					This study

Species	ID (isolate, strain[1], status[2], voucher)	Country, substrate/host	ITS	LSU	partial SSU–ITS–partial LSU	*gapdh*	*tef1*	Reference(s)
Cortinarius anomalosimilis	iNaturalist 58496002	USA	MZ234118					G.M. Taylor, unpubl.
Cortinarius anomalus	S:CFP1154, T	Sweden	KX302224					Dima et al. (2016)
Cortinarius armeniacus	CFP809, T	Sweden	DQ117925					Kytövuori et al. (2005)
Cortinarius atrocaeruleus	IB1951-0161, T	Austria	MT934892					Liimatainen et al. (2020)
Cortinarius badioflavidus	WTU:J.F. Ammirati 13668, T	USA	NR_153055					J.F. Ammirati, M. Beug, D. Bojantchev, O. Ceska, K. Liimatainen & T. Niskanen, unpubl.
Cortinarius boulderensis	MICH 10323, T	USA	NR_121207					Niskanen et al. (2006)
Cortinarius brunneoviscidus	HRL1296, T	Canada	MN751634					Landry et al. (2021)
Cortinarius brunneoviscidus	WTU-F-074618	USA	OM675979					This study
Cortinarius cagei	S:H. Lindström CFP1260, T	Sweden	KX964295					Liimatainen et al. (2017)
Cortinarius campester	PC:3883, T	France	MT934944					Liimatainen et al. (2020)
Cortinarius caninoides	PC:R. Henry 413, T	France	MH784825					A. Bidaud, J.M. Bellanger, X. Carteret, P. Reumaux & P. Moenne-Loccoz, unpubl.
Cortinarius caninus	S:CFP627, T	Sweden	KX302250					Dima et al. (2016)
Cortinarius decipiens	PML 366, T	France	FN428988					Suárez-Santiago et al. (2009)
Cortinarius duracinus	G:P. Moënne-Loccoz 349, T	France	KX964582					Liimatainen et al. (2017)
Cortinarius evernius	S:H. Lindström CFP792, T	Sweden	KX964331					Liimatainen et al. (2017)
Cortinarius falsosus	PC:3886, T	France	MT935040					Liimatainen et al. (2020)
Cortinarius fulvopaludosus	H:6033460, T	Finland	MG136823					Liimatainen (2017)
Cortinarius fuscoflexipes	IB:M. Moser 1983-0384, T	USA	MT935076					Liimatainen et al. (2020)
Cortinarius gentilis	CFP178, T	Norway	EU266692					Niskanen et al. (2009)
Cortinarius glandicolor	TN06-247, T	Finland	NR_119683					Niskanen et al. (2009)
Cortinarius grosmorneensis	TN07-227, T	Canada	NR_120094					Niskanen et al. (2012)
Cortinarius hinnuleocanadensis	H:7068025, T	Canada	MZ568648					Liimatainen & Niskanen (2021)
Cortinarius hinnuleus	CFP332, T	Sweden	DQ117926					Kytövuori et al. (2005)
Cortinarius leucopus	UBC:F19644	Canada	HQ604721					M.L. Berbee, A.R. Bradford & S.Y.M. Tang, unpubl.
Cortinarius neofallax	PC:PML1158, T	France	KF048129					Esteve-Raventós et al. (2013)
Cortinarius obliquus	NYS f2116, T	USA	NR_174909					Liimatainen et al. (2020)
Cortinarius occidentalisagacitas	H:7057491, T	USA	MT112152					Niskanen (2020)
Cortinarius oxytoneus	PC:R. Henry 931, T	France	KX964567					Liimatainen et al. (2017)
Cortinarius plumulosus	PC:R. Henry 3417, T	France	NR_153090					Liimatainen et al. (2017)
Cortinarius politus	WTU J.F. Ammirati 13416, T	USA	NR_131829					Niskanen et al. (2013)
Cortinarius psammocola	H:I. Kytövuori 99-722, T	Finland	MG136821					Liimatainen (2017)
Cortinarius pseudobovinus	IB 19890300, T	USA	NR_131791					Niskanen et al. (2006)
Cortinarius pseudofallax	PC 0124963, T	France	NR_131831					Esteve-Raventós et al. (2013)
Cortinarius quarciticus	S:H. Lindström CFP765, T	Sweden	MT935363					Liimatainen et al. (2020)
Cortinarius sagacitas	H:6033517, T	Finland	MT112148					Niskanen (2020)
Cortinarius spisnii	96140, T	Italy	MT935446					Liimatainen et al. (2020)
Cortinarius suberythrinus	G:56, T	France	MT935483					Liimatainen et al. (2020)
Cortinarius vernus	CFP443, T	Sweden	UDB000742*					Suárez-Santiago et al. (2009)
Diversispora aestuarii	clone Dae_407_3	Poland, soil			OL684647			Błaszkowski et al. (2022)
Diversispora aestuarii	clone Dae_407_9	Poland, soil			OL684648			Błaszkowski et al. (2022)
Diversispora alba [as D. aurantia]	isolate ASV_291	USA, soil			MT765585			Dirks & Jackson (2020)

Species	ID (isolate, strain[1], status[2], voucher)	Country, substrate/host	ITS	LSU	partial SSU–ITS–partial LSU	*gapdh*	*tef1*	Reference(s)
Diversispora alba [as *D. aurantia*]	isolate ASV_341	USA, soil			MT765635			Dirks & Jackson (2020)
Diversispora alba [as *D. aurantia*]	isolate ASV_364	USA, soil			MT765658			Dirks & Jackson (2020)
Diversispora alba	isolate DJ, T	Peru, soil			OP195880			This study
Diversispora alba	isolate DJ, T	Peru, soil			OP195881			This study
Diversispora alba	isolate DJ, T	Peru, soil			OP195882			This study
Diversispora alba	isolate DJ, T	Peru, soil			OP195883			This study
Diversispora alba	isolate DJ, T	Peru, soil			OP195884			This study
Diversispora alba	isolate DJ, T	Peru, soil			OP195885			This study
Diversispora alba	isolate W	Peru, soil			OP195886			This study
Diversispora alba	isolate W	Peru, soil			OP195887			This study
Diversispora alba	isolate W	Peru, soil			OP195888			This study
Diversispora alba	isolate W	Peru, soil			OP195889			This study
Diversispora alba	isolate W	Peru, soil			OP195890			This study
Diversispora alba	isolate W	Peru, soil			OP195891			This study
Diversispora arenaria	isolate 111-1-3b	Poland, soil			KJ850192			Balázs et al. (2015)
Diversispora arenaria	isolate 111-2-10	Poland, soil			KJ850193			Balázs et al. (2015)
Diversispora aurantia	DPP 2444, T	Israel, soil			AJ849468			Błaszkowski et al. (2004)
Diversispora aurantia	isolate Att1296-0, T	Israel, soil			FN547655			Stockinger et al. (2010)
Diversispora aurantia	isolate Att1296-0, T	Israel, soil			FN547656			Stockinger et al. (2010)
Diversispora aurantia	isolate Att1296-0, T	Israel, soil			FN547657			Stockinger et al. (2010)
Diversispora aurantia	isolate Att1296-0, T	Israel, soil			FN547658			Stockinger et al. (2010)
Diversispora aurantia	isolate Att1296-0, T	Israel, soil			FN547659			Stockinger et al. (2010)
Diversispora aurantia	isolate Att1296-0, T	Israel, soil			FN547660			Stockinger et al. (2010)
Diversispora aurantia	isolate Att1296-0, T	Israel, soil			FN547661			Stockinger et al. (2010)
Diversispora aurantia	isolate Att1296-0, T	Israel, soil			FN547662			Stockinger et al. (2010)
Diversispora aurantia	isolate Att1296-0, T	Israel, soil			FN547663			Stockinger et al. (2010)
Diversispora aurantia	isolate Att1296-0, T	Israel, soil			FN547664			Stockinger et al. (2010)
Diversispora aurantia	isolate Att1296-0, T	Israel, soil			FN547665			Stockinger et al. (2010)
Diversispora celata	isolate BEG231, T	UK, soil			AM713403			Gamper et al. (2009)
Diversispora celata	isolate BEG231, T	UK, soil			AM713404			Gamper et al. (2009)
Diversispora clara	isolate JP-2011	Spain, soil			FR873630			Estrada et al. (2011)
Diversispora clara	isolate JP-2011	Spain, soil			FR873633			Estrada et al. (2011)
Diversispora densissima	clone 5	Poland, soil			MT724384			Błaszkowski et al. (2022)
Diversispora densissima	clone 6	Poland, soil			MT724385			Błaszkowski et al. (2022)
Diversispora eburnea	isolate AZ420A, T	USA, soil			AM713405			Gamper et al. (2009)
Diversispora eburnea	isolate AZ420A, T	USA, soil			AM713406			Gamper et al. (2009)
Diversispora epigaea	isolate W3180	USA, soil			FR686938			Schüßler et al. (2011)
Diversispora epigaea	isolate W3180	USA, soil			FR686939			Schüßler et al. (2011)
Diversispora gibbosa	isolate 109-2-5	Poland, soil			KJ850203			Balázs et al. (2015)
Diversispora gibbosa	isolate 109-2-6	Poland, soil			KJ850204			Balázs et al. (2015)
Diversispora insculpta	isolate 142-1-71	Poland, soil			KJ850195			Balázs et al. (2015)
Diversispora insculpta	isolate 142-2-91	Poland, soil			KJ850197			Balázs et al. (2015)
Diversispora jakucsiae	isolate 238-1-10	Hungary, soil			KJ850181			Balázs et al. (2015)
Diversispora jakucsiae	isolate 238-1-8	Hungary, soil			KJ850182			Balázs et al. (2015)
Diversispora marina	clone 18	Poland, soil			MT725499			Błaszkowski et al. (2022)

Species	ID (isolate, strain[1], status[2], voucher)	Country, substrate/host	ITS	LSU	partial SSU–ITS–partial LSU	*gapdh*	*tef1*	Reference(s)
Diversispora marina	clone 19	Poland, soil			MT725500			Błaszkowski et al. (2022)
Diversispora peloponnesiaca	clone dp7	Greece, soil			MN306207			Błaszkowski et al. (2019)
Diversispora peloponnesiaca	clone dp9	Greece, soil			MN306208			Błaszkowski et al. (2019)
Diversispora peridiata	isolate 4	Poland, soil			KT444714			Błaszkowski et al. (2015)
Diversispora peridiata	isolate 5	Poland, soil			KT444715			Błaszkowski et al. (2015)
Diversispora sabulosa	isolate 336-2	Lithuania, soil			MG459214			Symanczik et al. (2018)
Diversispora sabulosa	isolate 336-4	Lithuania, soil			MG459215			Symanczik et al. (2018)
Diversispora slowinskiensis	isolate gl14a3	Poland, soil			KT444720			Błaszkowski et al. (2015)
Diversispora slowinskiensis	isolate gl14a1	Poland, soil			KT444721			Błaszkowski et al. (2015)
Diversispora sporocarpia	isolate Ds4	Poland, soil			MK036787			Jobim et al. (2019)
Diversispora sporocarpia	isolate Ds5	Poland, soil			MK036788			Jobim et al. (2019)
Diversispora spurca	isolate Att246-18, T	USA, soil			FN547643			Stockinger et al. (2010)
Diversispora spurca	isolate Att246-18, T	USA, soil			FN547652			Stockinger et al. (2010)
Diversispora trimurales	isolate 131-1-42	unknown, soil			KJ850199			Błaszkowski et al. (2015)
Diversispora trimurales	isolate 131-2-5	unknown, soil			KJ850200			Błaszkowski et al. (2015)
Diversispora valentina	isolate P37_Con	Spain, soil			MT985515			Guillén et al. (2020)
Diversispora valentina	isolate P11_Con	Spain, soil			MT985516			Guillén et al. (2020)
Diversispora varaderana	isolate 3	Cuba, soil			KT444710			Błaszkowski et al. (2015)
Diversispora varaderana	isolate 7	Cuba, soil			KT444711			Błaszkowski et al. (2015)
Diversispora versiformis	isolate BEG47	USA, soil			FM876815			Krüger et al. (2009)
Diversispora versiformis	isolate BEG47	USA, soil			FM876816			Krüger et al. (2009)
Exserohilum rostratum	CBS 320.64	USA, Bromus inermis				LT882579		Hernández-Restrepo et al. (2018)
Gelidatrema spencermartinsiae	CBS 10760, T	Argentina	NR_137691	DQ513279			KF037089	de García et al. (2010), Liu et al. (2015)
Inocybe calida	MCVE 21558	Italy	JF908226					Osmundson et al. (2013)
Inocybe lineata	DED8019	Thailand	EU569861					Horak et al. (2015)
Inocybe nigroumbonata	LAH35272	Pakistan	ON262107					This study
Inocybe parvibulbosa	SFSU:DED8021	Thailand	GQ892999					Horak et al. (2015)
Inocybe parvibulbosa	ZT10105	Thailand	GQ893003					Horak et al. (2015)
Inocybe parvibulbosa	ZT10078	Thailand	GQ893001					Horak et al. (2015)
Inocybe parvibulbosa	ZT10099, holotype	Thailand	GQ893000					Horak et al. (2015)
Inocybe sejuncta	TENN:068374	Australia	KP308818					Matheny & Bougher (2017)
Inocybe tumidula	PBM3764	Australia	KP171089					Matheny & Bougher (2017)
Inocybe tumidula	PBM3770	Australia	KP171090					Matheny & Bougher (2017)
Inocybe sp. AU84	REH9668	Australia	KP308828					Matheny & Bougher (2017)
Inocybe sp. AU106	TENN:067002	Australia	KP641638					Matheny & Bougher (2017)
Inocybe sp. AU106	TENN:066996	Australia	KP641637					Matheny & Bougher (2017)
Inocybe sp. AU110	CBG:8916878	Australia	KP636838					Matheny & Bougher (2017)
Inocybe sp. PBM3335	CO4327	Australia	KP636850					Matheny & Bougher (2017)
Inocybe sp. PBM3335	TENN:063942	Australia	KP636849					Matheny & Bougher (2017)
Inocybe sp. ZT10031	ZT10031	Thailand	GQ893020					Horak et al. (2015)
Mycena alphitophora	BAP 591	São Tomé & Principe	MH414553					Cooper et al. (2018)
Mycena alphitophora	HMJAU 43498	China	MH136830					Na & Bau (2019a)
Mycena alphitophora	HMJAU 43686	China	MH136831					Na & Bau (2019a)
Mycena amoena	L0607541	The Netherlands	OL772666					This study
Mycena amoena	L0607542	The Netherlands	OL772667					This study
Mycena antennae	BAP 660	São Tomé & Principe	MH414550					Cooper et al. (2018)

Species	ID (isolate, strain[1], status[2], voucher)	Country, substrate/host	ITS	LSU	partial SSU–ITS–partial LSU	*gapdh*	*tef1*	Reference(s)
Mycena bicystidiata	HMJAU 43648	China	MK309773					Na & Bau (2019b)
Mycena bicystidiata	HMJAU 43593	China	MK309775					Na & Bau (2019b)
Mycena bicystidiata	HMJAU 43589	China	MK309774					Na & Bau (2019b)
Mycena bicystidiata	HMJAU 43744	China	MK309776					Na & Bau (2019b)
Mycena capillata	L0063217	Brazil	OL772669					This study
Mycena castaneicola	HMJAU 43578	China	MH136826					Na & Bau (2019b)
Mycena castaneicola	HMJAU 43581	China	MH136827					Na & Bau (2019b)
Mycena chloroxantha var. *chloroxantha*	L0063621	Brazil	OL772668					This study
Mycena chloroxantha var. *appalachienensis*	KL-BK 59708	Austria	MK795669					Brodegger et al. (2019)
Mycena corynephora	MCVE 30/N	Italy	JF908368					Odmundson et al. (2013)
Mycena corynephora	MCVE 30/I	Italy	JF908366					Odmundson et al. (2013)
Mycena corynephora	MCVE 30/L	Switzerland	JF908367					Odmundson et al. (2013)
Mycena corynephora	MCVE 30/Q	Italy	JF908369					Odmundson et al. (2013)
Mycena corynephora	HMJAU 43574	China	MH136832					Na & Bau (2019a)
Mycena corynephora	HMJAU 43576	China	MH136833					Na & Bau (2019a)
Mycena corynephora	HMJAU 43580	China	MH136834					Na & Bau (2019a)
Mycena cyanorhiza	MCVE 120/B	Italy	JF908385					Odmundson et al. (2013)
Mycena cyanorhiza	J24082010	Finland	MW540696					C.B. Harder, B. Dima, T. Niskanen & T.V. Bonsdorff, unpubl.
Mycena diosma	CBH400	Denmark	FN394617					Harder et al. (2013)
Mycena aff. *discobasis*	BAP658	São Tomé & Principe	MH414554					Cooper et al. (2018)
Mycena aff. *discobasis*	DED8211	São Tomé & Principe	MH414555					Cooper et al. (2018)
Mycena discogena	BAP649	São Tomé & Principe	MH414556					Cooper et al. (2018)
Mycena eucalypticola	AH56005	Spain	MZ393494					Traba-Velay et al. (2021)
Mycena griseotincta	HMJAU 43800	China	MK309783					Na & Bau (2019b)
Mycena griseotincta	HMJAU 43805	China	MK309782					Na & Bau (2019b)
Mycena griseotincta	HMJAU 43819	China	MK309784					Na & Bau (2019b)
Mycena heteracantha	HMJAU 43709	China	MK309785					Na & Bau (2019b)
Mycena heteracantha	HMJAU 43711	China	MK309786					Na & Bau (2019b)
Mycena heteracantha	HMJAU 43716	China	MK309787					Na & Bau (2019b)
Mycena hyalinostipitata	HMJAU 43693	China	MH136828					Na & Bau (2019a)
Mycena hyalinostipitata	HMJAU 43701	China	MH136829					Na & Bau (2019a)
Mycena hygrophoroides	HMJAU 43417	China	MK309780					Na & Bau (2019b)
Mycena hygrophoroides	HMJAU 43421	China	MK309781					Na & Bau (2019b)
Mycena lasiopus	BAP603	São Tomé & Principe	MH414558					Cooper et al (2018)
Mycena lasiopus	BAP635	São Tomé & Principe	MH414557					Cooper et al (2018)
Mycena longiqua	BAP648	São Tomé & Principe	MH414552					Cooper et al (2018)
Mycena lourensis	AH56003	Spain	MZ393491					Traba-Velay et al. (2021)
Mycena lourensis	ACP2091XL	Mexico	MZ393492					Traba-Velay et al. (2021)
Mycena melanovelis	AH56004	Spain	MZ393493					Traba-Velay et al. (2021)
Mycena miscanthi	HMJAU 43584	China	MK309779					Na & Bau (2019b)
Mycena miscanthi	HMJAU 43573	China	MK309777					Na & Bau (2019b)
Mycena miscanthi	HMJAU 43582	China	MK309778					Na & Bau (2019b)
Mycena perlae	ACP1353	Mexico	MG926690					Córtes-Pérez et al. (2019)
Mycena perlae	ACP1669	Mexico	MG926691					Córtes-Pérez et al. (2019)

Species	ID (isolate, strain[1], status[2], voucher)	Country, substrate/host	ITS	LSU	partial SSU–ITS–partial LSU	*gapdh*	*tef1*	Reference(s)
Mycena pura	CBH128	Denmark	FN394575					Harder et al. (2013)
Mycena oboensis	BAP669	São Tomé & Principe	MH414559					Cooper et al. (2018)
Mycena spinosissima	ACP2022XAL	Mexico	MZ393495					Traba-Velay et al. (2021)
Mycena substylobates	HMJAU 43418	China	MH216189					Na & Bau (2019a)
Mycena substylobates	HMJAU 43444	China	MH216190					Na & Bau (2019a)
Mycena tenerrima group I	L0607549	The Netherlands	OL772664					This study
Mycena tenerrima group I	HMJAU 43646	China	MK309795					Na & Bau (2019b)
Mycena tenerrima group I	HMJAU 43816	China	MK309796					Na & Bau (2019b)
Mycena tenerrima group I	Aronsen120803	Norway	KT900140					Aronsen & Larsson (2015)
Mycena tenerrima group I	Orstadius329-05	Sweden	KT900141					Aronsen & Larsson (2015)
Mycena tenerrima group I	Aronsen061119	Norway	KT900142					Aronsen & Larsson (2015)
Mycena tenerrima group I	Aronsen120826/1	Norway	KT900143					Aronsen & Larsson (2015)
Mycena tenerrima group II	L0607551	The Netherlands	OL772670					This study
Mycena tenerrima group II	UBC:F19725	United States	HQ604774					M.L. Berbee, A.R. Bradford & S.Y.M. Tang, unpubl.
Mycena tenerrima group II	L0607550	The Netherlands	OL772665					This study
Mycena tenerrima group II	G.M. 2014-09-30.5	Luxembourg	MZ467320					S. Hermant & G. Marson, unpubl.
Mycena tenerrima group II	MCVE 35/H	Italy	JF908419					Odmundson et al. (2013)
Mycena tenerrima group II	MCVE 35/M	Italy	JF908420					Odmundson et al. (2013)
Phaeotremella camelliae	CGMCC 2.6141, T	China	MN450769	MN450769			MN450796	Sun et al. (2020)
Phaeotremella dejopia	MICH 340451, T	USA Wisconsin	MT913629	OM311634				This study
Phaeotremella dejopia	ARIZ AN 043301	USA Arizona	MT122147	OM311635			OM322340	T.A. Clements, unpubl.; this study
Phaeotremella eugeniae	LE 262894	Russia		MF076942			MF095828	Spirin et al. (2018)
Phaeotremella eugeniae	LE 303429, T	Russia	NR_158846	NG_060192			MF095825	Spirin et al. (2018)
Phaeotremella fagi	CBS 9964, T	The Netherlands	NR_119558	NG_057744			KF037051	Middelhoven (2006), Liu et al. (2015)
Phaeotremella fimbriata	Niemalä 7897	Finland	MF076910	MF076927				Spirin et al. (2018)
Phaeotremella fimbriata	Spirin 11139, T	Norway	NR_158848	NG_060191			MF095842	Spirin et al. (2018)
Phaeotremella fimbriata	Spirin 11114	Norway	MF076909				MF095831	Spirin et al. (2018)
Phaeotremella foliacea	CBS 5029, T	USA Oregon	NR_073211	AF189835			KF037088	Fell et al. (2000), Scorzetti et al. (2002), Liu et al. (2015)
Phaeotremella foliacea	CBS 8474, CCJ 1203, T	Taiwan	KY104489	KY108756				Vu et al. (2016)
Phaeotremella foliacea	Spirin 7721	Russia	MF076913	MF076930			MF095834	Spirin et al. (2018)
Phaeotremella foliacea	Miettinen 14610, T	Sweden	NR_158847	MF076933			MF095837	Spirin et al. (2018)
Phaeotremella foliacea	Spirin 11170	Russia	MF076917	MF076934			MF095838	Spirin et al. (2018)
Phaeotremella foliacea	Miettinen 14812.2	USA Massachusetts	MF076920	MF076937				Spirin et al. (2018)
Phaeotremella foliacea	Prillinger 1985/53/1	Germany	MF580586	MF581008			MF581769	Spirin et al. (2018)
Phaeotremella foliacea	LE 303431	Russia	MF076906				MF095827	Spirin et al. (2018)
Phaeotremella frondosa	LE 206897, T	Russia	MF076907	MF076925			MF095829	Spirin et al. (2018)
Phaeotremella frondosa	Spirin 10969	Russia	MF076911	MF076928			MF095832	Spirin et al. (2018)
Phaeotremella frondosa	Miettinen 19896	Finland	MF076915	MF076932			MF095836	Spirin et al. (2018)
Phaeotremella frondosa	Spirin 11202	Norway	MF076918	MF076935			MF095839	Spirin et al. (2018)
Phaeotremella frondosa	Spirin 11204	Russia	MF076919	MF076936			MF095840	Spirin et al. (2018)
Phaeotremella frondosa	Bandoni 554-6, T	Canada	NR_155680	NG_058368				Vu et al. (2016)
Phaeotremella frondosa	FLAS-F-60268	USA Florida	MF153056	OM311636				B. Kaminsky, M.E. Smith, R. Healy, B. Spakes Richter, A. Mujic, A. Corrales, et al., unpubl.; this study
Phaeotremella frondosa	MU 000297136	USA Ohio	OM311633	OM311637				This study

Species	ID (isolate, strain[1], status[2], voucher)	Country, substrate/host	ITS	LSU	partial SSU–ITS–partial LSU	*gapdh*	*tef1*	Reference(s)
Phaeotremella fuscosuccinea	Spirin 7905	Russia	MF076921	MF076938			MF095841	Spirin et al. (2018)
Phaeotremella fuscosuccinea	Spirin 7337	Russia	MF076923	MF076940			MF095843	Spirin et al. (2018)
Phaeotremella lactea	CGMCC 2.5810, T	China	MK050280	MK050280				Li et al. (2020)
Phaeotremella lacus	CGMCC 2.5580, T	China	MG909557	KY614525			MH187169	Li et al. (2019)
Phaeotremella mycetophiloides	Prillinger 1987/15	Germany	MF580587	LN870265			MF581770	Spirin et al. (2018)
Phaeotremella mycophaga	FO 23461	Germany	MF580589	AF042249			MF581772	Chen (1998), Spirin et al. (2018)
Phaeotremella ovata	CGMCC 2.5614, T	China	MK050281	MK050281				Li et al. (2020)
Phaeotremella roseotincta	LE 303436	Russia	KP986504	KP986539				Malysheva et al. (2015)
Phaeotremella roseotincta	LE 303428	Russia	KP986505					Malysheva et al. (2015)
Phaeotremella simplex	FO31782	Germany	AF042428	AF042246			LT905059	Chen (1998); M.A. Yurkov, unpubl.
Phaeotremella translucens	CBS 14981	Japan	LC203431	LC203432				Degawa et al. (2022)
Phaeotremella translucens	CBS 14982	Japan	LC203434	LC203435				Degawa et al. (2022)
Phaeotremella yunnanensis	BJFC 019725	China	MK559396	MK559398			MK559400	Yuan et al. (2020)
Phaeotremella yunnanensis	BJFC 019764, T	China	MK559397	MK559399			MK559401	Yuan et al. (2020)
Porpoloma portentosum	MICH 00011834, T	Argentina	NR_154301					Sánchez-Garcia et al. (2014)
Pseudotricholoma umbrosum	MICH 00012331	Canada	NR_154304					Sánchez-Garcia et al. (2014)
Thaxterogaster caesiophylloides	H:6029792, T	Finland	NR_130303					Liimatainen et al. (2014)
Thaxterogaster frondosomultiformis [as Cortinarius frondosomultiformis]	TG2000-218, T	Italy	KM504516					Brandrud et al. (2014)
Thaxterogaster multiformis	S:F44806, T	Sweden	NR_130232					Liimatainen et al. (2014)
Thaxterogaster talimultiformis	UPS A. Taylor 2004096, T	Sweden	NR_130306					Liimatainen et al. (2014)
Thaxterogaster talus	S:F44793, T	Sweden	NR_130275					Liimatainen et al. (2014)
Tricholoma albobrunneum	TUF106242	Estonia	UDB011126*					I. Saar, unpubl.
Tricholoma albobrunneum	C-F-96268	France	LT000077					Heilmann-Clausen et al. (2017)
Tricholoma aff. *albobrunneum*	QFB32594	Canada	MW628036					Landry et al. (2022)
Tricholoma aff. *albobrunneum*	HRL1852, QFB32636	Canada	MW627973					Landry et al. (2022)
Tricholoma aff. *albobrunneum*	YL4171, CMMF024667	Canada	MW628092					Landry et al. (2022)
Tricholoma ammophilum	WTU-F-073015, T	USA	MW597199					Trudell & Parker (2021)
Tricholoma ammophilum	CMMF003005	Canada	MW628083					Landry et al. (2022)
Tricholoma argyraceum	L0374886, T	Netherlands	LT000198					Heilmann-Clausen et al. (2017)
Tricholoma arvernense	DBG:18239	USA	MF034264					Reschke et al. (2018)
Tricholoma arvernense	MB<DEU-Marburg>:002876	Austria	MF034215					Reschke et al. (2018)
Tricholoma arvernense	C-F-59255	France	LT000078					Heilmann-Clausen et al. (2017)
Tricholoma arvernense	C-F-59014	Sweden	LT000157					Heilmann-Clausen et al. (2017)
Tricholoma arvernense	YL4388, CMMF024674	Canada	ON256899					Landry et al. (2022)
Tricholoma aurantio-olivaceum	MICH 12313, T	USA	MN809569					M. Gordon, unpubl.
Tricholoma aurantium	TUF101569	Estonia	UDB011542*					I. Saar, unpubl.

Species	ID (isolate, strain[1], status[2], voucher)	Country, substrate/host	ITS	LSU	partial SSU–ITS–partial LSU	*gapdh*	*tef1*	Reference(s)
Tricholoma arvernense	TENN:066037	USA	KU058507					Sánchez-Garcia & Matheny (2016)
Tricholoma badicephalum	WTU-F-073095, T	USA	MW597309					Trudell & Parker (2021)
Tricholoma boudieri	C-F-90092, CFT-0395, T	Slovenia	LT000136					Heilmann-Clausen et al. (2017)
Tricholoma dryophilum	KMS362	USA	AF377239					Bidartondo et al. (2002)
Tricholoma dryophilum	WTU-F-073055, T	USA	MW597274					Trudell & Parker (2021)
Tricholoma focale	C-F-27500, CFT-0398, T	Sweden	LT000166					Heilmann-Clausen et al. (2017)
Tricholoma forteflavescens	HKAS:93511	China	NR_160587					Reschke et al. (2018)
Tricholoma fulvimarginatum	pat10091201, CMMF024686	Canada	MW627928					Landry et al. (2022)
Tricholoma fulvimarginatum	YL4169, CMMF024666	Canada	MW627933					Landry et al. (2022)
Tricholoma fulvimarginatum	HRL2816, QFB32648	Canada	MW627974					Landry et al. (2022)
Tricholoma fulvimarginatum	CMMF002688	Canada	MW627986					Landry et al. (2022)
Tricholoma fulvimarginatum	JLAB874, CMMF009290	Canada	MW628015					Landry et al. (2022)
Tricholoma fulvimarginatum	HL1668, QFB32593	Canada	MW628035					Landry et al. (2022)
Tricholoma fulvimarginatum	CMMF003587	Canada	MW628056					Landry et al. (2022)
Tricholoma fulvimarginatum	HRL0634, QFB32609	Canada	MW628080					Landry et al. (2022)
Tricholoma fulvimarginatum	HRL3617, QFB33141	Canada	ON256900					Landry et al. (2022)
Tricholoma fulvimarginatum	Halling 3234, T	USA	OP221720					This study
Tricholoma fulvum	C-F-96195	Sweden	LT000171					Heilmann-Clausen et al. (2017)
Tricholoma hemisulphureum	C-F-96217	Estonia	LT000065					Heilmann-Clausen et al. (2017)
Tricholoma hemisulphureum	C-F-96217	Estonia	LT000065					Heilmann-Clausen et al. (2017)
Tricholoma ilkkae	S_F_513823, T	Sweden	LT222029					Heilmann-Clausen et al. (2017)
Tricholoma imbricatoides	HRL3100, QFB32654, T	Canada	MW628100					Landry et al. (2022)
Tricholoma imbricatoides	CMMF002109	Canada	MW627977					Landry et al. (2022)
Tricholoma imbricatoides	HL0395, QFB31069	Canada	MW628128					Landry et al. (2022)
Tricholoma imbricatoides	QFB30736	Canada	MW628048					Landry et al. (2022)
Tricholoma imbricatoides	CMMF007436	Canada	MW627952					Landry et al. (2022)
Tricholoma imbricatoides	CMMF007466	Canada	MW628091					Landry et al. (2022)
Tricholoma imbricatoides	CMMF002729	Canada	MW627909					Landry et al. (2022)
Tricholoma imbricatoides	CMMF005038	Canada	MW628018					Landry et al. (2022)
Tricholoma imbricatoides [as *T. imbricatum*]	HRL1001	Canada	KJ705242					J.A. Bérubé, J. Gadomski, R. Labbe, R. Lebeuf, P. Gagne, J. Dube, et al., unpubl.
Tricholoma imbricatoides [as *T. aurantio-olivaceum*]	WTU-F-073038	USA	MW597257					S.A. Trudell, M. Gordon & E.T. Cline, unpubl.
Tricholoma imbricatoides [as *T. imbricatum*]	DBG:18375	USA	MF034266					Reschke et al. (2018)
Tricholoma imbricatoides [as *T. imbricatum*]	DBG:23986	USA	MF034274					Reschke et al. (2018)
Tricholoma imbricatoides [as *T. imbricatum*]	WTU-F-073019	USA	MW597202					S.A. Trudell, M. Gordon & E.T. Cline, unpubl.
Tricholoma imbricatoides [as *T. imbricatum*]	KMS296	USA	AF377242					Bidartondo et al. (2002)
Tricholoma imbricatoides [as *T. imbricatum*]	trh895	USA	AF462636					M. Horton, unpubl.
Tricholoma imbricatum	C-F-59268, CFT-0394, T	Denmark	LT000024					Heilmann-Clausen et al. (2017)
Tricholoma imbricatum	TIK2-X-10	Montenegro	JQ685732					Lazarevic et al., unpubl.
Tricholoma imbricatum	TUF101431	Estonia	UDB011626*					I. Saar, unpubl.
Tricholoma imbricatum	MB<DEU-Marburg>:102330	Austria	MF034301					Reschke et al. (2018)

Species	ID (isolate, strain[1], status[2], voucher)	Country, substrate/host	ITS	LSU	partial SSU–ITS–partial LSU	*gapdh*	*tef1*	Reference(s)
Tricholoma inamoenum	C-F-35182, CFT-0399, T	Sweden	LT000173					Heilmann-Clausen et al. (2017)
Tricholoma magnivelare	NYSf2421, T	USA	LT220177					Heilmann-Clausen et al. (2017)
Tricholoma mcneilii	HRL2835, QFB32650, T	Canada	MW628021					Landry et al. (2022)
Tricholoma mcneilii	QFB32579	Canada	MW628115					Landry et al. (2022)
Tricholoma mcneilii	QFB32581	Canada	MW627953					Landry et al. (2022)
Tricholoma mcneilii [as *Tricholoma* sp.]	iNaturalist # 18259629	USA	MZ215771					G.M. Taylor, unpubl.
Tricholoma mcneilii [as *Tricholoma* sp.]	iNaturalist # 17610322	USA	MZ206359					G.M. Taylor, unpubl.
Tricholoma nigrum	SFSU-F-000790, T	USA	MN809565					M. Gordon, unpubl.
Tricholoma nigrum	WTU-F-073017	USA	MW597201					S.A. Trudell, M. Gordon & E.T. Cline, unpubl.
Tricholoma nigrum	WTU-F-073070	USA	MW597288					S.A. Trudell, M. Gordon & E.T. Cline, unpubl.
Tricholoma nigrum	WTU-F-000660	USA	MW597231					S.A. Trudell, M. Gordon & E.T. Cline, unpubl.
Tricholoma nigrum [as *T. luteomaculosum*]	UBC F19693		HM240543					M.L. Berbee & S.R. Lim, unpubl.
Tricholoma nigrum [as *T. luteomaculosum*]	trh914		AF458446					M. Horton, unpubl.
Tricholoma nigrum [as *T. luteomaculosum*]	trh1033		AF458447					M. Horton, unpubl.
Tricholoma olivaceum	MB<DEU-Marburg>:002991	China	MF034294					Reschke et al. (2018)
Tricholoma olivaceum	MB<DEU-Marburg>:30191	China	MF034307					Reschke et al. (2018)
Tricholoma olivaceum	MB<DEU-Marburg>:301918	China	MF034306					Reschke et al. (2018)
Tricholoma olivaceum	HKAS:93513, T	China	NR_160588					Reschke et al. (2018)
Tricholoma pallens	CMMF003782	Canada	MW628013					Landry et al. (2022)
Tricholoma pallens	HRL3381, QFB33134, T	Canada	ON256907					Landry et al. (2022)
Tricholoma pallens	HRL2642	Canada	ON206668					P. Alvarado, unpubl.
Tricholoma pallens [as *T. olivaceum*]	MICH340356	USA	OM985826					H. Su, J.K. Stallman, J. Johnson, B. Roy, D.J. Lodge, B. Sheehan & S.D. Russell, unpubl.
Tricholoma pallens [as *T. saponaceum*]	iNaturalist # 59500740	USA	MW031156					S. Jakob, unpubl.
Tricholoma pallens [as *T. saponaceum*]	#20	China	MW192470					Gao et al. (2022)
Tricholoma pallens [as *Tricholoma* sp. 'IN07']	iNaturalist # 92048539	USA	OM972428					S.D Russell, unpubl.
Tricholoma pallens [as *Tricholoma* sp. 'IN07']	iNaturalist # 92048667	USA	OM972427					S.D. Russell, unpubl.
Tricholoma pessundatum	C-F-43780, CFT-0400, T	Denmark	LT000032					Heilmann-Clausen et al. (2017)
Tricholoma pessundatum	CMMF009347	Canada	MW628012					Landry et al. (2022)
Tricholoma populinum	TUF120226	Estonia	UDB024626*					I. Saar, unpubl.
Tricholoma populinum	TUF118836	Estonia	UDB019508*					I. Saar, unpubl.
Tricholoma psammopus	DG30	United Kingdom	JQ888219					Pickles et al. (2012)
Tricholoma pseudoterreum	CMMF001539	Canada	MW628017					Landry et al. (2022)
Tricholoma pseudoterreum	CMMF006864	Canada	MW627947					Landry et al. (2022)
Tricholoma pseudoterreum	HRL1886, QFB32637, T	Canada	MW628106					Landry et al. (2022)
Tricholoma pseudoterreum	HL0403-QFB31074	Canada	MW627965					Landry et al. (2022)
Tricholoma pseudoterreum	CMMF005015	Canada	MW628105					Landry et al. (2022)
Tricholoma pseudoterreum	CMMF004855	Canada	MW627887					Landry et al. (2022)

Species	ID (isolate, strain[1], status[2], voucher)	Country, substrate/host	ITS	LSU	partial SSU–ITS–partial LSU	*gapdh*	*tef1*	Reference(s)
Tricholoma pseudoterreum	CMMF002096	Canada	MW627927					Landry et al. (2022)
Tricholoma rapipes	C-F-59258, CFT-0406	France	LT000085					Heilmann-Clausen et al. (2017)
Tricholoma robustipes	YL4219, CMMF024670	Canada	MW628124					Landry et al. (2022)
Tricholoma robustipes	CMMF002303	Canada	MW627932					Landry et al. (2022)
Tricholoma robustipes	HRL0983	Canada	KJ705247					Bérubé et al. unpubl.
Tricholoma robustipes	HRL3316, QFB33132 T	Canada	ON256909					Landry et al. (2022)
Tricholoma robustipes	HRL0923	Canada	KJ705246					J.A. Bérubé, J. Gadomski, R. Labbe, R. Lebeuf, P. Gagne, J. Dube, et al., unpubl.
Tricholoma robustipes	HRL0295, QFB32601	Canada	MW628006					Landry et al. (2022)
Tricholoma saponaceum	C-F-96276	France	LT000087					Heilmann-Clausen et al. (2017)
Tricholoma saponaceum	C-F-96192	Slovakia	LT000133					Heilmann-Clausen et al. (2017)
Tricholoma saponaceum	C-F-23337	Denmark	LT000038					Heilmann-Clausen et al. (2017)
Tricholoma saponaceum	AFTOL-ID 672	USA	DQ494700					Matheny et al. (2006)
Tricholoma saponaceum	TUF106254	Estonia	UDB011570*					I. Saar, unpubl.
Tricholoma saponaceum	MHHNU 30742	China	MK214390					Z.H. Chen & P. Zhang, unpubl.
Tricholoma aff. *saponaceum*	HRL0787, QFB32612	Canada	MW627994					Landry et al. (2022)
Tricholoma aff. *saponaceum*	CMMF000214	Canada	MW628019					Landry et al. (2022)
Tricholoma sp.	iNAT:17426370	USA	MZ206356					G.M. Taylor, unpubl.
Tricholoma sp.	TRTC156508	Canada	JULY072-08**					J.M. Moncalvo, unpubl.
Tricholoma stans	C-F-59042, CFT-0396, T	Sweden	LT000189					Heilmann-Clausen et al. (2017)
Tricholoma stans	HRL1012	Canada	KJ705239					J.A. Bérubé, J. Gadomski, R. Labbe, R. Lebeuf, P. Gagne, J. Dube, et al., unpubl.
Tricholoma stans	QFB32589	Canada	MW628001					Landry et al. (2022)
Tricholoma stans	HRL3087, QFB32653	Canada	MW628050					Landry et al. (2022)
Tricholoma stans	CMMF006893	Canada	MW628052					Landry et al. (2022)
Tricholoma stans	QFB32597	Canada	MW627910					Landry et al. (2022)
Tricholoma stans	C-F-96258	Norway	LT000124					Heilmann-Clausen et al. (2017)
Tricholoma sudum	C-F-90094, CFT-0403, T	Denmark	LT000051					Heilmann-Clausen et al. (2017)
Tricholoma terreum	L0374887, T	Germany	LT000098					Heilmann-Clausen et al. (2017)
Tricholoma ustale	MB<DEU-Marburg>:002924	Germany	MF034288					Reschke et al. (2018)
Tricholoma ustaloides	MB<DEU-Marburg>:002929	Germany	MF034291					Reschke et al. (2018)
Tricholoma vaccinum	C-F-96228	Slovenia	LT000150					Heilmann-Clausen et al. (2017)
Tricholoma vaccinum	TUF106239	Estonia	UDB011642*					I. Saar, unpubl.
Tricholoma vaccinum	QFB30744	Canada	MW627975					Landry et al. (2022)
Tricholoma vaccinum	QFB31081	Canada	MW628029					Landry et al. (2022)
Tricholoma aff. vaccinum	CMMF009312	Canada	MW627878					Landry et al. (2022)
Tricholoma aff. vaccinum	HRL2795, QFB32647	Canada	MW627929					Landry et al. (2022)
Tricholoma viridiolivaceum	OTA:61887	New Zealand	JX178633					Teasdale et al. (2013)
Tricholoma viridiolivaceum	C-F-96257	New Zealand	LT000117					Heilmann-Clausen et al. (2017)

yses were performed on the CIPRES Science Gateway (Miller et al. 2010) using RAxML-HPC version 8. The ML analysis used the GTRCAT model. The rapid bootstrapping algorithm was employed with 1000 replicates.

A *Mycena* dataset consisting of 62 ITS sequences downloaded from GenBank and 7 ITS sequences generated during this study (Tab. 1) was compiled and aligned using the iterative aligner Canopy version 0.1.5 (http://wasabiapp.org/software/canopy). Two species placed in *Mycena* sect. *Calodontes*, *M. diosma* Krieglst. & Schwöbel and *M. pura* (Pers.) P. Kumm., were chosen as the outgroup. Settings for Canopy were as follows: the initial aligner and alignment merger were set to PRANK (Löytynoja & Goldman 2005, 2008), the iterative aligner was set to PAGAN (Löytynoja et al. 2012), and the tree estimator was set to RAxML with the GTRCAT substitution model (Stamatakis 2014). PRANK was called with the +F argument. The iterative aligner ran for a maximum of 50 iterations. The final alignment had a total length of 2289 sites. The alignment was partitioned corresponding with the SSU, ITS1, 5.8S rDNA, ITS2, and LSU regions. Boundaries for each region were determined with ITSx (Bengtsson-Palme et al. 2013). In some cases, manual adjustment was needed. ML analysis was conducted in RAxML-NG version 1.0.1 (Kozlov et al. 2019). The best fit substitution models were determined with ModelTest-NG version 0.1.6 (Flouri et al. 2014, Darriba et al. 2020). Freerate models (+R) were not considered to prevent overparameterization. Models that simultaneously include a proportion of invariable sites and discrete gamma rate categories (+G+I) were not tested, since their biological relevance has been contested and to prevent a 'ping–pong effect' (Stamatakis 2006, Jia et al. 2014). The ML bootstrap (MLBS) analysis was run for a maximum of 2000 iterations, or until autoMRE bootstopping convergence criteria were met. BI was performed with BEAST version 2.6.2 (Bouckaert et al. 2019). The best-fit substitution models were determined and applied using bModelTest version 1.9.0 (Bouckaert & Drummond 2017). The MCMC chain was run for 25,000,000 generations, with sampling every 10,000 generations. TreeAnnotator version 1.10 (Drummond & Rambaut 2007) was used to discard the first 10 % of the sampled trees as burn-in and to subsequently combine all remaining trees. Trees resulting from ML and BI analyses were visualized using FigTree version 1.4.2 and edited in Adobe Illustrator CC 2015.

ITS, LSU, and *tef1* sequences of 39 *Phaeotremella* specimens—representing a complete sampling of the *Phaeotremella* species with publicly available sequence data—and one belonging to *Gelidatrema* (Phaeotremellaceae) serving as an outgroup (Tab. 1) were aligned with MUSCLE in SeaView version 5.0.4 (Gouy et al. 2010). The alignments were trimmed with TrimAl version 1.2 using automatic settings (Capella-Gutiérrez et al. 2009). For each locus, the best model of nucleotide substitution was determined with ModelFinder according to the Bayesion information criterion as implemented in IQ-TREE version 1.6.12 (Nguyen et al. 2015, Kalyaanamoorthy et al. 2017). Single-locus and concatenated multi-locus phylogenetic trees were inferred with IQ-TREE using 1000 ultrafast bootstrap replicates and the following models: TIM2e+R2 (ITS), TNe+R2 (LSU), and TIM2e+I+G4 (*tef1*) (Chernomor et al. 2016, Hoang et al. 2018). The alignments (https://doi.org/10.6084/m9.figshare.20352642.v2) and phylogenetic trees (https://doi.org/10.6084/m9.figshare.20352663.v2) were uploaded to the figshare online repository.

Newly generated *Tricholoma* sequences (Landry et al. 2022) were supplemented with sequences of closely related species found by BLAST searches in NCBI GenBank, UNITE (Abarenkov et al. 2010), or the Barcode of Life Data System (BOLD, http://boldsystems.org/) and of species belonging to closely related sections as delimited in recent infrageneric classification studies (Heilmann-Clausen et al. 2017, Reschke et al. 2018). Sequences were aligned using MUSCLE version 3.7 (Edgar 2004) and corrected manually as needed. Phylogenetic trees were constructed with the help of MEGA7 (Kumar et al. 2016) with default settings. Maximum likelihood (ML) was inferred based on the Tamura-Nei model (Tamura & Nei 1993). ML bootstrap (MLBS) analysis was performed with 100 replicates. Initial tree(s) for the heuristic search were obtained automatically by applying Neighbor-Joining (NJ) and BioNJ algorithms to a matrix of pairwise distances estimated using the Maximum Composite Likelihood approach, and then selecting the topology with superior log likelihood value.

Taxonomy

Ascomycota, Dothideomycetes, Pleosporales, Pleosporaceae

Bipolaris chusqueae Madrid, Cantillo & R. Castillo, **sp. nov.** – Fig. 1
MycoBank no.: MB 843173

D i a g n o s i s . – Different from similar species, such as *Bipolaris austrostipae*, *B. axonopodicola*, and *B. coffeana* in the number of conidial distosepta and in several differences in

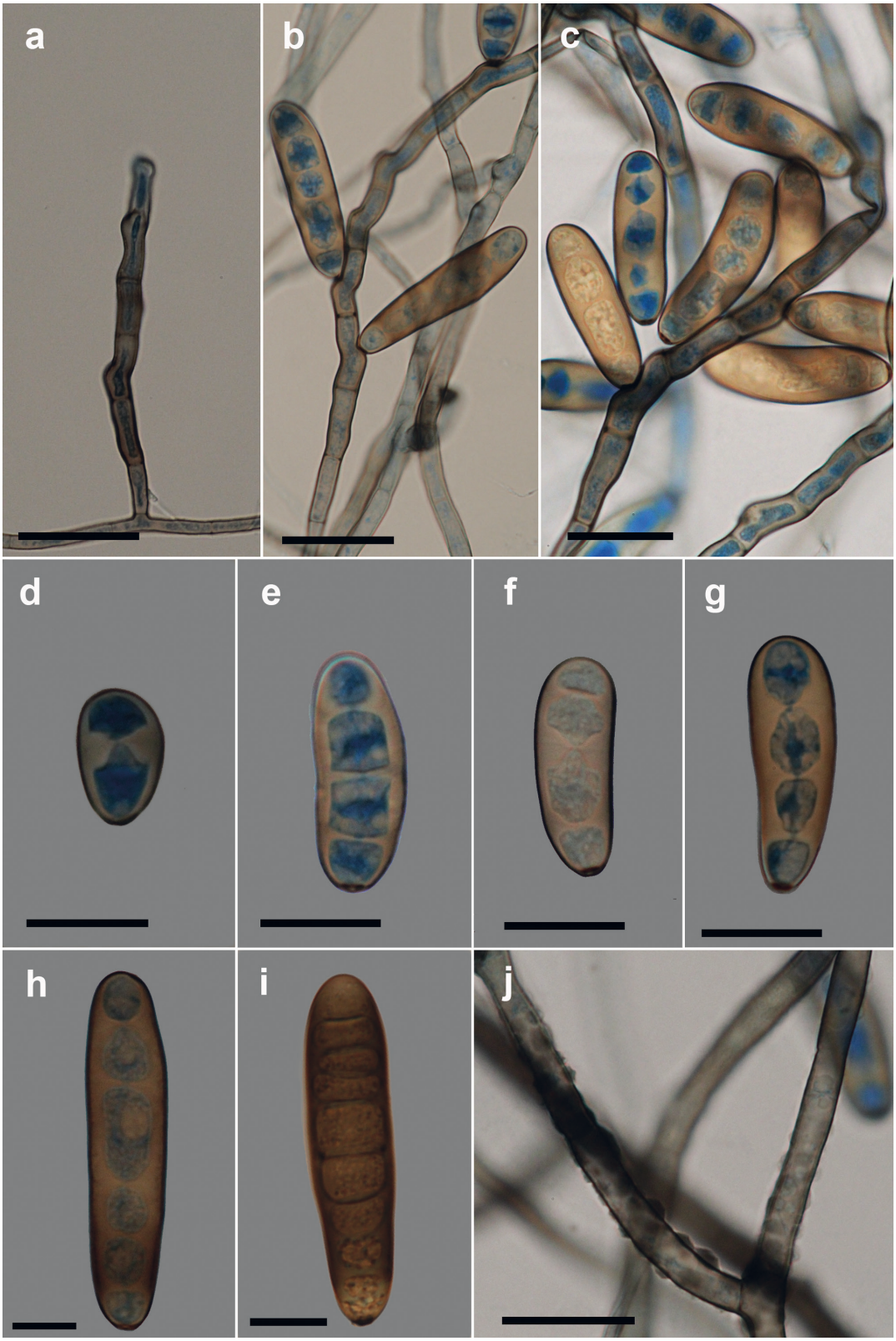

Fig. 1. *Bipolaris chusqueae*, collection SGO 166370 (holotype). **a.** Conidiophore. **b, c.** Conidiogenous cells and conidia. **d–i.** Conidia. **j.** Verruculose hyphae. Scale bars a–c 30 µm, d–g 25 µm, h–j 10 µm.

both ITS and *gapdh* loci. Conidia straight to slightly curved, measuring (17–)26–50(–68) × 10–12(–15) µm, with 2–9 (mostly 3) conspicuous distosepta.

Holotypus. – CHILE. Valparaíso Region, Marga Marga Province, La Campana National Park, on branches of *Chusquea cumingii*, 30 June 2015, *leg.* H. Madrid (SGO 166370; holotype). Sequences ex-holotype: OM914401 (ITS), OM914400 (LSU), OM912808 (*gapdh*).

Description. – Colonies on water agar with sterilized corn leaves hairy to cottony. Vegetative hyphae septate, branched, light olivaceous to mid brown, thin- to thick-walled, 1.5–7.0 µm wide, mostly smooth to verruculose, but occasionally showing incrustations and wart-like deposits of a mucilaginous dark brown material. – Conidiophores macronematous, mononematous, mostly solitary, but sometimes caespitose, septate, simple, straight to flexuous, more or less geniculate at the fertile portion, light olivaceous brown to dark brown, often paler at the apex, smooth to verruculose with cell walls often thicker than those of the supporting vegetative hyphae, 31–350 × 5–8 µm with subnodulose to nodulose intercalary swellings up to 10 µm wide. – Conidiogenous cells integrated, terminal and intercalary, mostly subcylindrical, mono- to polytretic, proliferating sympodially, 12–30 µm long. – Conidia subcylindrical to narrowly clavate, straight to slightly curved, light olivaceous brown to dark brown, smooth, (17–)26–50(–68) × 10–12(–15) µm, with 2–9 (mostly 3) distosepta, with a rounded apex and an obconically truncate or rounded base; hilum thick and dark with a conspicuous central germ pore. – Sexual morph not observed.

Etymology. – Referring to the bamboo genus *Chusquea*, from which this fungus was isolated.

Habitat and distribution. – On branches of *Chusquea cumingii*. Thus far only known from the type locality in Chile.

Notes. – *Bipolaris chusqueae* was isolated from *Chusquea cumingii*, an endemic bamboo species found in areas of central Chile. Due to mobility restrictions during the SARS-CoV-2 pandemic, the ex-type strain that was preserved in sterile water, could not be properly maintained for several months and died. However, the holotype was deposited at SGO and ex-holotype sequences are available in NCBI GenBank. BLAST searches with the ITS sequence of *B. chusqueae* revealed that this fungus is closely related to *B. cynodontis* (Marignoni) Shoemaker (CBS 109894, ex-type strain, GenBank accession no. KJ909767, 99.30 % shared identity), *B. axonopodicola* Y.P. Tan & R.G. Shivas (BRIP 11740, ex-type strain, KX452443, 99.30 %), *B. austrostipae* Y.P. Tan & R.G. Shivas (BRIP 12490, ex-type strain, KX452442, 99.15 %), and *B. coffeana* Sivan. (BRIP 14845 = CBS 126976, ex-type strain, MH864366, 99.15 %).

The *gapdh* sequence of *B. chusqueae* shares 98.62 % identity with *B. austrostipae* (BRIP 12490, ex-type strain, GenBank accession no. KX452408) and 97.80 % with *B. cynodontis* (CBS 285.51, LT715772). Conidia of *B. cynodontis* are larger (27–100 × 10–20 µm) than those of *B. chusqueae* (Manamgoda et al. 2014). However, the conidia of *B. austrostipae*, *B. axonopodicola*, and *B. coffeana* are similar in size to those of *B. chusqueae*, but they are distinguished by the number of distosepta, i.e., 6–9, 5–10, 4–7, and 2–9 (mostly 3), respectively (Manamgoda et al. 2014, Tan et al. 2016). In addition, no *Bipolaris* species other than *B. chusqueae* has been reported from a member of *Chusquea*.

Bipolaris axonopodicola and *B. chusqueae* were retrieved as sister taxa in the *gapdh* phylogenetic tree (Fig. 2). However, this relationship was poorly supported and these species were separated by a considerable genetic distance. *Bipolaris austrostipae*, *B. axonopodicola*, *B. chusqueae*, *B. coffeana*, and *B. cynodontis* formed a moderately supported clade (MLBS = 70).

Authors: H. Madrid, T. Cantillo & R. Castillo

Basidiomycota, Agaricomycetes, Agaricales, Cortinariaceae

Cortinarius* subgenus *Telamonia

Cortinarius anomalosimilis Lebeuf, Healy, Ammirati, J. Landry & G. Taylor **sp. nov**. – Fig. 3
MycoBank no.: MB 843004

Holotypus. – CANADA. Québec, Hinchinbrooke, Réserve écologique du Boisé-des-Muir, 45°05'07.0"N, 74°06'52.4"W, 67 m a.s.l., in an old-growth forest of *Carya cordiformis*, *Tsuga canadensis*, and *Fagus grandifolia*, 23 September 2012, *leg.* R. Lebeuf & A. Paul, HRL1298 (CMMF024817; holotype).

Description. – Pileus 15–40 mm in diameter, conico-convex to convex then campanulate with an inflexed margin, fibrillose, greyish with a violet tinge to pale violet (18A2, 19A2), pale ochraceous (around 5B5) on disc. – Lamellae emarginate, distant to close, whitish to violet at first, later rusty brown. – Universal veil white, copious, often leaving a fibrillose annular zone in upper to mid-stipe. – Cortina white. – Stipe 25–55 mm long, 3–7 mm thick at apex, 5–10 mm thick at base, equal to clavate, white silky fibrillose to pale greyish violet, often darker violet towards apex, staining brown where bruised. – Context cream to

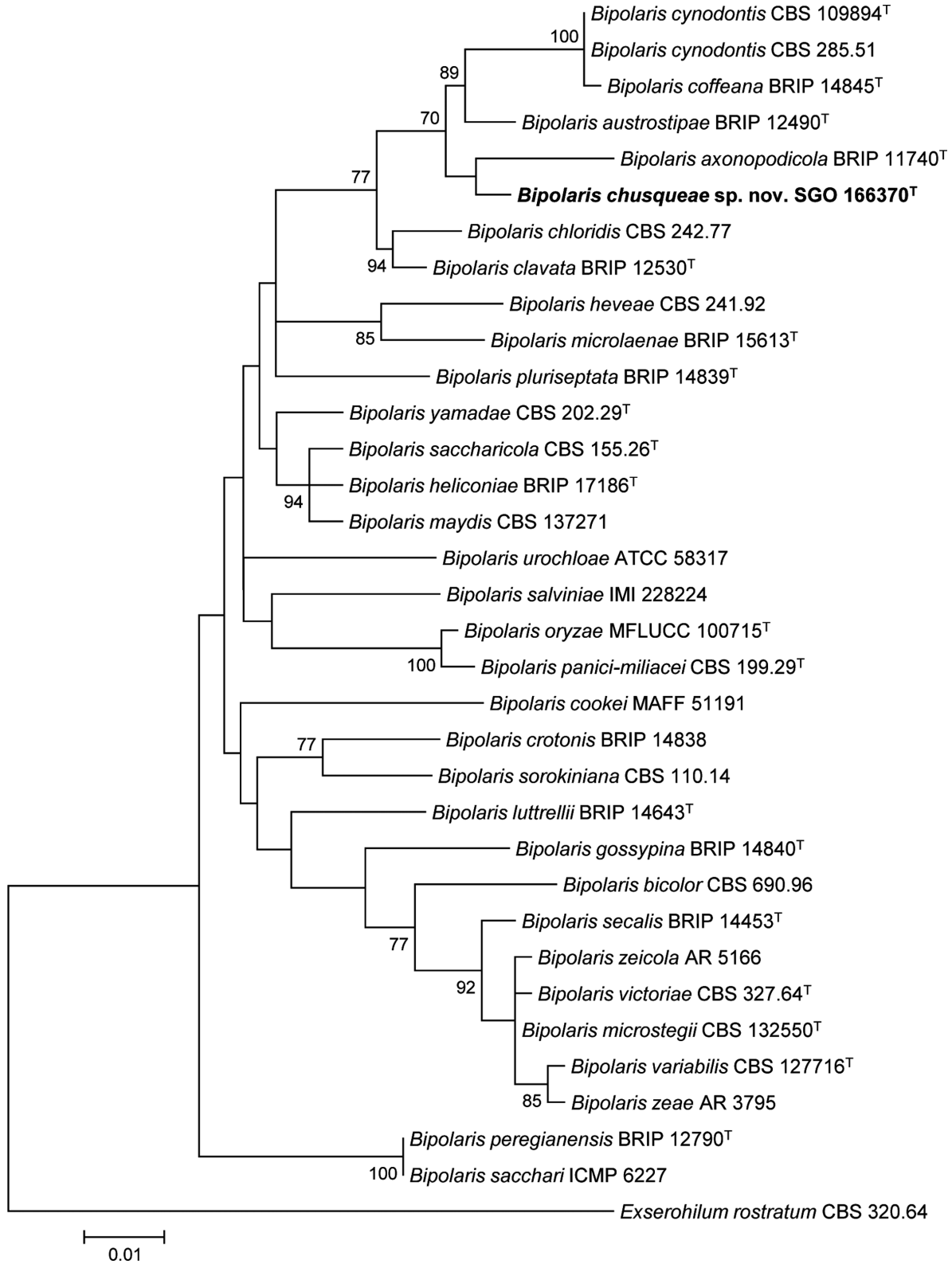

Fig. 2. Phylogeny of *Bipolaris* reconstructed from a *gapdh* dataset. The topology is the result of ML inference performed with MEGA X. ML bootstrap (MLBS) values ≥70 are shown at the nodes, T indicates ex-type sequences. The new species, *B. chusqueae*, is highlighted in boldface.

Fig. 3. *Cortinarius anomalosimilis*. **a.** Basidiomata *in situ*, collection CMMF024817 (holotype). **b.** Basidiomata *in situ*, collection CMMF024818. **c.** Basidiospores. **d.** Pileipellis section in SDS Congo Red. Scale bars c 10 µm, d 25 µm. Photos R. Lebeuf (a), G. Taylor (b).

pale violet, often darker violet at stipe apex or in top half. – Odor indistinct. – Exsiccatae cinnamon (6C5, 6D5). – Basidiospores (8.0–)8.5–11.6(–14.8) × (5.0–)5.4–6.8(–7.5) µm, av. 9.9 × 6.1 µm, Q = 1.37–2.27, Q_{av} = 1.63 [210/10/7], not dextrinoid, generally ellipsoid, oblong to subamygdaloid, generally moderately to ± coarsely verrucose, often more so at distal end, in some collections many rather narrow with a sharp, extended apiculus, nearly smooth to slightly, moderately or more coarsely ornamented, especially at distal end. – Basidia 33–42 × 8–10 µm, 4-spored, in some collections 2- and 4-spored, clavate to narrowly clavate, colorless, in age greyish, yellowish to yellow-brown. – Lamellar trama hyphae colorless, yellowish or yellow-brown, with refractive walls, not encrusted. – Pileipellis duplex: epicutis hyphae radially arranged to ± interwoven, cylindrical, smooth, colorless to yellowish, 3–10 µm wide, covered in places with a ± thin surface layer (veil) of cylindrical, colorless, smooth hyphae 2–7 µm wide; hypocutis hyphae cylindrical to broadly cylindrical or enlarged, colorless to yellowish or yellow-brown, with refractive walls, smooth, mostly 30–60 × 6–25 µm wide. – Clamp connections present in all tissues. – Macrochemical reaction dark grey on pileus surface with 10 % KOH.

Etymology. – Named for its similarity to *Cortinarius* species belonging to section *Anomali*.

Habitat and distribution. – Gregarious in hardwood forests dominated by *Quercus* or *Carya*, in the fall. So far known from Canada (Québec) and the USA (Iowa, New York).

Additional material examined. – *Ibid.* (QFB29866; isotype). Sequences ex-isotype: MN751619 (ITS). – CANADA. Québec, Hinchinbrooke, Réserve écologique du Boisé-des-Muir, in a mixed forest, under *Carya cordiformis* and *Tsuga canadensis*, 30 August 2011, *leg.* R. Lebeuf, HRL0862 (TENN-F-071093; in HRL). – USA. Iowa, Webster County, Fort Dodge, Diggings Preserve, in a small natural area that was the former site of a coal mine, in woods dominated by

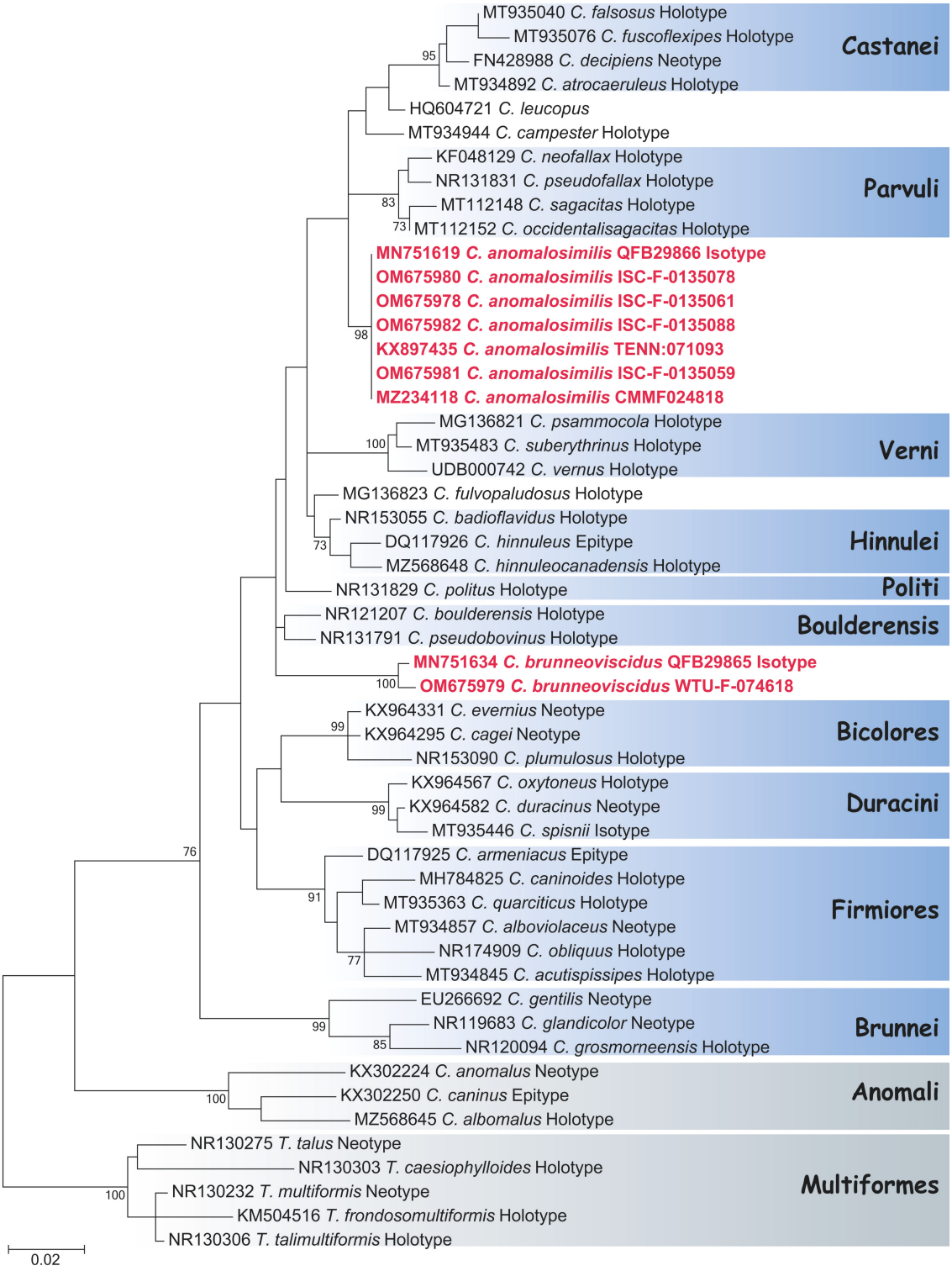

Fig. 4. Phylogeny of *Cortinarius* species in various sections of subgenus *Telamonia* (blue boxes) as defined by Liimatainen et al. (2020) and in section *Anomali* reconstructed from an ITS dataset. The tree topology with the highest log likelihood (-lnL = 3708.7478) is shown, resulting from ML inference performed in MEGA7. Selected species in genus *Thaxterogaster* section *Multiformes* served as outgroup taxa. MLBS values (if ≥70) are shown at the nodes. Tree drawn to scale, with branch lengths proportional to the number of substitutions per site; new species highlighted in red; bar indicating the expected number of substitutions per site.

Quercus alba, *Q. rubra*, *Carya ovata*, and *Tilia americana*, 7 September 2006, *leg*. R. Healy (ISC-F-0135061); Story County, Ames, Iowa State University Campus, Pammel Woods, small riparian hardwoods dominated by *Q. macrocarpa*, 22 September 2006, *leg*. R. Healy (ISC-F-0135088); Webster County, Brushy Creek State Preserve, in upland hardwoods dominated by *Q. rubra* and *C. ovata*, 17 September 2007, *leg*. R. Healy (ISC-F-0135078); Polk County, Des Moines, Brown Woods Preserve, small urban forest dominated by *Q. alba* and *C. ovata*, 29 September 2007, *leg*. R. Healy (ISC-F-0135059); New York, Livingstone County, MacKay Wildlife Preserve, in a deciduous forest of *Q. alba*, *Q. rubra*, and *Carya cordiformis*, 3 September 2020, *leg*. G. Taylor, iNaturalist observation #58496002 (CMMF024818).

Notes. – The ITS sequence of *Cortinarius anomalosimilis* is distinct from that of other members of subgenus *Telamonia*, deviating by at least 10 substitutions and indels from the closest known species, *Cortinarius fulvopaludosus* Kytöv., Niskanen & Liimat. (Fig. 4). With its pale violet colors, dry pileus and stipe, silky pileus, and violet lamellae, *C. anomalosimilis* bears resemblance to members of section *Anomali* and to certain species belonging to sect. *Firmiores* sensu Liimatainen et al. (2020), namely *C. acutispissipes* Rob. Henry, *C. alboviolaceus* (Pers.) Fr., *C. obliquus* Peck, and *C. paralbocyaneus* Eyssart.

Members of sect. *Anomali* differ by their generally subglobose to broadly ellipsoid spores, and the yellowish to brownish universal veil remnants often present on the stipe (Dima et al. 2021). The four species mentioned above in sect. *Firmiores* have a more robust stipe and smaller spores. Three are known from Europe and North America: *C. acutispissipes*, *C. alboviolaceus*, and *C. paralbocyaneus* (Liimatainen et al. 2020, Landry et al. 2021). *Cortinarius alboviolaceus* is a more robust species compared to *C. anomalosimilis* with a pileus up to 90 mm wide, a larger stipe 50–120 mm long, 5–10 mm wide at apex, and up to 20 mm wide at base, and with generally smaller spores, 8.5–10 × 6–6.5 µm (Brandrud et al. 1990–2014). It is common in western North America. *Cortinarius acutispissipes* has a larger stipe, 40–80 mm long, 7–13 mm broad at apex, and 11–25 mm broad at base, an earthy odor, and it produces smaller, almost smooth to finely verrucose spores, 7–8.5 × 4–5.5 µm (R. Lebeuf, pers. obs.). It is the most common of the three transcontinental species in Québec, Canada. *Cortinarius paralbocyaneus* lacks ochraceous tones on the pileus and produces smaller, finely verrucose spores measuring 7.5–9 × 5.6 µm (Bidaud et al. 2002). *Cortinarius obliquus* has only been reported from North America thus far. It is a more robust species with a pileus 40–75 mm broad, a prominently marginate stipe 8–15 mm broad at apex and 16–26 mm broad at bulb, lamellae with a long-persistent dark violet color, an earthy odor, and smaller spores measuring 6.5–9 × 4.5–6 µm (R. Lebeuf, unpubl.).

One of the noticeable features of *C. anomalosimilis* is the large variation in spore size, shape and ornamentation observed in some collections. For example, in collection ISC-F-0135059, spores varied from 8.1 × 5.9 µm (Q = 1.37) to 14.8 × 6.7 µm (Q = 2.21), they were ellipsoid, oblong to subamygdaloid, smooth to strongly verrucose, and many were malformed with extended apiculus. Two-spored aborted basidia were also observed in that collection, which probably gave rise to the larger spores.

Authors: R. Lebeuf, R.A. Healy, J.F. Ammirati, J. Landry & G. Taylor

Basidiomycota, Agaricomycetes, Agaricales, Cortinariaceae

Cortinarius* subgenus *Telamonia

Cortinarius brunneoviscidus Lebeuf, Healy, Ammirati & J. Landry, **sp. nov.** – Fig. 5
MycoBank no.: MB 843005

Holotypus. – CANADA. Québec, Hinchinbrooke, Réserve écologique du Boisé-des-Muir, 45°05'07.0"N, 74°06'52.4"W, 67 m a.s.l., in an old-growth mixed forest, under *Fagus grandifolia* and *Acer* sp., 23 September 2012, *leg.* R. Lebeuf & A. Paul, HRL1296 (CMMF004500; holotype).

Description. – Pileus 30–80 mm in diameter, hemispherical then convex with a broadly deflexed and undulating margin, smooth, slightly viscid, hygrophanous, orange-brown (around 7E7) when humid, yellowish brown (around 5C6) when dried, with darker brown streaks, edge of margin decorated with a narrow band of white fibrils. – Lamellae emarginate, subdistant to close, pale cream at first, later light brown (café au lait), broad (up to 9 mm). – Universal veil white, sparse, evanescent. – Stipe 20–80 mm long, 8–15 mm thick at apex, up to 30 mm thick at base, clavate to bulbous, sometimes connate, white. – Context of pileus and stipe cream to pale brown. – Odor absent. – Exsiccatae pileus blackish brown, stipe greyish brown (6C4). – Basidiospores (7.5–)8.0–9.6(–13.3) × 4.5–5.9(–7.4) µm, av. 8.6 × 5.1 µm, Q = 1.41–1.96, Q_{av} = 1.68 [90/4/2], not dextrinoid, ellipsoid to subamygdaloid, moderately to ± coarsely verrucose, often more so at distal end. – Basidia 30–36 × 7–9 µm, 4-spored, clavate to narrowly clavate, colorless, becoming length brown to brown pigmented in age. – Lamellar trama hyphae not or only slightly encrusted. – Pileipellis duplex: epicutis a thin ixocutis, upper layer (veil) thin to moderately thick, made of

Fig. 5. *Cortinarius brunneoviscidus*. **a.** Basidiomata *in situ*, collection CMMF004500 (holotype). **b.** Basidiomata *in situ*, collection WTU-F-074618. **c.** Basidiospores. **d, e.** Pileipellis section in SDS Congo Red. Scale bars c, e 10 mm, d 25 µm. Photos R. Lebeuf (a), R. Healy (b).

narrow, cylindrical hyphae, mostly 2–6 µm wide, colorless to yellowish, smooth or spirally-encrusted; lower layer made of subparallel to slightly interwoven cylindrical hyphae, slightly gelatinized, mostly 2–6(–9) µm wide, colorless to yellowish brown with refractive walls, spirally-incrusted or smooth; hypocutis made of cylindrical hyphae to enlarged cells measuring 18–70 × 5–30 µm, enlarged cells generally smooth with a yellowish brown intraparietal pigment, and cylindrical hyphae often slightly or more coarsely encrusted. – Clamp connections present in all tissues. – Macrochemical reaction black on pileus surface with 10 % KOH.

Etymology. – Named for the color of the pileus and its viscidity, an unusual character in *Cortinarius* subgenus *Telamonia*.

Habitat and distribution. – Gregarious to caespitose in hardwood forests dominated by *Quercus*, *Carya* or *Fagus*, in the fall. So far known from only two sites, in Canada (Québec) and the USA (Iowa).

Additional material examined. – *Ibid.* (QFB29865; isotype). Sequences ex-isotype: MN751634 (ITS). – USA. Iowa, Webster County, Brushy Creek State Preserve, in upland hardwoods dominated by *Quercus rubra* and *Carya ovata*, 26 September 2006, *leg.* R. Healy (WTU-F-074618).

Notes. – The ITS sequence of *Cortinarius brunneoviscidus* is distinct from that of other members of subgenus *Telamonia*, deviating by more than 20 substitutions and indels from its closest relatives, *Cortinarius badioflavidus* Ammirati, Beug, Niskanen, Liimat. & Bojantchev (section *Hinnulei*) and *Cortinarius boulderensis* A.H. Sm. (section *Boulderenses*), and far away from somewhat phenotypically similar species in genus *Thaxterogaster* section *Multiformes* as defined by Liimatainen et al. (2022) (Fig. 4). *Cortinarius brunneoviscidus* is found in hardwood forests of *Carya*, *Quercus*, or *Fagus*. It has the general appearance of a phlegmacioid ow-

ing to its robust habit, slightly gelatinous pileus surface and clavate to bulbous stipe, but its hygrophanous pileus is characteristic of subgenus *Telamonia*.

Members of *Thaxterogaster* section *Multiformes* are similar in appearance but have a distinct gelatinous pileipellis. In *C. brunneoviscidus*, the gelatinous layer of the pileipellis is very thin and difficult to observe microscopically. The basidiospore ornamentation in section *Multiformes* usually consists of irregular, low, rounded and often confluent warts, which can appear rather diffuse in the microscope. In *C. brunneoviscidus* the basidiospores are ellipsoid to subamygdaloid and moderately to coarsely verrucose.

Authors: R. Lebeuf, R.A. Healy, J.F. Ammirati & J. Landry

Glomeromycota, Glomeromycetes, Diversisporales, Diversisporaceae

Diversispora alba Corazon-Guivin, G.A. Silva & Oehl, **sp. nov.** – Fig. 6
Mycobank no.: MB 845974

Diagnosis. – Spores white, 63–120 µm, with a four-layered spore wall. Differs from *Diversispora aurantia*, which has triple-layered, orange spores of similar size (70–120 µm); and from *D. spurca*, which has white spores of similar size (40–120 µm) but with two wall layers.

Holotypus. – PERU. San Martín State, Lamas Province, Paucarpata, 6°26'8.82"S, 76°31'52.1"W, 502 m a.s.l., in a coffee plantation, 15 March 2021, *leg.* M.A. Corzaon-Guivin (ZT Myc 66904; holotype). Derived from a bait culture established on the two host plants *Brachiaria brizantha* and *Sorghum vulgare* in the greenhouse of the Universidad Nacional de San Martín.

Description. – Spores formed terminally on subtending hyphae (SH) singly; white, globose to subglobose to rarely oblong or irregular, (63–)70–102(–125) × (63–)70–102(–120) µm. – Spore wall with four layers; outer layer (SWL1) hyaline to subhyaline, evanescent, 0.6–1.2 µm thick, often partly degraded giving a roughening appearance of the outer spore surface, where in addition some soil debris might stick on; second layer (SWL2) also hyaline to subhyaline, semi-evanescent, and 0.6–1.2 µm thick, both SWL1 and SWL2 layers, when intact, often ballooning in lactic acid and might easily separate from each other, while ballooning; third layer (SWL3) structural, persistent, laminate, white, 2.6–4.1(–4.9) µm thick; innermost layer (SWL4) flexible, white, 0.5–1.2 µm thick, usually tightly adherent to

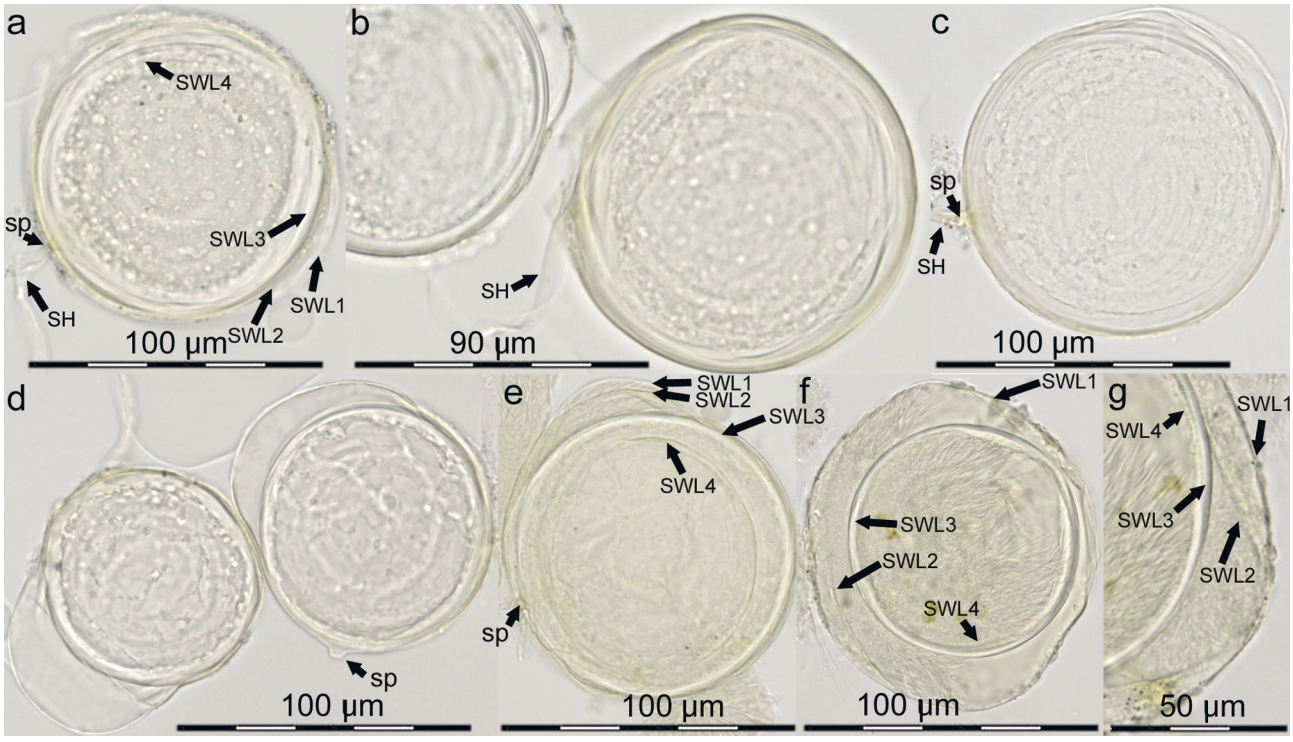

Fig. 6. *Diversispora alba*. **a–f.** Uncrushed spores with a four-layered spore wall (SWL1–4), a single, cylindrical subtending hypha (SH), and a septum (sp) arising directly or at some distance from the base. SWL1 and SWL2 partially or completely ballooning from the laminate SWL3. **f–g.** Crushed spore to show the four-layered spore wall. SWL1 in degradation stages covered with some debris. None of the layers stains in the 1:1 mixture of PVLG and Melzer's reagent.

SWL3, sometimes separating or showing several folds in crushed spores, SWL3 and SWL4 often resembling endospore, without continuing into the subtending hypha; no layers staining in Melzer's reagent. – Subtending hyphae (SH) cylindrical to slightly funnel-shaped or slightly constricted, sometimes recurved, 5.0–9.2 µm broad and 15–40 µm long; only SWL1 and SWL2 continue, as SHL1 and SHL2, on subtending hyphae towards the mycelia hyphae, tapering from 1.2–2.4 µm to 0.6–1.2 µm within the first 5–10 µm from the base causing the flexible fragile portion of the SH to break from the mature spore where the septum separates the spore contents from the hyphal contents; SWL2, SWL3, or both layers, close spore pore at spore base, but more commonly within the subtending hyphae in a short distance from the spore base (1.5–5.0 µm); SH layers not staining in Melzer's reagent. – Arbuscular mycorrhizal formation not observed thus far.

Etymology. – Referring to the white spores.

Habitat and distribution. – Found in trap cultures inoculated with rhizosphere soils and root fragments of coffee, and in pot cultures with *Brachiaria brizantha* and *Sorghum vulgare*. Thus far known from Lamas Province, Peru. Environmental sequences from Japan and the USA indicate a broader distribution.

Additional material examined. – *Ibid.* (ZT Myc 66905, isotype). Sequences ex-isotype: OP195880–OP195885 (partial SSU–ITS–partial LSU). – PERU. San Martín State. Lamas Province, Pamashto, 6°21'8.59"S, 76°32'15.66"W, 831 m a.s.l., 15 March 2021, *leg.* M.A. Corzaon-Guivin (ZT Myc 66906).

Notes. – *Diversispora alba* can be easily distinguished from all other species in the Diversisporales by diversisporoid spore formation singly in rhizosphere soils or inside roots, the white spores, and the four spore wall layers. In the genus *Diversispora*, only three other species are known that have four spore wall layers: *D. aestuarii* Błaszk., B.T. Goto, Niezgoda & Magurno, *D. sporocarpia* Chachuła, Mleczko, Zubek, Niezgoda, A. Kozłowska, Jobim, B.T. Goto & Błaszk., and *D. valentina* A. Guillén, Serrano-Tamay, Peris & I. Arrill. (Jobim et al. 2019, Guillén et al. 2020, Błaszkowski et al. 2022). However, these three species all form pigmented spores, i.e., yellow to yellowish-brown in *D. aestuarii*, yellow to light brown in *D. sporocarpia*, and orange to dark brown in *D. valentina*.

BLAST searches of the SSU–ITS–LSU sequences of *D. alba* resulted in *D. aurantia* and *D. spurca* as closest matches with ~96 % shared identity. The phylogenetic analyses based on partial SSU–ITS–partial LSU placed multiple isolates of the new species in a separate clade with high support, sister to *D. aurantia* (Błaszk., Blanke, Renker & Buscot) C. Walker & A. Schüßler and *D. spurca* (C.M. Pfeiff., C. Walker & Bloss) C. Walker & A. Schüßler (Fig. 7). LSU environmental sequences with >97 % shared identity with *D. alba* were obtained from rhizosphere soil of *Elymus mollis* (Poales, Poaceae) in Japan (GenBank accession no. AB640743), roots of *Miscanthus sinensis* (Poales, Poaceae) in Japan (AB561118), and soil from hardwood forest in Michigan, USA (Castillo et al. 2018). ITS environmental sequences with >97 % shared identity with *D. alba* have not been found thus far. Three ~1500 bp AM fungal sequences from switchgrass soil in Wisconsin, USA (GenBank accession nos. MT765585, MT765635, MT765658), referred to as *D. aurantia* by Dirks & Jackson (2020) represent the fungus described here, as they were retrieved in the *D. alba* clade among our Peruvian isolates (Fig. 7). It can be concluded that *D. alba* has a wide geographical distribution and may occur in a wide range of different habitats, as is known for many other *Diversispora* species.

Phylogenetically, *D. alba* is closely related to *D. aurantia*, which, however, forms orange spores with a three-layered spore wall (Błaszkowski et al. 2004), and to *D. spurca*, which forms whitish, but double-layered spores (Kennedy et al. 1999). *Diversispora spurca* is described to incorporate large amounts of debris on the spore surface during degradation of the evanescent outer spore layer. This can also be observed in *D. alba* but to a much lower degree. On the other hand, *D. alba* shares with *D. aurantia* the ballooning nature of the outer spore wall layer, which in *D. alba* may also include the second layer SWL2.

Diversispora alba is the eleventh species of Glomeromycota described from the Peruvian Amazon region (Corazon-Guivin et al. 2019a, 2019b, 2019c, 2019d, 2022a, 2022c; Song et al. 2019; Lebeuf et al. 2022) after *Acaulospora aspera* Corazon-Guivin, Oehl & G.A. Silva, *A. flava* Corazon-Guivin, G.A. Silva & Oehl, *A. flavopapillosa* Corazon-Guivin, G.A. Silva & Oehl (Diversisporales, Acaulosporaceae), *Funneliglomus sanmartinense* Corazon-Guivin, G.A. Silva & Oehl, *Microkamienskia peruviana* Corazon-Guivin, G.A. Silva & Oehl, *Nanoglomus plukenetiae* Corazon-Guivin, G.A. Silva & Oehl, *Rhizoglomus cacao* Corazon-Guivin, G.A. Silva & Oehl, *R. variabile* Corazon-Guivin, Oehl & G.A. Silva (Glomerales, Glomeraceae), *Paraglomus occidentale* Corazon-Guivin, G.A. Silva & Oehl, and *P. peruvianum* Corazon-Guivin, G.A. Silva & Oehl

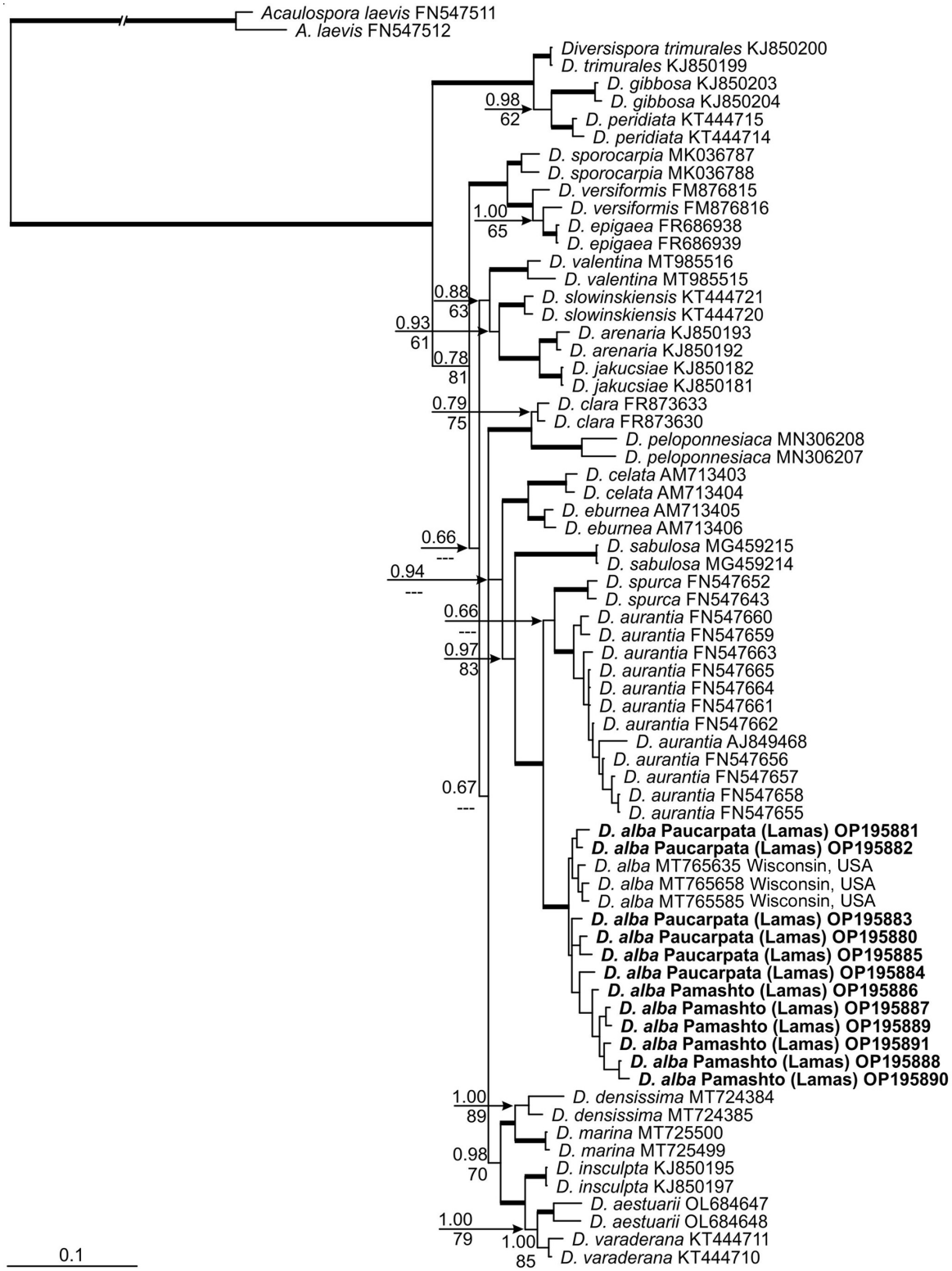

Fig. 7. Phylogeny of *Diversispora* reconstructed from a partial SSU–ITS–partial LSU dataset. *Acaulospora laevis* served as outgroup. For each node, MLBS ≥60 and BI posterior probability (BIPP) ≥0.60 values are presented, as MLBS/BIPP. Thick branches represent clades with more than 90 % of support in both analyses. Sequences labeled with their GenBank accession numbers, sequences obtained in this study highlighted in boldface.

(Paraglomerales, Paraglomeraceae). To our knowledge, only one other species has thus far been described from other parts of the Amazonian rainforest in South America, *Sclerocarpum amazonicum* Jobim, Błaszk., Niezgoda, A. Kozłowska & B.T. Goto (Jobim et al. 2019).

Authors: M.A. Corazon-Guivin, A. Vallejos-Tapullima, V.M. Santos, G.A. da Silva & F. Oehl

Basidiomycota, Agaricomycetes, Agaricales, Inocybaceae

Inocybe nigroumbonata Naseer & Khalid, **sp. nov.** – Figs. 8, 9
MycoBank no.: MB 843794

Holotypus. – PAKISTAN. Khyber Pakhtunkhwa Province, Swat District, Shawar valley, 2100 m a.s.l., solitary on soil under *Quercus incana*, 14 July 2014, *leg.* A. Naseer & A.N. Khalid, ASSW38 (LAH35272; holotype). Sequences ex-holotype: ON262107 (ITS).

Description. – Pileus 2.0–2.9 cm diameter, at first conical, then expanded to convex, with large pronounced umbo, radially fibrillose of black color when young, margins slightly incurved, fimbriated, cracked; greyish black fibrils when young, then light brown (3.3Y 5.8/6.2) with creamy white fibrils (7.1Y 7.3/7.1), paler between the spreading fibrils, black color confined to umbo only with maturity, black to greyish black umbo (6.1G 6/6), cortina not observed. – Lamellae moderately crowded (approx. 35–45, lamellulae = 1–3), narrowly adnate, subdistant, (sub)ventricose, regular, pale pink, concolorous, one tier of lamellulae. – Stipe 3.5–4 × 0.3–0.5 cm, central, cylindrical with distinct marginate to rounder basal bulb 0.4–0.6 cm wide; entirely pruinose, curved, brownish orange (8.7 GY 5.5/5), silvery white (4.3 GY 7.1/1.4) at apex and base, creamy white in bulb. – Odor mild, not remarkable. – Basidiospores (7.2–)7.4–9.3(–9.9) × (5.0–)5.2–7.1(–7.6), av. 8.29 × 5.92, Q = (1.1–)1.2–1.5(–1.6), Q_{av} = 1.40, nodulose, thin-walled, apiculus small and distinct, pale brown to yellowish brown in 5 % KOH. – Basidia 22.7–22.8 × 9.0–9.6 µm, clavate, usually four-spored, thin-walled, guttutaled, hyaline in 5 % KOH, long sterigmata, up to 2.2–6.3 µm. – Cheilocystidia 46.8–59.1 × 17.21–22.5 µm, fusiform to utriform, light green in 5 % KOH, metalloids, with crystalliferous apex. – Pleurocystidia similar to cheilocystidia, different in color and size, 30–60 × 15.5–30.0 µm, hyaline in 5 % KOH. – Caulocystidia 40.8–68.5 µm, variable, utriform, some broadly clavate, metuloids, thick-walled, with crystalliferous apex. – Caulo-paracystidia present below the mid-region of the stipe, slender to subcylindrical, hyaline in 5 % KOH, thin-walled. – Pileipellis a cutis of cylindrical hyphae, 3.2–4.7 µm diameter, yellowish brown in 5 % KOH, thin-walled, septate, encrusted. – Stipitipellis a cutis of cylindrical hyphae, 2.9–4.0 µm diameter. – Clamp connections frequently present.

Additional material examined. – PAKISTAN. Khyber Pakhtunkhwa Province, Swat District, Matta, 2000 m a.s.l., solitary on soil under *Quercus incana*, 15 July 2018, *leg.* A. Naseer & A.N. Khalid, ASSW40 (LAH35277).

Habitat and distribution. – Thus far only known under *Quercus incana* from Khyber Pakhtunkhwa Province, Pakistan.

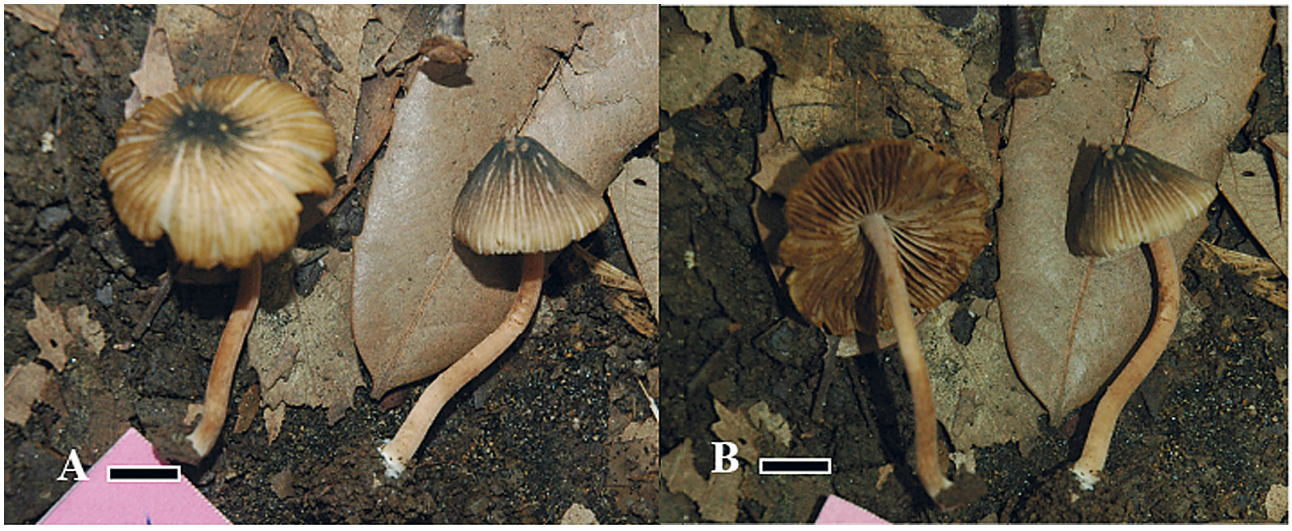

Fig. 8. *Inocybe nigroumbonata*. **A, B.** Basidiomata *in situ*. Scale Bars 0.87 cm.

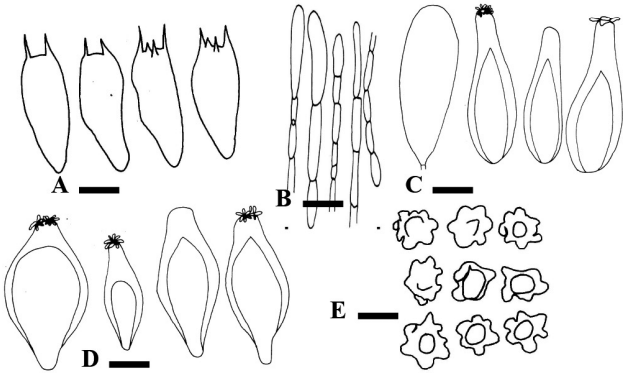

Fig. 9. Micromorphological characteristics of *Inocybe nigroumbonata*, collection LAH35272 (holotype). **A.** Basidia. **B.** Pileipellis. **C.** Cheilocystidia; **D.** Pleurocystidia. **E.** Basidiospores. Scale bars A–D 8.8 µm, E 7.86 µm.

Notes. – Around 40 species of *Inocybe* sensu lato have thus far been reported from Pakistan (Naseer et al. 2019, Jabeen & Khalid 2020, Saba & Khalid 2020, Saba et al. 2020, Khan et al. 2022, this study). *Inocybe nigroumbonata* is characterized by the combination of the following morphological characteristics: basidiomata medium-sized; pileus light brown, with a black umbo and radial greyish-black fibrils; pale pink lamellae; stipe pruinose, brownish-orange, with apex and base silvery white, and bulb creamy white with tightened adhered soil; basidiospores nodulose, measuring 7.4–9.3 × 5.2–7.1 µm; and basidia clavate, measuring 22.7–22.8 × 9.0–9.6 µm. The phylogenetically closest relatives of *I. nigroumbonata* are *I. calida* Velen. and *I. parvibulbosa* E. Horak, Matheny & Desjardin (Fig. 10).

Inocybe calida and *I. nigroumbonata* are morphologically similar, particularly in the shape and size of basidiomata, pruinose stipe, and nodulose basidiospores. *Inocybe nigroumbonata*, characterized by a pileus that is radially fibrillose and colored light brown with a black umbo. In contrast, *I. calida* has a rimulose, reddish-brown, umbonate pileus. *Inocybe nigroumbonata* is further distinguished by its brownish-orange stipe, with slightly clavate bulb with tightly adhering soil (Horak et al. 2015). Microscopically, *I. nigroumbonata* has longer basidiospores compared to *I. calida* (7.4–9.3 µm vs. 5.6–87.1 µm) and shorter, clavate basidia (22.7–22.8 µm vs. 23–28 µm). *Inocybe parvibulbosa* can be easily differentiated from *I. nigroumbonata* by its very small size (pileus diameter 0.6–1.8 cm vs. 2.0–2.9 cm in *I. nigroumbonata*), cinnamon brown to dark hazel brown pileus (vs. light brown with black umbo and radial greyish-black fibrils), and cinnamon lamellae (vs. pale pink). In addition, *I. parvibulbosa* has thus far only been found in association with *Dipterocarpus obtusifolius* and *Tectona grandis* in Thailand (Horak et al. 2015).

Authors: A. Naseer & A.N. Khalid

Basidiomycota, Agaricomycetes, Agaricales, Mycenaceae

Mycena amoena Jagers, Aronsen, Holzapfel & Nuytinck, **sp. nov.** – Figs. 11–13
MycoBank no.: MB 842232

Diagnosis. – Differs from *Mycena lasiopus* by its smaller size, pale grey to white pileus, small granulose not lamellate basal disc, more conspicuously lobed cherocytes covered with warts and spinulae, completely spinulose caulocystidia, and very few cheilocystidia and clamps.

Holotypus. – THE NETHERLANDS. Overijssel Province, Enschede, Boeldershoek, 52°13'26.7"N, 6°47'37.4"E, 25 m a.s.l., 9 May 2019, *leg.* M. Jagers, MJD19019 (L0607542; holotype). Sequences ex-holotype: OL772667 (ITS).

Description. – Pileus up to 2.0(–2.3) mm diameter, initially paraboloid, expanding to obtusely conic or broadly convex in age; young covered all over with groups of grey to dark grey (sometimes nearly blackish grey) 'sugar-like' granules on a pale grey surface, mature white, still bearing small amounts of granules especially in the center, translucent-striate, margin crenulate, old very thin-fleshed, translucent. – Lamellae subventricose to ventricose, adnexed to narrowly adnate, with lamellulae of variable length, (6–)8–10 reaching the stipe, white. – Stipe 8–20 × 0.08-0.2 mm, central, filiform, hirsute, watery grey to watery white, at the base slightly inflated, with a small basal disc, not always easily seen and sometimes apparently absent; disc margin granulose. – Primordia hemispherical to paraboloid, covered with dark grey granules, initially forming a closed layer, soon breaking up to a non-contiguous layer upon a light grey surface, more whitish at the margin; dried dark grey. – Smell and taste insignificant. – Basidiospores 7.3–8.7–10.2 × 3.9–4.7–5.5 µm, Q = 1.54–1.87–2.19, Q_{av} = 1.81–1.91 [100/5], ellipsoid, smooth, hyaline, thin-walled, amyloid. – Basidia 9–20 × 7–10 µm, short clavate to obpyriform, 4-spored, rarely 2-spored, sterigmata 2–4 µm long. – Cheilocystidia very sparse or absent, 8–24 × 5.5–13 µm, clavate to broadly clavate, sparsely spinulose in the upper part but more densely spinulose near the pileus margin; spinulae 0.5–1.0 × 0.5 µm, cylindrical to subconical. – Pleurocystidia absent. – Pileipellis a cutis with acanthocysts and cherocytes; hyphae 1.5–13 µm diameter, spinulose or smooth, dextrinoid. – Central acanthocysts globose, subglobose, thin-walled, 8–22 ×

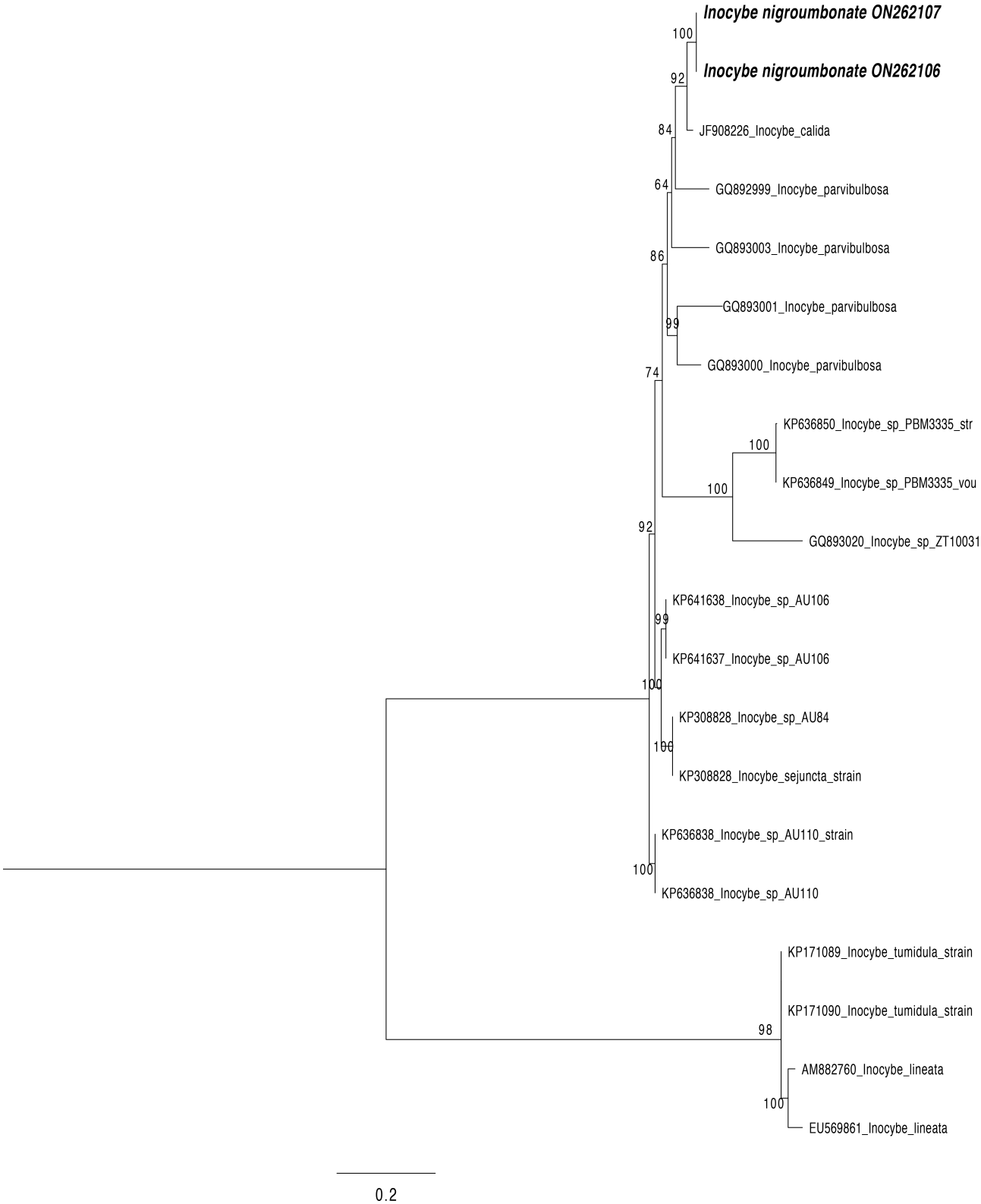

Fig. 10. Phylogeny of selected species of *Inocybe* reconstructed from a single-locus dataset including ITS sequences only. The topology is the result of ML inference with RAxML. MLBS values (if ≥70) are shown at the nodes. The new species, *I. nigroumbonata*, is highlighted in boldface.

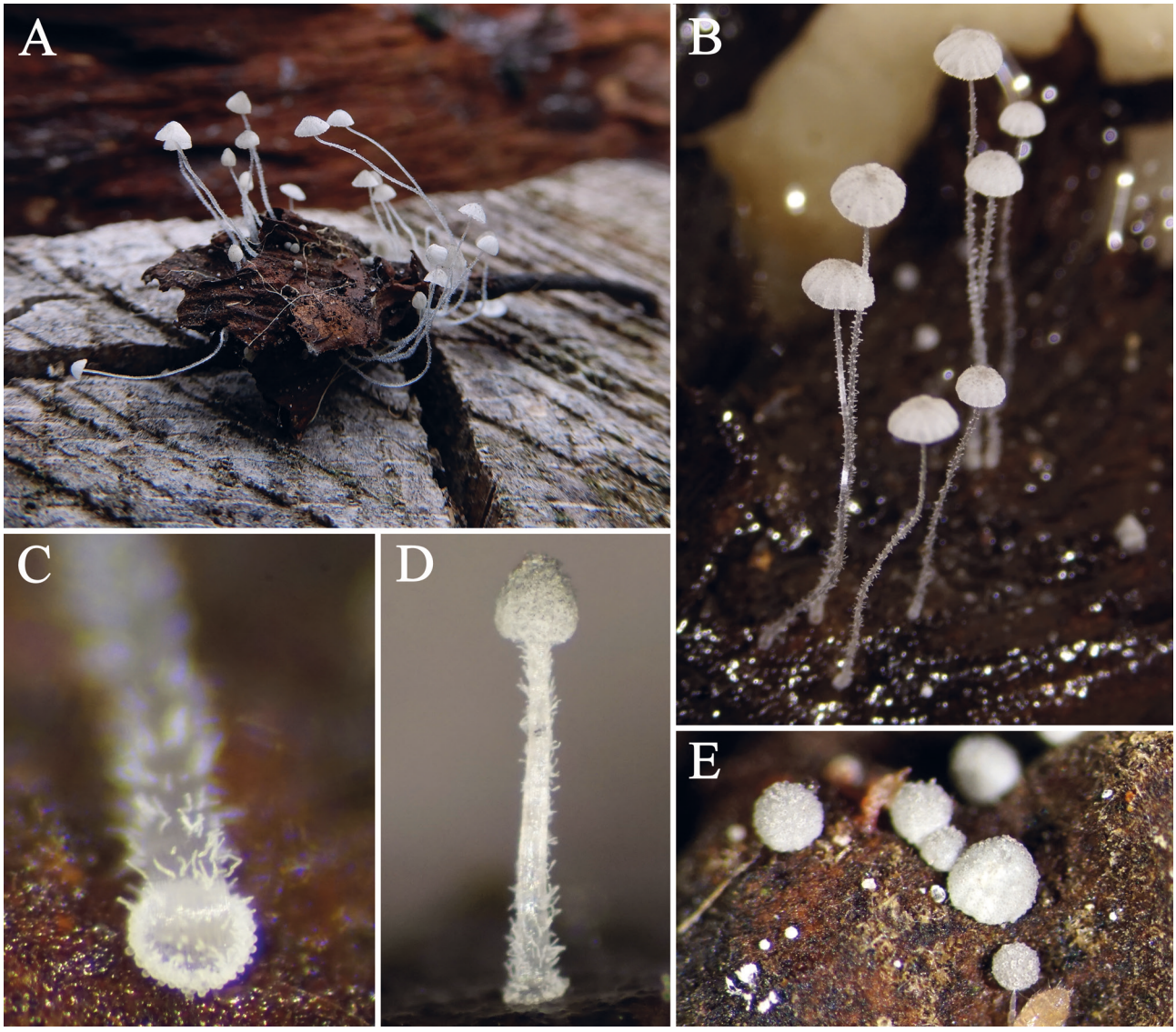

Fig. 11. *Mycena amoena*, collection L0607542 (holotype). **A–B.** Basidiomata *in situ*. **C.** Young basidioma in detail. **D.** Stipe base in detail. **E.** Primordia.

9.0–19.5 µm, densely spinulose, grey-brown, grey, or hyaline, inamyloid, sometimes seen originating from septate, thin-walled, smooth or spinulose hyphae of about 3 µm diameter; spinulae 0.5–1.0 × 0.5–1.5 µm, cylindric or subconical. – Marginal acanthocysts clavate, broadly clavate, ovoid, or subglobose, thin-walled, 11–28 × 8–13 µm, densely spinulose, grey or hyaline, inamyloid, spinulae 0.5–1.0 × 0.5–1.5 µm, cylindrical or subconical. – Cherocytes roundish to obtuse angular, with 2–6(–7) obtuse or obtusely conical lobes and with dark grey brown, slightly dextrinoid, vacuolar contents, covered with spinulae and warts; 9–28 × 9–25 µm (disregarding lobes), thick-walled, walls grey or hyaline, up to 5 µm, lobes extending up to 11 µm, warts hemispherical, 0.5–2.5 × 0.5–3.0 µm, often seen originating from septate, slightly thick-walled, smooth or spinulose hyphae of about 3 µm diameter. – Hypodermium composed of inflated hyphae up to 28 µm diameter, dextrinoid. – Lamellar trama composed of inflated hyphae up to 18 µm, dextrinoid. – Cortical and medullary hyphae of the stipe 3–19 µm diameter, parallel, smooth, dextrinoid. – Basal disc cystidia globose to subglobose, spinulose, connected to the stipe base by a dense layer of short, smooth or spinulose cells from about 3–5 × 6 µm, partly loosening with age; 9–23 × 6–20 µm diameter,

grey or hyaline, inamyloid; spinulae 0.5–1.0 × 0.5 µm, cylindrical, conical, or subconical. – Caulocystidia abundant, 9–142 × 4.5–16 µm, hyaline, thin-walled, inamyloid, ranging from short and broadly clavate or subcylindrical to long and cylindrical, apex even or somewhat wider, obtuse, densely and evenly spinulose overall, spinulae 0.5–1.0(–2.0) × 0.5–1.0 µm, cylindrical or subconical. – Clamp connections present but very rare, only seen at the base of a few basidia.

Etymology. – *Amoenus* (Latin), referring to the graceful basidiomata.

Habitat and distribution. – Scattered or gregarious on nuts and husks (seldom on leaves) of *Corylus avellana* from May to the end of October. Known only from type locality in the Netherlands.

Additional material examined. – *Ibid.*, 9 June 2018, *leg.* M. Jagers (L0607541); 1 May 2020, *leg.* M. Jagers (L0607543); 6 June 2021, *leg.* M. Jagers (L0607544).

Notes. – Species belonging to *Mycena* section *Sacchariferae* Kühner ex Singer are recognizable by their small size, granular ('sugar coated') pileus and hairy stipe (Desjardin 1995). The presence of a universal veil, a unique feature of the members of this section and best observed on primordia, provides the ornamented surface of the pileus. Desjardin (1995) provisionally subdivided sect. *Sacchariferae* into three stirpes, based on the shape of the veil cells, shape of the caulocystidia and the presence or absence of a basal disc. These are *Adscendens* Desjardin, *Alphitophora* Desjardin, and *Amparoina* Desjardin. Species in stirps *Adscendens* and *Alphitophora* have a veil consisting of thin-walled cells, named acanthocysts. Species in stirps *Adscendens* have smooth caulocystidia and a basal disc, whereas species in stirps *Alphitophora* have spinulose caulocystidia and no basal disc. Species in stirps *Amparoina* have a veil consisting of thick-walled cells, named cherocytes, and spinulose caulocystidia. A basal disc may be present or not. Maas Geesteranus & de Meijer (1998) suggested a fourth stirps, *Fuscinea* nom. prov., whose two members only differ from those in stirps *Alphitophora* by the dark content of their acanthocysts. Desjardin (1995) described the cherocytes of stirps *Amparoina* as variously shaped, densely spinulose, with 1–12 thick-walled, spine-like projections, varying between species. He accepted eight species and two varieties in stirps *Amparoina*. In the course of time, 16 new species were added (Maas Geesteranus & de Meijer 1997, 1998; Desjardin et al. 2007; Bougher 2009; Aravindakshan & Manimohan 2015; Cooper et al. 2018; Cortés Pérez et al. 2019; Na & Bau 2019a). Desjardin (1995) already included an exception in stirps *Amparoina*, *M. sotae* Singer, a species that has lobed or irregularly-shaped acanthocysts without spine-like projections. This placement encouraged some of the aforementioned authors to include some of their new species, with a veil consisting of cherocytes without spines, into stirps *Amparoina* (Maas Geesteranus & de Meijer 1998, Aravindakshan & Manimohan 2015, Cooper et al. 2018). To date, little phylogenetic research has been done on the species belonging to *Mycena* sect. *Sacchariferae*. Some recent phylogenetic studies, in which only a few species from the section were included, showed a clear separation between stirps *Adscendens* on the one hand and stirps *Alphitophora* and *Amparoina* on the other (Cooper et al. 2018, Na & Bau 2019a). In a subsequent study, Na & Bau (2019b) introduced a new section based on both molecular phylogenetic reconstruction and morphological characters: *M.* sect. *Amparoina* T. Bau & Q. Na. This section consisted of stirps *Alphitophora* and stirps *Amparoina* (containing only two species), next to sect. *Sacchariferae* consisting of stirps *Adscendens* only.

In our phylogenetic analysis, a well-supported monophyletic stirps *Alphitophora* was similarly recovered, but stirps *Amparoina* as defined by Na & Bau (2019a, 2019b) was not (Fig. 14). This is largely due to the placement of *M. castaneicola*, formerly a member of stirps *Amparoina* (Na & Bau 2019a), on an earlier-diverging branch with respect to stirps *Alphitophora* and the clade containing the remainder of analysed species or species placed in stirps *Amparoina*. Although this split was well-supported by ML, it only received marginal support by BI (MLBS = 100, BIPP = 0.85). Therefore, we see no merit in subdividing sect. *Amparoina* into stirpes *Alphitophora* and *Amparoina* at this time. Subsequent authors should carefully consider the taxonomic value and continued use of the aforementioned stirpes, perhaps supported with more comprehensive phylogenetic analyses.

Mycena species belonging to sect. *Sacchariferae* and sect. *Amparoina* can be found all over the world. According to the various descriptions, those species from sect. *Amparoina* that have a veil consisting of cherocytes, all prefer a tropical or subtropical climate. They were only recorded in Europe from tropical greenhouses (Robich 2007, Gubitz 2012, Brodegger et al. 2019). However, in 2018 and subsequent years we found basidiomata of *M. amoena* on fallen nuts and husks of several *Corylus avellana* shrubs, planted in 1996. On many nuts basidiomata of *Mycena tenerrima* (Berk.) Quél. (= *M. adscendens* Maas Geesteranus) were collected (col-

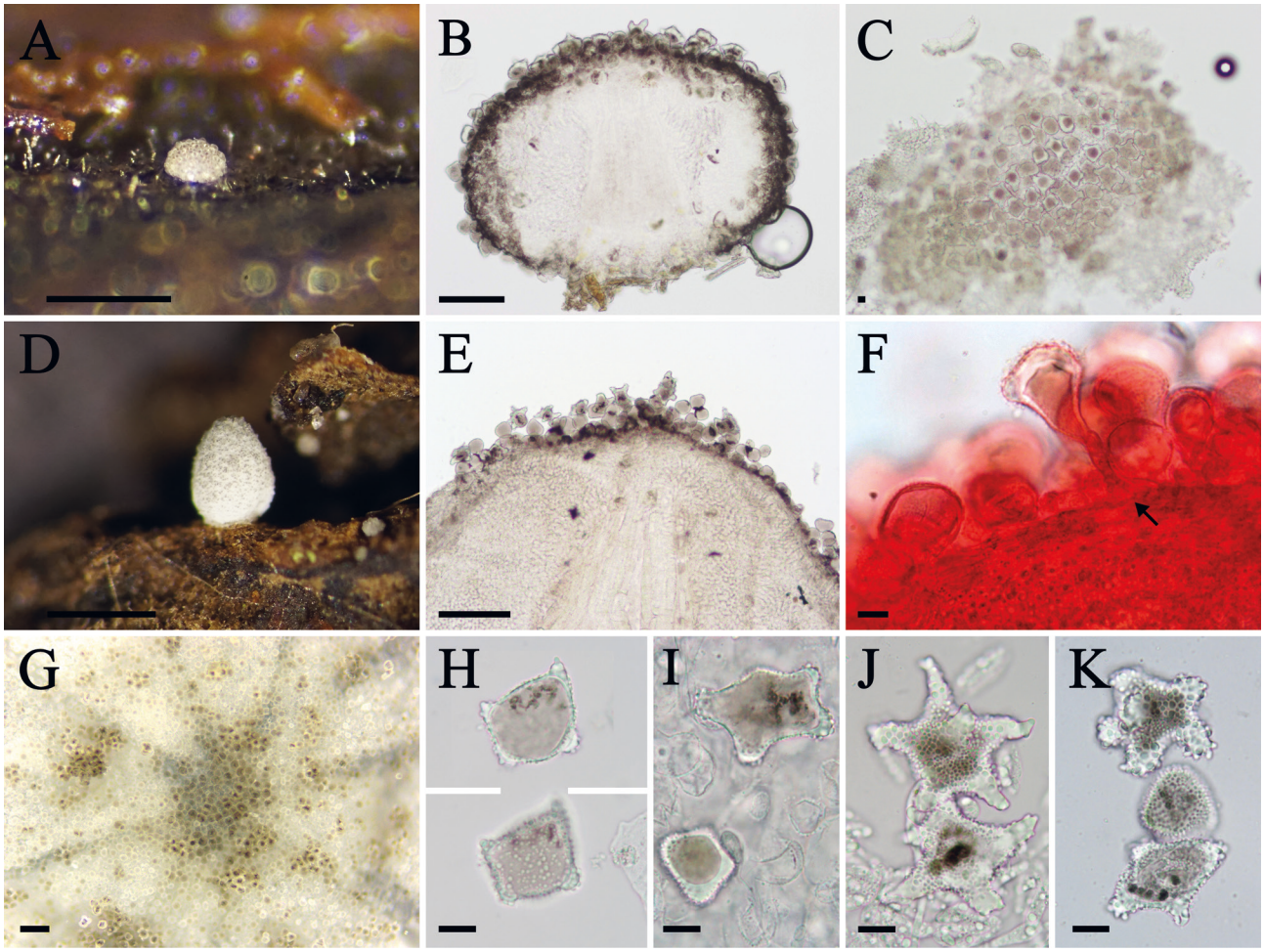

Figs. 12. *Mycena amoena*, cherocytes. **A.** Primordium of ~ 0.05 mm in diameter. **B.** Vertical section primordium of ~ 0.05 mm in diameter, in water, showing a veil consisting of cherocytes. **C.** Scalp of the top of a primordium of ~ 0.05 mm in diameter, in water. **D.** Primordium ~ 0.8 mm in diameter. **E.** Vertical section primordium ~ 0.8 mm in diameter, in water, showing cherocytes and acanthocysts. **F.** Cherocyte connected to the pileipellis by a hypha, in Congo red. **G.** Pileus center of a mature basidioma seen from above. **H.** Two pictures of the same cherocyte; above inside, a grey-brown colored vacuole surrounded by a thick-walled, lobed wall, below outside, covered with warts, in water. **I.** Two differently shaped cherocytes showing a grey-brown colored vacuole surrounded by a thick-walled, lobed wall, in water. **J–K.** Some strikingly formed cherocytes, especially seen on primordia, in water. Scale bars A 100 µm; B, C 10 µm; D 1 mm; E, F = 10 µm; G 100 µm; H–K 10 µm.

lection number L0607549, 16 June 2019, leg. M. Jagers). Primordia of both species even appeared at a distance of just one mm. Basidiomata of *M. tenerrima* can be distinguished from those of *M. amoena* in being taller, having white to light grey veil cells, finer hairs on the stipe, and a rather well-developed, hirsute basal disc. More significantly, they lack cherocytes and have smooth caulocystidia and elongated basal disc cystidia.

Our phylogenetic analysis covered a total of 69 ITS sequences, 60 of which belong to species of sect. *Sacchariferae* and sect. *Amparoina* (Tab. 1), including two newly generated sequences from *M. amoena* (L0607542, holotype; L0607541), three from *M. tenerrima* (L0607549, L0607550, L0607551), one from *M. chloroxantha* Singer var. *chloroxantha* from 1997 (L0063621, Maas Geesteranus & de Meijer 1997), and one from type material of *M. capillata* Maas G. & de Meijer (L0063217, holotype; Maas Geesteranus & de Meijer 1998). In accordance with Na & Bau (2019b), sect. *Amparoina* was recovered as a monophyletic lineage separate from sect. *Sacchariferae* sensu Na & Bau (Fig. 14). Based on both pairwise identity and phylogenetic placement, the phylogenetically closest related species to *M. amoena* are *M. melanovelis* Traba, Couciero & M. Villareal nom. prov. (Traba-Velay et al. 2021) and *M. lasiopus* BAP635 (and BAP603, Cooper et al. 2018). As

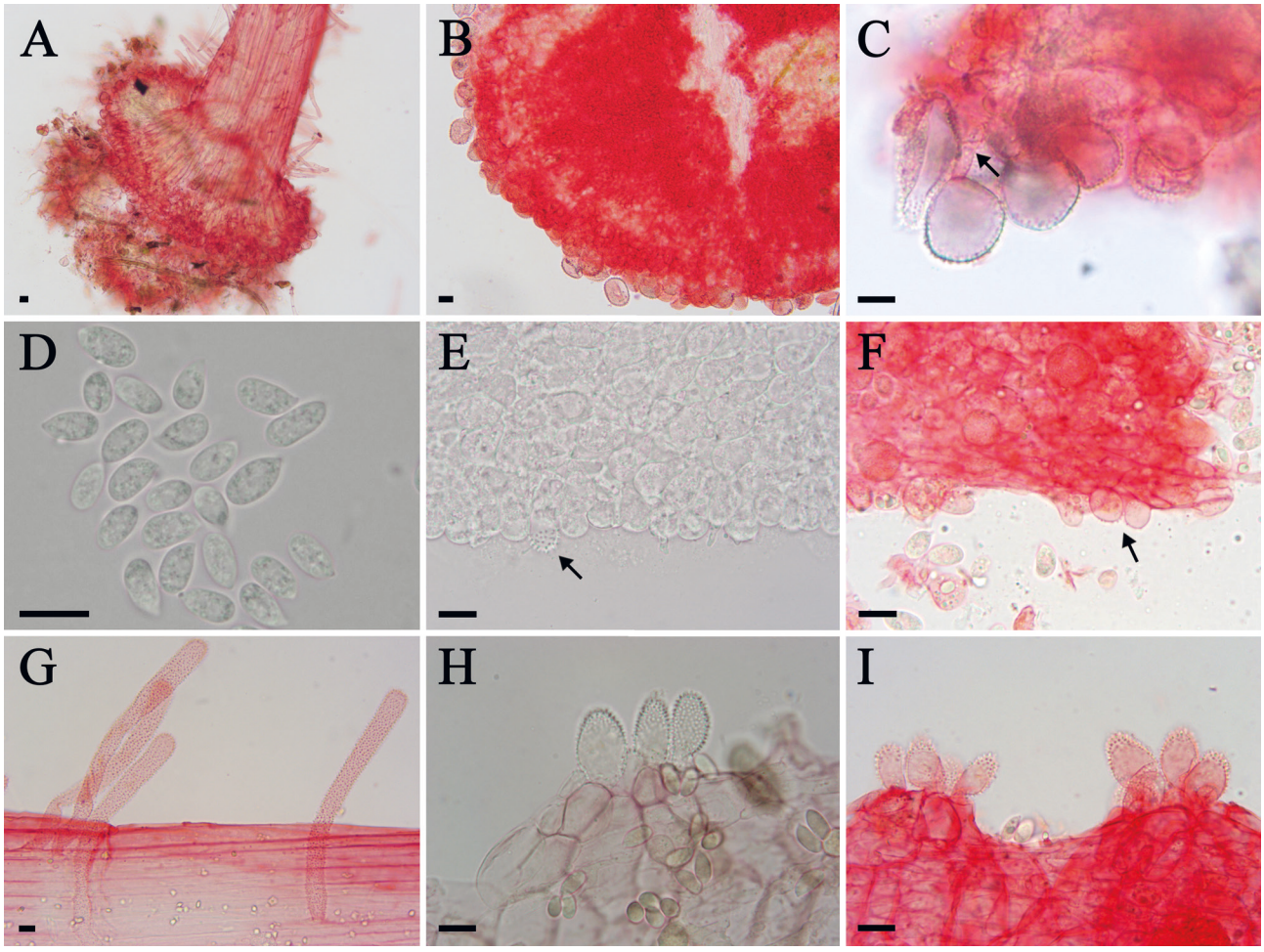

Fig. 13. *Mycena amoena*, micromorphological characteristics. **A–B.** Basal disc cystidia in Congo red. **C.** Basal disc cystidium connected by a hypha (arrow). **D.** Basidiospores in water. **E.** Cheilocystidium on lamellar edge (arrow), in water. **F.** Cheilocystidia on lamellar edge (arrow), in Congo red. **G.** Caulocystidia in Congo red. **H.** Pileipellis marginal acantohocysts in Melzer's reagent. **I.** Pileipellis marginal acanthocysts in Congo red. Scale bars 10 µm.

expected, *M. chloroxantha* var. *chloroxantha* L0063621 and the holotype of *M. capillata* (L0063217) are similarly placed in sect. *Amparoina*, the former being closest related to *M. chloroxantha* var. *appalachiensis* KL-BK 59708. *Mycena alphitophora* BAP591 from São Tomé and Principe does not belong to the same species as *M. alphitophora* HMJAU 43498 and HMJAU 43686, which had already been noticed by Cooper et al. (2018).

At the time of writing, the ITS sequence of *M. alphitophora* BAP591 is the most divergent and most difficult to align among all publicly available ITS sequences from species and collections placed in sect. *Amparoina*. It is represented by the most unstable branch in all iterations of the phylogenetic tree, which makes its true phylogenetic placement rather uncertain. In our phylogenetic tree, several species placed in the larger clade containing *M. amoena, M. chloroxantha*, and *M. heteracantha*, among others, lack basal discs (Fig. 14): *M. chloroxantha* var. *appalachiensis* KL-BK 59708 (Brodegger et al. 2019), *M. castaneicola* (Na & Bau 2019a), and the recently described provisional species *M. eucalypticola* Traba, Couceiro & M. Villarreal nom prov., *M. lourensis* Traba, A Cortés-Pérez, Couceiro & M. Villarreal nom. prov., and *M. melanovelis* nom. prov. (Traba-Velay et al. 2021). Remarkably, collections from China identified as *M. heteracantha* (HMJAU 43709, HMJAU 43716, HMJAU 43693) were observed possessing basal discs (Na & Bau 2019b, 2020) while according to Singer (1976) and Desjardin (1995), *M. heteracantha* should lack a basal disc. Cherocytes may or may not have colored vacuolar contents, as is the case within the clade containing

M. amoena and the closely related species *M. melanovelis* nom. prov. and *M. lasiopus*. However, the presence of cherocytes with vacuolar contents may not be entirely phylogenetically informative, as *M. oboensis* is not closely related to other species who share this trait (Fig. 14). *Mycena oboensis* is, like *M. amoena*, a small species with a small basal disc with cherocytes that are covered with warts but differs

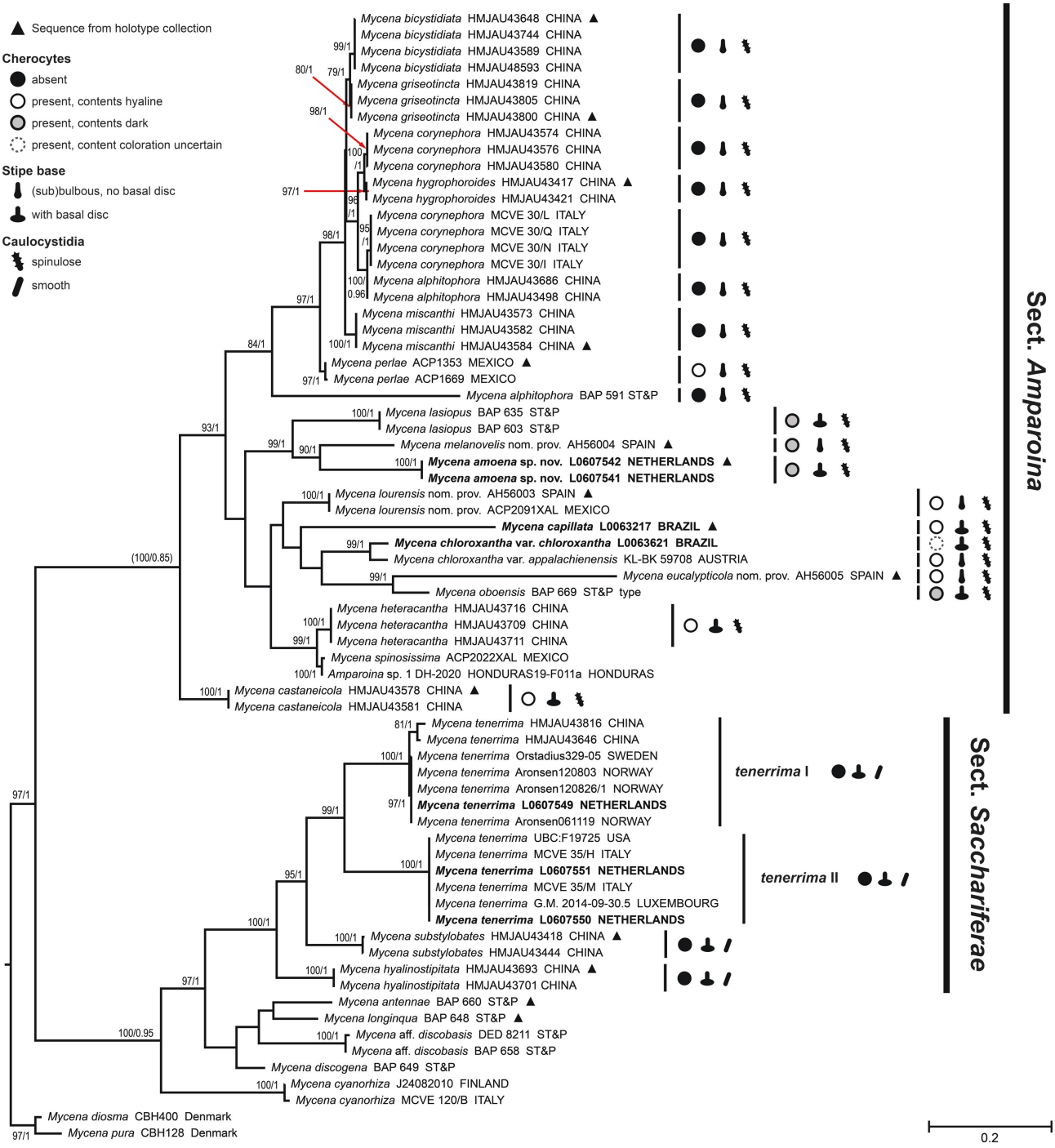

Fig. 14. Phylogeny of selected *Mycena* species, with emphasis on sect. *Amparoina* and sect. *Sacchariferae*, reconstructed from an ITS dataset. *Mycena diosma* and *M. pura* were selected as outgroup taxa. MLBS ≥70 and BIPP ≥0.90 are shown on or near branches (MLBS/BIPP). Newly obtained sequences shown in boldface, ex-holotype sequences indicated with black triangles (▲), some morphological features shown for species in *Mycena* sect. *Amparoina* and sect. *Sacchariferae*. ST&P: São Tomé and Príncipe.

from *M. amoena* in having two-spored basidia, smaller basidiospores, clamps in all tissues, and no cheilocystidia. *Mycena lasiopus* differs from *M. amoena* in having a somewhat larger, rather dark pileus, a radially lamellate basal disc, clamps in all tissues, broader basidiospores, numerous cheilocystidia, and caulocystidia that are almost smooth at the apex. Moreover, we note that a fourth species is known having lobed cherocytes with dark-colored contents, *M. albinea* Aravind. & Manim (not represented in our phylogenetic tree, since no ITS sequences are available). This species differs from *M. amoena* by having a pale brownish to off-white pileus, a radially lamellate basal disc, larger basidiospores, and longer caulocystidia (Aravindakshan & Manimohan 2015). *Mycena amoena*'s closest relative in our phylogenetic tree, *M. melanovelis* nom. prov., also has cherocytes with colored vacuolar contents, but contrary to *M. amoena,* its cherocytes have small spines instead of lobes. It also differs from *M. amoena* by lacking a basal disc and having larger basidiomata, smaller basidiospores, and cheilocystidia forming a sterile band.

Interestingly, *M. tenerrima* was found to consist of two distinct phylogenetic species, referred to as *M. tenerrima* groups I and II. Both species appear to occur in the Netherlands. It is important to note that alignments of adequate quality for downstream use in phylogenetic analyses could not be obtained with conventional alignment tools like MAFFT (Katoh & Standley 2013), resulting in unstable trees and low support values; topologies shifted substantially with addition or removal of sequences, and also heavily depended on phylogenetic tree estimation tools, partitioning schemes, evolutionary models, and comparatively small adjustments of the initial alignments (data not shown). These phylogenetic uncertainties likely arose due to undersampling (i.e., a limited number of relevant sequences in public databases) and highly divergent sequences. Alignments revealed a high number of gap-rich and nearly unalignable regions within the ITS sequences of species in sect. *Amparoina*, which may have arisen as a result of frequent indel events (data not shown). For instance, the longest unalignable region was observed in the ITS1 region of *M. oboensis* BAP 669, which was 203 nucleotides in length. Indeed, the ITS regions of several clades of fungi are known to be rapidly evolving and often contain indel-rich regions, which may lead to inaccurate alignments and distorted phylogenies (Caligiorne et al. 2005, Ogden & Rosenberg 2006, Tóth et al. 2013, Brown et al. 2014, Wächter & Melzer 2020). Based on our observations, this appears to also hold true for sect. *Amparoina*, if not for the genus *Mycena* as a whole. Tóth et al. (2013) and Wächter & Melzer (2020) have used phylogeny-aware alignment tools in conjunction with iterative guide trees to improve the accuracy of large ITS alignments. To approximate the alignment strategy used by Tóth et al. (2013) and Wächter & Melzer (2020), Canopy, an iterative phylogeny-aware alignment tool with iterative guide tree estimation, was used to align our dataset. Both ML and BI phylogenetic trees constructed with the Canopy alignment appear more robust and are supported by higher likelihoods and branch support values. Although our final phylogenetic trees are stable and branches are comparatively well-supported, the observed instability of the tree prior to adapting alternative alignment strategies should be noted and carefully considered. Nonetheless, all iterations of our phylogenetic analyses, including the final tree, support a monophyletic *Mycena* sect. *Amparoina* (Fig. 14). Sequences currently placed within sect. *Amparoina* might be especially vulnerable to long branch attraction, since a large part of this clade primarily consists of highly variable sequences connected by long branches. Again, this could be the result of undersampling in this clade. In future studies, this could be amended by addition of more sequences from species placed in sect. *Amparoina*, or through multi-gene phylogenetic analyses. Therefore, we stress that some caution should be exercised in inferring (higher) taxonomic relationships from our phylogenetic tree, since it might not accurately reflect the 'true' phylogeny.

Authors: M. Jagers, A. Aronsen, Q.M. Holzapfel & J. Nuytinck

Basidiomycota, Tremellomycetes, Tremellales, Phaeotremellaceae

Phaeotremella dejopia Dirks, **sp. nov.** – Fig. 15
MycoBank no.: MB 842948

H o l o t y p u s . – USA. Wisconsin, Dane County, Olson Oak Woods State Natural Area, 42°56'41.64"N, 89°35'13.56"W, 310 m a.s.l., on a fallen deciduous tree trunk in association with *Stereum gausapatum* (Fr.) Fr., 7 October 2018, *leg.* Alden C. Dirks, ACD0048, https://mushroomobserver.org/294641 (MICH 340451; holotype). Sequences ex-holotype: MT913629 (ITS), OM311634 (LSU).

D e s c r i p t i o n . – B a s i d i o m a t a foliaceous, sessile, gelatinous, ca. 15 cm in diameter, with undulate, cespitose lobes, transitioning from translucent tan, pinkish, or pale brown at the margin to darker brown to black at the point of attachment, darkening when dried. – H y p h a e with clamp connections, (2.0–)3.0–4.1(–4.4) µm in diameter [20/2].

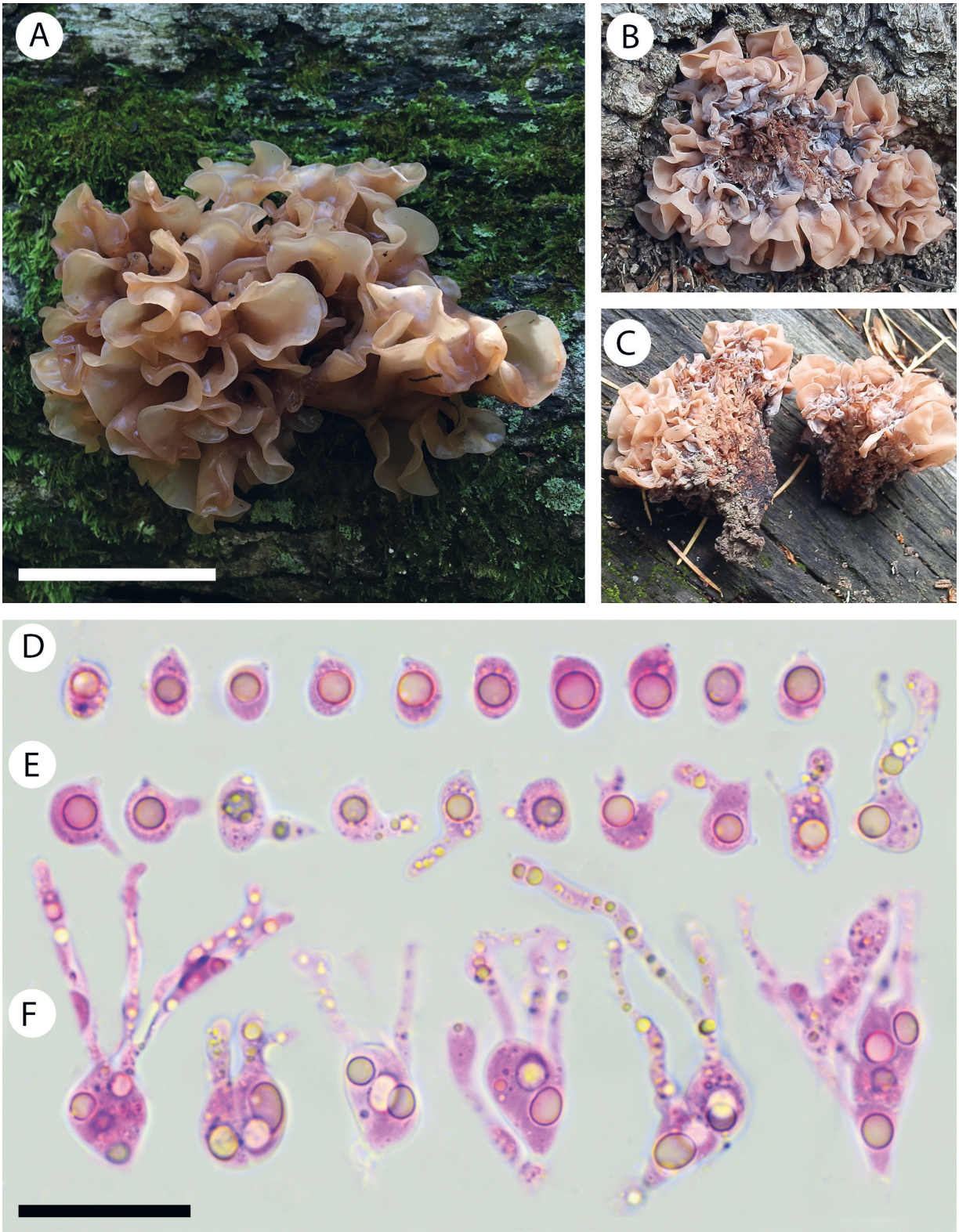

Fig. 15. *Phaeotremella dejopia*, basidiomata and microscopic structures. **A.** Basidiomata, collection MICH 340451 (holotype). **B–C.** Basidiomata, collection ARIZ AN 043301, illustrating darker base. **D.** Basidiospores, not germinating. **E.** Basidiospores, germinating. **F.** Heterobasidia with vertical and horizontal septation. Scale bars A 5 cm, D–F 20 µm.

– Basidia globose, ovoid, or clavate, cruciate septate or less frequently transversely septate, with or without (depending on specimen) prominent oil droplets, (8.8–)8.9–15.3(–21.2) × (6.3–)7.1–10.0(–10.8) µm, av. 12.1 × 8.5 µm, with up to four sterigmata, (12.3–)13.0–30.9(–43.9) µm long, sometimes with a swollen apex [20/2]. – Basidiospores broadly ellipsoid to ellipsoid or ovoid; smooth, hyaline, inamyloid, apiculate, frequently observed germinating, sometimes repetitive, with or without (depending on specimen) a prominent oil droplet; (4.5–)5.7–8.3(–10.0) × (3.5–)4.3–6.5(–7.7) µm, av. 7.0 × 5.4 µm, Q = (1.0–)1.2–1.5(–1.7), Q_{av} = 1.3 [90/2]. – Conidia not observed.

Etymology. – Referring to Dejope, the name of the region from which the holotype was collected, in the Ho-Chunk language. Dejope translates to "four waters" and refers to the four lakes of the Madison area in Wisconsin—Mendota, Monona, Waubesa, and Kegonsa—where the Ho-Chunk people have lived for over ten millennia. The suffix "-ia" is vocally similar and a play on the Ho-Chunk suffix "-eja" meaning "that place" or "there". Therefore, *Phaeotremella dejopia* means the *Phaeotremella* of the place of four waters. The newly minted Ho-Chunk common name for this species is "TeeHųųcnįk", which means "little water bear".

Habitat and distribution. – Only known from the USA (Arizona and Wisconsin) perhaps in association with *Stereum gausapatum* on dead hardwood. Full geographic distribution, potential host species, and substrates not yet determined.

Additional material examined. – USA. Arizona, Coconino County, on deadwood of *Quercus gambelii* Nutt., *Stereum* host unknown, 2 October 2016, *leg.* Teresa A. Clements, TAC 1632, https://mushroomobserver.org/254834 (ARIZ AN 043301).

Notes. – *Phaeotremella* jelly fungi are conspicuous members of the forest funga, producing foliar, gelatinous basidiomata in mycoparasitic association with *Stereum* Hill ex Pers. crust fungi (Roberts 1999, Spirin et al. 2018). The genus was resurrected by Liu et al. (2015) for the *Tremella foliacea* Pers. group, which was resolved as a well-supported monophyletic clade, and now harbors fungi that produce macroscopic basidiomata as well yeasts with no known sexual sporocarps (Wedin et al. 2016; Spirin et al. 2018; Li et al. 2019, 2020; Sun et al. 2020; Yuan et al. 2020; Degawa et al. 2022). *Phaeotremella* is well-situated for "plug-and-play" phylogenetics given that all 16 currently described species in the genus have published sequence data for at least two of three common DNA barcodes—ITS, LSU, and *tef1*—and 10 species have sequence data from type material.

Based on phylogeny, biogeography, morphology, and ecology, a new species of *Phaeotremella*, *P. dejopia*, is here described from the USA. *Phaeotremella dejopia* belongs to a well-supported clade sister to *P. frondosa* (Fr.) Spirin & V. Malysheva, along with *P. fuscosuccinea* (Chee J. Chen) Spirin & Yurkov, *P. roseotincta* (Lloyd) V. Malysheva, and *P. yunnanensis* L.F. Fan, F. Wu & Y.C. Dai (Fig. 16). The close phylogenetic relationship between these four taxa and their monophyly was consistent across independent loci, although incomplete lineage sorting resulted in strongly supported, conflicting hypotheses concerning which share a most recent common ancestor (*P. fuscosuccinea* and *P. dejopia* vs. *P. dejopia* and *P. yunnanensis*). As a result, the concatenated analysis shows a polytomy that will need to be resolved by sequencing more loci. *Phaeotremella fuscosuccinea*, *P. roseotincta*, and *P. yunnanensis* have been documented exclusively in Asia, namely China, Taiwan, Japan, and the Russian Far East (Lloyd 1923, Chen 1998, Malysheva et al. 2015, Spirin et al. 2018, Yuan et al. 2020), whereas *P. dejopia* is thus far restricted to North America, found along with *P. foliacea* (Pers.) Wedin, J.C. Zamora & Millanes and *P. frondosa*.

Compared to these other five species, *P. dejopia* seems to reach the greatest size (15 cm vs. 10 cm or less) and the coloration of the fronds is notably paler. In both traits, *P. dejopia* is most like *P. fuscosuccinea*. Although *P. dejopia* has the smallest basidiospores on average (largely due to especially small dimensions in the holotype specimen), the basidiospores of all these taxa range widely in size and overlap extensively, making identification via microscopy less than ideal (Tab. 2). However, ITS sequences can readily distinguish these semi-cryptic taxa. *Phaeotremella dejopia* has low intraspecific ITS divergence (99.6 % identical, 1 nucleotide difference, 1 ambiguous nucleotide), but relatively high divergence from *P. roseotincta* and *P. yunnanensis* (96.5–97.3 % shared identity), and even more from *P. fuscosuccinea* (90.2–90.4 % shared identity). Ecologically, *P. dejopia*, *P. frondosa*, *P. roseotincta*, and *P. yunnanensis* are reported on deciduous wood whereas *P. foliacea* and *P. fuscosuccinea* are reported on conifers. Therefore, in North America, assuming one has knowledge of the substrate, *P. dejopia* and *P. frondosa* are the only two taxa that could be confused with each other but should be separable by morphology or ITS sequencing (Chen 1998, Malysheva et al. 2015, Spirin et al. 2018, Yuan et al. 2020).

Tab. 2. Sizes of basidiospores of select *Phaeotremella* species and *Tremella aspera*.

Species/specimen	Length (µm)	av. L	Width (µm)	av. W	Q	Q_{av}	n	Reference
Phaeotremella dejopia	(4.5–)5.7–8.3(–10.0)	7.0	(3.5–)4.3–6.5(–7.7)	5.4	(1.0–)1.2–1.5(–1.7)	1.3	90/2	This study
MICH 340451 (Wisconsin)	(4.5–)5.3–6.6(–7.2)	6.0	(3.5–)3.9–5.1(–6.3)	4.5	(1.0–)1.2–1.4(–1.7)	1.3	45	This study
ARIZ AN 043301 (Arizona)	(6.2–)7.2–8.9(–10.0)	8.0	(4.4–)5.5–7(–7.7)	6.3	(1.0–)1.1–1.5(–1.7)	1.3	45	This study
Phaeotremella foliacea	(5.2–)5.3–9.1(–10.2)	7.3	(4.6–)4.7–8.5(–9.5)	6.4	1.0–1.3(–1.4)	1.2	280/9	Spirin et al. (2018)
Phaeotremella frondosa	(6.1–)6.4–10.2(–10.8)	8.1	(5.0–)5.1–8.7(–9.0)	6.7	1.0–1.5(–1.6)	1.2	240/8	Spirin et al. (2018)
Phaeotremella fuscosuccinea	(6.4–)7.1–10.2(–10.8)	8.7	(5.1–)5.2–8.1(–8.2)	6.7	(1.1–)1.2–1.5(–1.6)	1.3	90/3	Spirin et al. (2018)
Phaeotremella roseotincta	7.0–10.0	N/A	7.0–9.0	N/A	N/A	N/A	N/A	Malysheva et al. (2015)
Phaeotremella yunnanensis	(6.0–)7.0–8.0(–8.9)	7.4	6.0–7.3(–9.0)	6.9	N/A	1.1	30/1	Yuan et al. (2020)
Tremella aspera	8.6–11.8	N/A	8.6–11.8	N/A	N/A	N/A	N/A	Coker (1920)
BPI 724576 (North Carolina)	(10.2–)11.4–13.3(–14.0)	12.4	(9.5–)10.4–12.4(–14.0)	11.4	(1.0–)1.0–1.2(–1.2)	1.1	30/1	This study

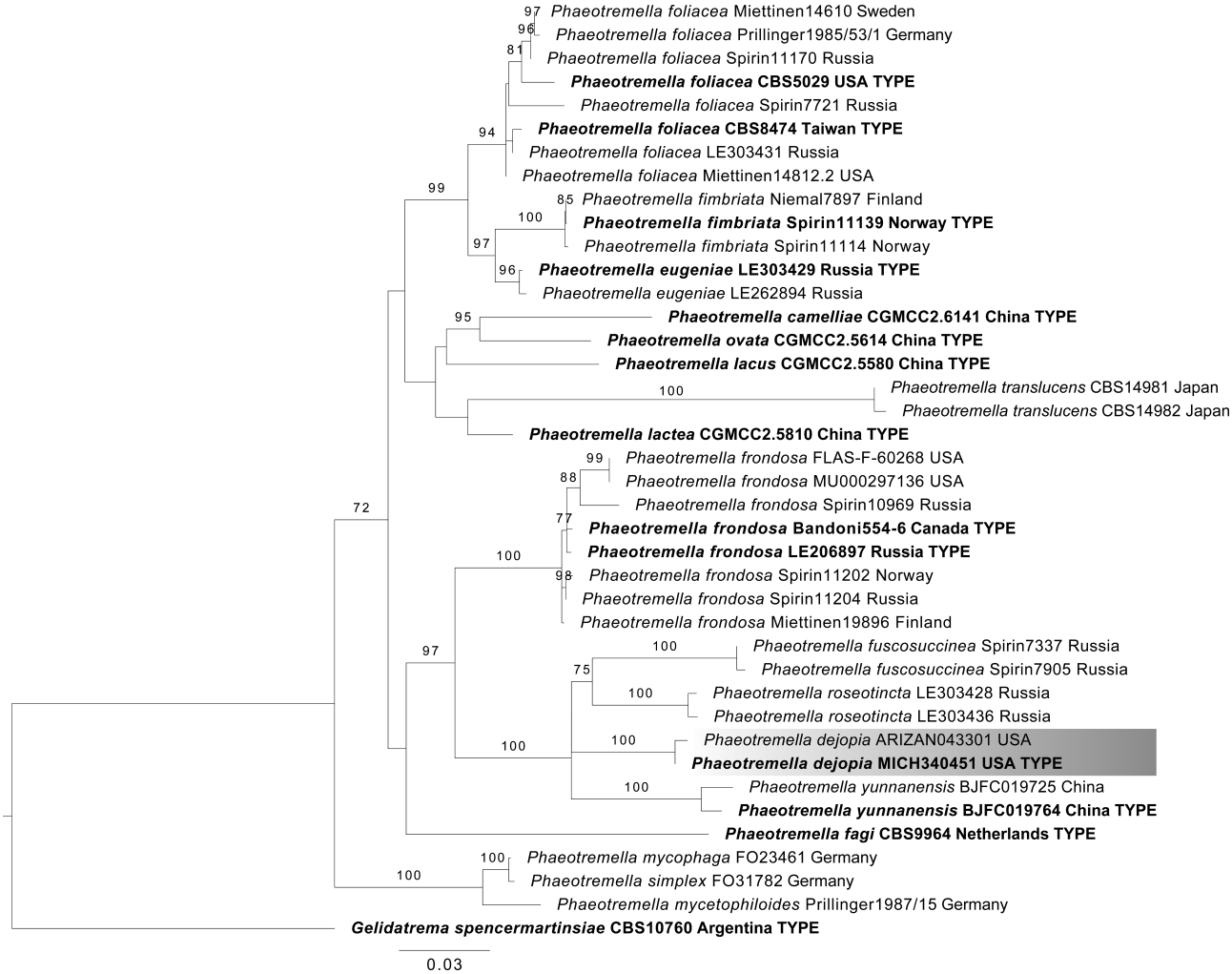

Fig. 16. Phylogeny of *Phaeotremella* reconstructed from a three-locus concatenated dataset (ITS, LSU, *tef1*). For each node, the MLBS (if ≥70) for 1000 replicates is presented on the branch leading to that node. Taxon names for sequences derived from type material are in boldface.

Tremella aspera shares a vaguely similar morphology and ecology with *P. dejopia*, warranting its study to determine whether they are synonymous. Described from an oak stump in North Carolina (Coker 1920), *T. aspera* is a forgotten name represented by only one other collection besides the holotype, from 1926 (MyCoPortal 2022). This collection was acquired and studied; unfortunately, the holotype was not accessed. Sequencing efforts failed, but microscopy revealed large, globose to broadly ellipsoid basidiospores, measuring (10.2–)11.4–13.3(–14) × (9.5–)10.4–12.4(–14) µm, av. 12.4 × 11.4 µm, Q = (1.0–)1.0–1.2(–1.2), Q_{av} = 1.1, and large basidia, 18.3–23.7 µm wide. The holotype was described as possessing basidiospores that were globose, 8.6–11.8 µm in diameter (Tab. 2), as well as large basidia 15.5–18.5 × 20.2–25.9 µm. The basidiomata of both specimens consist of dark, crumpled lobes that grow as an extensive mass across the substrate with multiple points of attachment in an *Exidia*-like fashion. Due to its subglobose spores, large basidia, and macromorphology, *T. aspera* is not synonymous with *P. dejopia*, which produces sizeable basidiomata that grow from a central point of attachment and have pale lobes, smaller ellipsoid spores, and smaller basidia. However, both the collector of the 1926 specimen, Ross W. Davidson, and a mycologist who later studied the holotype, heterobasidiomycete expert Robert J. Bandoni, believed *T. aspera* to be synonymous with *P. foliacea*/*P. frondosa*. Until more specimens from the type locality can be collected and studied or the holotype sequenced, *T. aspera* is regarded as a *nomen ambiguum*.

This study highlights the need for greater documentation of *Phaeotremella* fungi, with special attention paid to substrate and associated *Stereum* fungi or other potential hosts (e.g., *Aleurodiscus* spp., *Peniophora* spp., and *Trichaptum* spp.) (Spirin et al. 2018). The fact that *Stereum* species are often complexes of which taxonomic boundaries are poorly understood and in flux, requires that potential hosts also be collected, preserved, and DNA barcoded for accurate taxonomic assignment (Dai 2011, DeLong-Duhon & Bagley 2020). With increased metadata, consistent ecological differences among *Phaeotremella* species could be elucidated, providing more traits for field identification. Given the variable and overlapping morphologies of *Phaeotremella* jelly fungi, DNA sequence data will be crucial in the endeavor to understand the full diversity and range of *Phaeotremella* species. For example, sequencing of *Phaeotremella* specimens from Florida and Ohio for this study confirmed what could only be conjectured by Spirin et al. (2018): *P. frondosa* indeed has a broad distribution across North America.

Author: A.C. Dirks

Basidiomycota, Agaricomycetes, Agaricales, Tricholomataceae

Tricholoma* section *Genuina

Tricholoma mcneilii Lebeuf, A. Paul, J. Landry & G. Taylor, **sp. nov.** – Fig. 17
MycoBank no.: MB 843707

Diagnosis. – Differs from its sister species *Tricholoma stans* by its growth under various conifers (*Pinus*, *Abies*, *Tsuga*), occurrence in North America, and genetic distance at the ITS locus. Basidiospores 4.0–6.0 × 3.0–5.0 µm, on average 4.9 × 3.8 µm.

Holotypus. – CANADA. Québec, Saint-Casimir, route à Jean-Toutant, 46°42'13.7"N, 72°06'43.1"W, 57 m a.s.l., in a plantation of *Abies balsamea* with a few *Picea glauca* mixed in, 15 October 2018, *leg.* R. Lebeuf & A. Paul, HRL2835 (DAOM 985001; holotype).

Description. – Pileus 58–160 mm in diameter, convex then applanate and depressed at center, viscid to slightly viscid, reddish brown to brownish orange 6(C–D)(6–8), 8(D–E)(4–5), with innate darker brown fibrils sometimes giving a brushed aspect; margin inflexed for a long time then straight, costate or not, undulating with age, paler when young. – Lamellae emarginate, crowded, 5–8 mm broad, white to pallid at first, developing orange-brown to reddish brown spots with age, especially at edge. – Stipe 44–70 × 15–29 mm, equal or clavate, pointed or almost flattened at base, solid, slightly superficially fibrillose, sometimes floccose or scaly in upper part, cream at first, discoloring orange-brown with age or when bruised. – Context thick, fibrous, firm, white, browning when bruised. – Odor farinaceous. – Taste farinaceous, bitter. – Basidiospores (4.0–)4.2–5.5(–6.0) × (3.0–)3.2–4.2(–5.0) µm, av. 4.9 × 3.8 µm, Q = 1.11–1.38(–1.56), Q_{av} = 1.27 [141/5/5], predominantly broadly ellipsoid, also ovoid, ellipsoid or subglobose, inamyloid. – Basidia 23–43 × 5–7 µm, 4-spored, narrowly clavate. – Cheilocystidia absent. – Pileipellis an ixocutis 30–200 µm thick; hyphae in matrix 2–5 µm wide, repent to interwoven-ascending, pale to darker brown, smooth (and then with an intracellular pigment) or finely to moderately spirally-incrusted, cylindrical, thin-walled; underlying hyphae 3–7 µm in diameter, ± parallel, interwoven or in bundles, more darkly pigmented brown, yellowish brown or reddish brown, smooth to coarsely spirally-incrusted; subpellis not differentiated. – Stipitipellis a cutis made of

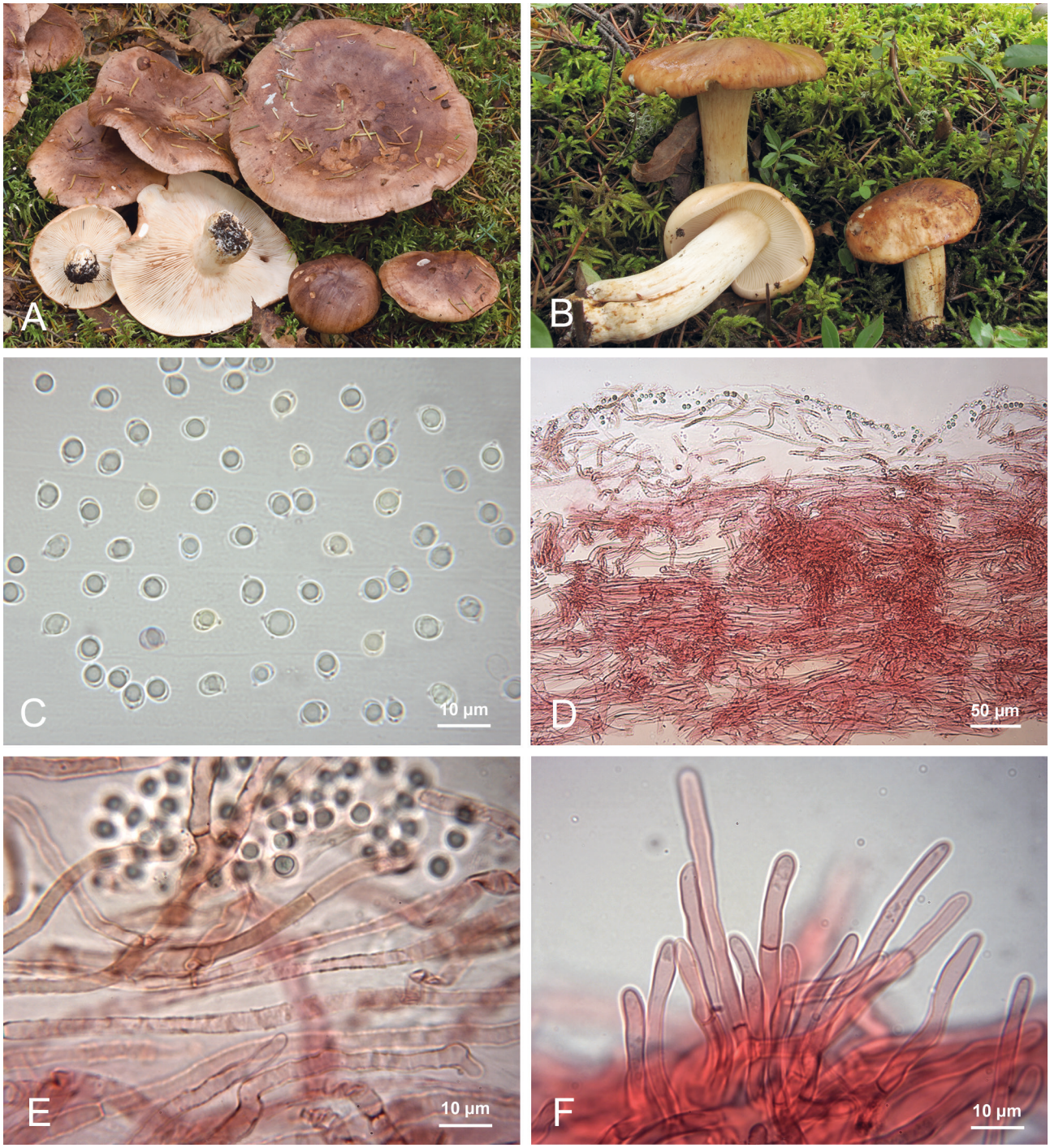

Fig. 17. *Tricholoma mcneilii*. **A.** Basidiomata *in situ*, collection DAOM 985001 (holotype). **B.** Basidiomata *in situ*, collection QFB32581. **C.** Basidiospores in 3 % KOH. **D–E.** Pileipellis section in SDS Congo Red. **F.** Caulocystidia.

2.5–7 µm wide cylindrical hyphae, longitudinal or superficially entangled, smooth and thin-walled or finely incrusted with slightly thickened walls (up to 0.5 µm broad). – Caulocystidia 20–60 × 3–6 µm, present as recurved end-cells or more rarely intercalary, arranged in small to large fascicles or entangled, cylindrical, cylindrical-flexuose, sometimes subcapitate or branched, particularly abundant at stipe apex, but also present on lower stipe. – Clamp connections absent in all examined tissues.

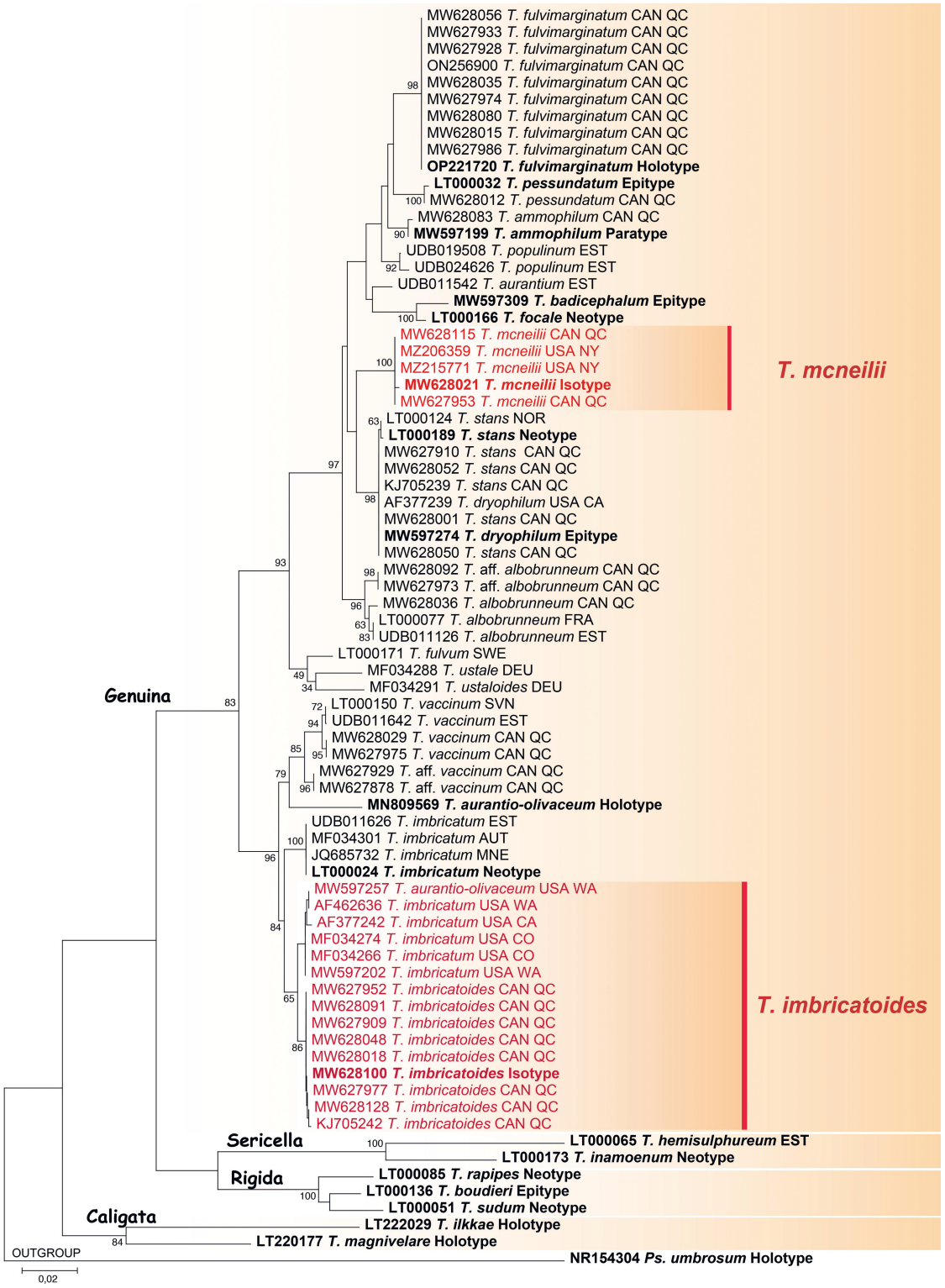

Fig. 18. Phylogeny of selected *Tricholoma* species in sections *Genuina*, *Sericella*, *Rigida* and *Caligata* reconstructed from an ITS dataset. The tree topology with the highest log likelihood (-lnL = 4122.0788) is shown, resulting from ML inference performed in MEGA7. MLBS values (if ≥60) are shown at the nodes. Section designations following Heilmann-Clausen et al. (2017) and Reschke et al. (2018), ex-type sequences in boldface, new species highlighted in red, bar indicating the expected number of substitutions per site.

Etymology. – Named in honor of Raymond McNeil, for his contributions to the knowledge of the Québec funga.

Habitat and distribution. – Gregarious to caespitose under various conifers, (*Abies balsamea*, *Pinus banksiana*, *Tsuga canadensis*), in acidic soil, in the fall. Thus far known from Canada (Québec) and the USA (New York).

Additional material examined. – *Ibid.* (QFB32650; isotype). Sequences ex-isotype: MW628021 (ITS). – CANADA. Québec, Amos, Lac-Gauvin, under *Pinus banksiana* and a few *Abies*, in a forested area in acidic soil, 15 September 2012, *leg.* H. Lambert, HL1230 (QFB32579); *ibid*, 11 September 2013, *leg.* H. Lambert, HL1302 (QFB32581). – USA. New York, Limestone, Allegany State Park, under *Tsuga canadensis*, 17 October 2018, *leg*. G. Taylor, iNaturalist ID 17610322 (CMMF024930); *ibid*, under *Tsuga canadensis* and *Betula alleghaniensis*, 7 November 2018, *leg*. G. Taylor, iNaturalist ID 18259629 (CMMF024931).

Notes. – The ITS sequence of the isotype is distinct from other members of section *Genuina*, deviating from *Tricholoma stans* (Fr.) Sacc. by 10 substitutions and indels. *Tricholoma mcneilii* belongs to the difficult group of species featuring a viscid orange-brown to reddish brown pileus, farinaceous odor and taste, small spores, lack of cheilocystidia, and undifferentiated subpellis. It is morphologically very similar to *T. stans*, but even though both species are present in eastern North America, our phylogenetic analysis suggests that they are reproductively isolated (Fig. 18). Ecologically speaking, *T. stans* is restricted to *Pinus* forests in Europe and eastern North America (Christensen & Heilmann-Clausen 2013) and is also associated with *Quercus* in Central America (Ovrebo et al. 2021), whereas *T. mcneilii* grows under various conifers (*Abies*, *Tsuga*, *Pinus*). Spore shape can also help distinguishing the two species in eastern North America. Indeed, although spores of both species have similar lengths, those of *T. stans* are mostly ellipsoid in eastern North America, with an average Q of 1.52–1.58 (R. Lebeuf, pers. obs.), while those of *T. mcneilii* are mostly broadly ellipsoid, with an average Q of 1.25–1.29. However, the spores of the European collections of *T. stans* are reported as broadly ellipsoid, with an average Q of 1.22–1.31 (Kibby 2012, Christensen & Heilmann-Clausen 2013). This discrepancy between American and European collections of *T. stans* remains to be resolved. Both *T. stans* and *T. mcneilii* can have a costate margin, but most collections of *T. stans* made in eastern North America by the authors and colleagues do not show that character, and it is also inconsistent in *T. mcneilii*. *Tricholoma albobrunneum* (Pers.) P. Kumm. and an as yet undescribed sister North American entity are also associated with *Pinus*, but they feature a white band at stipe apex, and their spores are mostly ellipsoid (average Q ~ 1.5). *Tricholoma pessundatum* (Fr.) Quél, associated with *Picea*, *Abies*, and *Pinus*, typically shows concentrically arranged dark round spots on the margin, and its spores are ellipsoid to oblong.

Authors: R. Lebeuf, J. Landry & A. Paul

Basidiomycota, Agaricomycetes, Agaricales, Tricholomataceae

Tricholoma* section *Genuina

Tricholoma imbricatoides Lebeuf, A. Paul & J. Landry, **sp. nov.** – Fig. 19
MycoBank no.: MB 843708

Diagnosis. – Differs from *Tricholoma imbricatum* by its generally smaller size, basidiospores mostly ellipsoid, 5–7 × 3.5–5.5 µm, on average 5.9 × 4.1 µm, occurrence restricted to North America, and genetic distance at the ITS locus.

Holotypus. – CANADA. Québec, Amos, in a pure stand of *Pinus banksiana*, in sandy soil, 27 September 2019, *leg.* R. Lebeuf & A. Paul, HRL3100 (DAOM 985002; holotype).

Description. – Pileus 25–80(–100) mm in diameter, convex then plano-convex to pulvinate often with a low umbo, with age applanate; surface dry, appressed-fibrillose then squamulose, sometimes felty, splitting with age, dark brick, dark brown, orange-brown, cinnamon or yellowish brown (6D(5–7), 7D6, 7½D4, 7½D6), darkest at center and paler towards margin, at times with a whitish band at edge of margin; margin inflexed for a long time then straight, undulating with age. – Lamellae emarginate to deeply emarginate, close to subdistant, 2–7 mm broad, white when young, developing light brown to yellowish brown spots or zones with age, particularly at margin. – Stipe 25–60(–80) × 6–15 mm, equal, pointed at base, flocculose and mostly white at apex, below longitudinally fibrillose and concolorous with pileus but paler, darkening to rusty brown from the base up with age, occasionally discoloring rusty brown in spots. – Context thick, firm, white, brownish under the pileipellis. – Odor indistinct. – Taste mild, bitterish or slightly acrid. – Basidiospores (5.0–)5.5–6.5(–7.0) × (3.5–)3.8–5.0(–5.5) µm, av. 5.9 × 4.1 µm, Q = 1.20–1.75, Q_{av} = 1.43 [135/5/5], predominantly ellipsoid, more rarely broadly ellipsoid, oblong to amygdaliform, smooth, inamyloid. – Basidia 28–42 × 6–7 µm, 4-spored, narrowly clavate. – Cheilocystidia absent. – Pileipellis a cutis made of radially arranged

Fig. 19. *Tricholoma imbricatoides*. **A.** Basidiomata *in situ*, collection DAOM 985002 (holotype). **B.** Basidiomata *in situ*, collection HRL1001. **C.** Basidiomata, collection CMMF002729. **D.** Basidiospores in 3 % KOH. **E.** Pileipellis section in SDS Congo Red. **F.** Pileipellis section in 3 % KOH. **G.** Caulocystidia.

hyphae 2–7(–12) µm broad, repent, parallel to interwoven, sometimes in bundles, thin-walled, the outermost hyphae smooth or incrusted with a dark brown pigment, the lower hyphae smooth, with an intracellular orangish brown or more rarely pale-yellow pigment; terminal cells cylindrical; subpellis not differentiated. – Stipitipellis a cutis made of 2–7 µm wide cylindrical hyphae, longitudinal or superficially entangled, smooth and thin-walled or finely incrusted with slightly thickened walls (up to

0.5 µm broad). – Caulocystidia 25–75 × 3–9 µm, present as recurved end-cells at stipe apex, single, arranged in fascicles or entangled, cylindrical, cylindrical-flexuose, narrowly clavate, moniliform. – Thromboplerous hyphae present in the pileipellis and pileitrama of some collections (Fig. 19F). – Clamp connections absent in all examined tissues.

Etymology. – Referring to the similarity with *Tricholoma imbricatum*.

Habitat and distribution. – Gregarious, sometimes caespitose, under *Pinus*, especially *P. banksiana* in eastern North America, in September and October. Frequent in Québec, Canada, and widely distributed in North America, from the east to the west coast.

Additional material examined. – *Ibid.* (QFB32654; isotype). Sequences ex-isotype: MW628100 (ITS). – CANADA. Québec, Saint-Roch-de-Richelieu, in a young *Pinus banksiana* plantation mixed with a few *Populus* sp., in sandy soil, 9 October 2011, *leg.* R. Lebeuf & A. Paul, HRL1001; *ibid*., 9 October 1995, *leg.* R. Archambault, YL2729 (CMMF002729); Sept-Îles, near the baseball field on Holliday Street, in *Pinus banksiana* needle litter, in sandy soil, 5 September 2001, *leg.* Raymond Boyer, BOY372 (CMMF005038); Sacré-Coeur, under *Pinus banksiana*, 11 October 2008, *leg.* H. Lambert, HL0395 (QFB31069).

Notes. – The ITS sequence of the isotype and other Québec collections positions the species within section *Genuina* in a sister relationship to the European species *T. imbricatum* (Fr.) P. Kumm., from which it differs by 10 substitutions and indels. The ITS sequence also differs from collections made in Colorado and the west coast by substitution at two positions, one of which being ambiguous in some collections, seemingly resulting from intragenomic heterogeneities. These differences appear insufficient to separate the eastern and western entities (Fig. 18). Morphologically, although much similar to *T. imbricatum*, *T. imbricatoides* is generally less robust, with a smaller pileus and a shorter and narrower stipe, and its spores are predominantly ellipsoid, whereas they are mostly broadly ellipsoid in *T. imbricatum* (Breitenbach & Kränzlin 1991, Christensen & Heilmann-Clausen 2013). Other brown species of *Tricholoma* growing under *Pinus* – *T. albobrunneum* and a close North American variant (referred to as *T.* aff. *albobrunneum* in Fig. 18), *T. mcneilii* (described above), *T. pessundatum*, and *T. stans* – have a viscid pileus and farinaceous odor and taste. *Tricholoma vaccinum* (Schaeff.) P. Kumm. differs by its squamose pileus with a floccose margin and farinaceous odor and taste.

Authors: R. Lebeuf, J. Landry & A. Paul

Basidiomycota, Agaricomycetes, Agaricales, Tricholomataceae

***Tricholoma* clade /Arvernense**

Tricholoma pseudoterreum Lebeuf, Y. Lamoureux, A. Paul & J. Landry, **sp. nov.** – Fig. 20
MycoBank no.: MB 843709

Diagnosis. – Differs from other grey species of *Tricholoma* by the combination of tomentose to felty pileus in young age becoming squamulose in age; lack of cortinoid partial veil; farinaceous odor and mild taste; abundant polymorphic cheilocystidia; duplex pileipellis; and presence of clamp connections at the base of basidia and in the pileitrama, lamellar trama, and pileipellis. Basidiospores 5.0–8.5 × 4.0–6.5 µm, on average 6.3 × 4.8 µm.

Holotypus. – CANADA. Québec, Hervey-Jonction, ZEC Tawachiche, 46°56’59.55”N, 72°26’48.65”W, 187 m a.s.l., under *Abies balsamea* in mossy and sandy soil, 28 September 2014, *leg.* R. Lebeuf & A. Paul, HRL1886 (DAOM 984999; holotype).

Description. – Pileus 40–75 mm in diameter, conical to convex, then applanate, usually with a broad and low umbo; surface dry, tomentose to felty at first, becoming radially fibrillose-virgate then squamulose, dark brownish grey at center, grey to paler brownish grey at margin, with age paler and becoming greyish brown; margin inflexed then straight, undate with age. – Lamellae emarginate, close, broad, segmentiform, white then pale grey, with edge finely fimbriate under hand lens and black-spotted with age. – Cortinoid veil absent. – Stipe 45–100 × 7–23 mm, equal or clavate with a pointed base, rooting, fibrillose, white to greyish, solid, becoming dirty yellowish at base when bruised. – Context rather thin in pileus, white to pale grey, fibrous in stipe. – Odor farinaceous. – Taste farinaceous, mild. – Basidiospores (5.0–)5.5–7.5(–8.5) × (4.0–)4.2–5.5(–6.5) µm, av. 6.3 × 4.8 µm, Q = 1.11–1.67, Q_{av} = 1.32 [148/5/5], broadly ellipsoid, ellipsoid, inamyloid, smooth, with granular content. – Basidia (25–)30–45 × 6–8 µm, (2–)4-spored, narrowly clavate, sometimes misshapen near lamellar edge, clamped. – Cheilocystidia 16–55 × 5–16 µm, numerous, polymorphic (cylindrical, cylindrical-curved, pestle-shaped, clavate, bifurcate, L-shaped, etc.), sometimes with long and narrow excrescences or mucronate, often septate, with refractive thin walls, very rarely clamped. – Pileipellis duplex: suprapellis a cutis partly breaking up into small trichoderm scales, hyphae ± parallel, smooth and then hyaline or with an intracellular or intraparietal brown, yellowish brown or yellow pigment, or spirally incrusted with a brown pigment, in masses pale to dark brown, 2–8 µm wide, very rarely clamped; subpellis well differentiated, made of several rows of thin-walled enlarged cells

Fig. 20. *Tricholoma pseudoterreum*. **A.** Basidiomata *in situ*, collection DAOM 984999 (holotype). **B.** Basidiomata, collection CMMF002096. **C.** Basidiospores in 3 % KOH. **D.** Cheilocystidia. **E.** Pileipellis section in SDS Congo Red. **F.** Pileipellis section in 3 % KOH. **G.** Caulocystidia. **H–L.** Clamp connections (H) in suprapellis, (I) in hyphae underlying the pileipellis, (J) in lamellar trama, (K) at the base of basidia, (L) in stipitipellis.

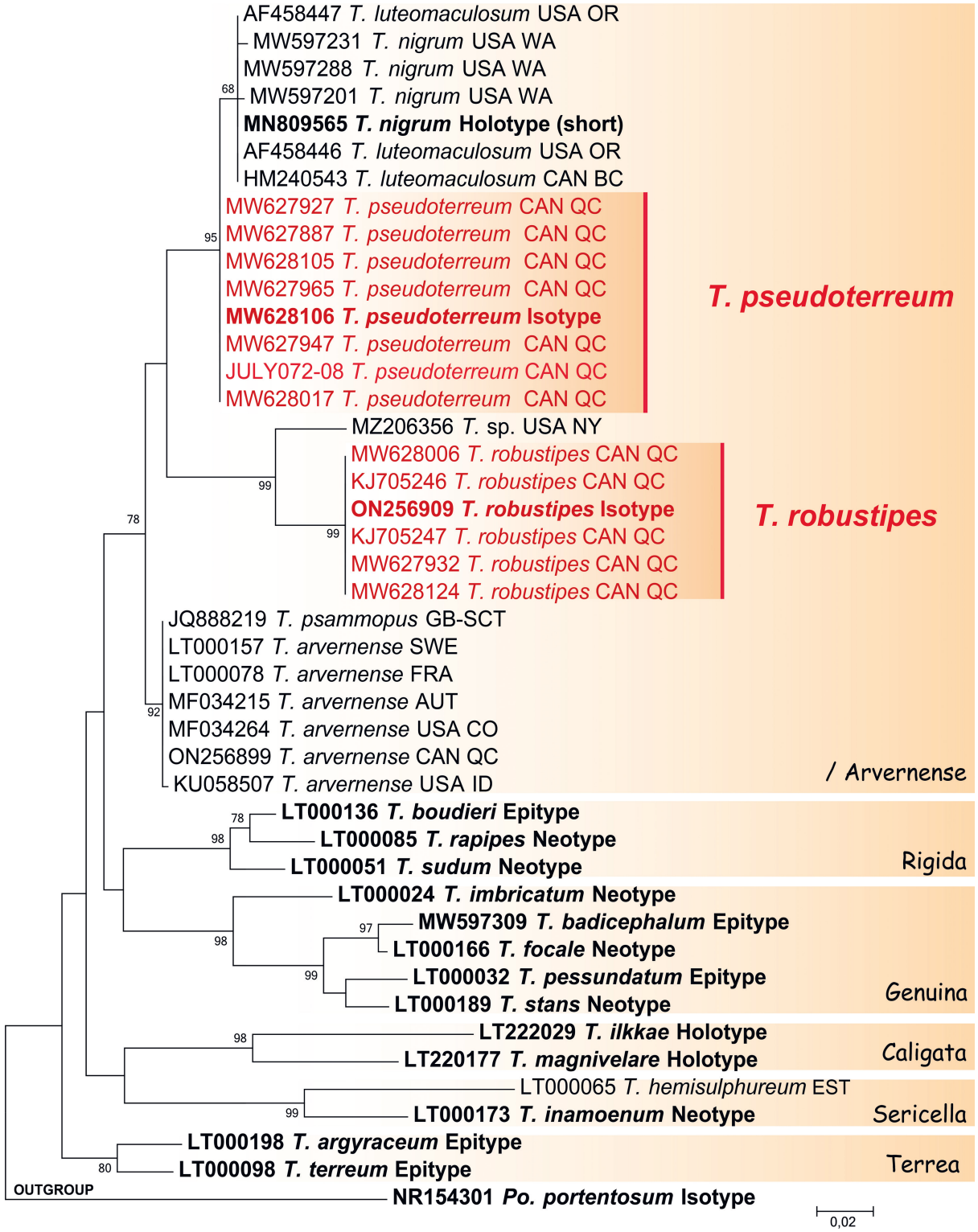

Fig. 21. Phylogeny of selected *Tricholoma* species closely related to the new species (clade /Arvernense) or in sections *Genuina*, *Sericella*, *Rigida*, *Terrea*, and *Caligata* reconstructed from an ITS dataset. The tree topology with the highest log likelihood (-lnL = 3875.0134) is shown, resulting from ML inference performed in MEGA7. MLBS values (if ≥60) are shown at the nodes. Section designations following Heilmann-Clausen et al. (2017) and Reschke et al. (2018), ex-type sequences in boldface, new species highlighted in red, bar indicating the expected number of substitutions per site.

measuring 15–70 × 6–30 µm, mostly hyaline, in some collections lowest cells heavily coated with a dark brown pigment in plaques, rarely clamped; underlying hyphae 3–10 µm in diameter, ± parallel to slightly interwoven, brown-pigmented, clamped. – Pileitrama hyphae 4–20(–25) µm broad, clamped. – Lamellar trama subregular, hyphae 3–17 µm wide, clamped. – Stipitipellis a cutis made of 2–6 µm wide cylindrical hyphae, longitudinal, smooth and thin-walled or finely incrusted with slightly thickened walls (up to 0.5 µm broad), occasionally clamped. – Caulocystidia 20–85 × 3.5–11 µm, present as recurved end-cells, frequent or scattered, more numerous at stipe apex, single, in fascicles or entangled, cylindrical, narrowly clavate, cylindrical-flexuose, sometimes capitate, not clamped, thin-walled and smooth or finely incrusted with slightly thickened walls (up to 0.5 µm).

Etymology. – Named for its macromorphological resemblance to *Tricholoma terreum*.

Habitat and distribution. – Uncommonly encountered in small groups under various conifers (*Abies balsamea*, *Picea* sp., *Pinus* sp.) in litter. Thus far only known from Québec, Canada.

Additional material examined. – *Ibid.* (QFB32637; isotype). Sequences ex-isotype: MW628106 (ITS). – CANADA. Québec, Lachute, in an old *Picea* sp. and two-needled *Pinus* plantation, in sandy and mossy soil, 29 September 1993, *leg.* Y. Lamoureux, YL2096 (CMMF002096); *ibid*., in needle litter, 14 September 1986, *leg.* R. McNeil, McN1895 (CMMF006864); Sept-Îles, near the baseball field on Holliday Street, in *Pinus banksiana* needle litter, 5 September 2001, *leg.* Raymond Boyer, BOY370 (CMMF005015); Sacré-Coeur, under *Pinus banksiana*, with a few *Abies balsamea* and *Populus tremuloides* at a distance, 11 October 2008, *leg.* H. Lambert, HL0403 (QFB31074).

Notes. – The ITS sequence of the isotype differs from other species of the /Arvernense clade, deviating from *T. nigrum* Shanks & Ovrebo by 7–9 substitutions and indels. The phylogenetic analysis reveals a sister relationship between the two species, *T. nigrum* being apparently restricted to western USA and *T. pseudoterreum* thus far only found in Eastern Canada (Fig. 21). *Tricholoma pseudoterreum* can be recognized by a tomentose to felty brownish grey to grey pileus in young age becoming squamulose and greyish brown in age, lack of cortinoid partial veil, farinaceous odor and mild taste, and microscopically by broadly ellipsoid to ellipsoid spores measuring 5.0–8.5 × 4.0–6.5 µm, on average 6.3 × 4.8 µm, abundant polymorphic cheilocystidia, duplex pileipellis, and presence of clamp connections at the base of basidia and in the pileitrama, lamellar trama, and rarely in the pileipellis. It is found in association with *Abies balsamea* and two-needled *Pinus* spp. *Tricholoma nigrum* differs in several ways: the viscid pileus is very dark grey when young; blackish squamules are often present on the stipe upper half or near the apex; basidiospores are larger, measuring 6.7–8.6 × 4.8–5.8 µm, on average 7.2–8.2 × 5.2–5.8 µm; cheilocystidia, not always conspicuous, are clavate to broadly clavate; the pileipellis has a gelatinous layer and the subpellis is not always well differentiated; and clamp connections are absent (Shanks 1996, Bessette et al. 2013).

Macroscopically, *T. pseudoterreum* is also similar to species in section *Terrea*, but it can be distinguished by the presence of clamp connections. Moreover, in that section, *T. terreum* (Schaeff.) P. Kumm. has clavate, regular cheilocystidia, and its odor is mild, not farinaceous. *Tricholoma argyraceum* (Bull.) Gillet has a distinctly umbonate pileus at maturity and a well-developed partial veil. Microscopically, its spores are smaller and mostly oblong, with an average Q of 1.60–1.98; the cheilocystidia are absent or inconspicuous, mostly cylindrical to clavate; and the pileipellis has no differentiated subpellis. It can associate with conifers or deciduous trees (e.g., *Picea* and *Populus*) (Riva 1988, Christensen & Heilmann-Clausen 2013). *Tricholoma scalpturatum* (Fr.) Quél. grows with a wide range of deciduous trees or more occasionally with conifer trees, it has smaller, narrower spores, and its subpellis is poorly differentiated (Kibby 2012, Christensen & Heilmann-Clausen 2013). Among other North American grey *Tricholoma* species with a dry pileus, *T. argenteum* Ovrebo, *T. atrodiscum* Ovrebo, *T. subacutum* Peck, *T. pullum* Ovrebo, and *T. acre* Peck do not have a farinaceous odor and have a bitter or acrid taste. The first three are associated with conifers, and the last two are found under deciduous trees (*Quercus*, *Fagus*, *Carya*) (Ovrebo 1980, 1989). *Tricholoma michiganense* A.H. Sm. has a coal tar odor (but rather peppery in collections made in Québec by the authors) and a very unpleasant taste, its lamellae discolor orange when bruised, and it is associated with *Quercus* (Smith 1942).

Authors: R. Lebeuf, J. Landry, Y. Lamoureux & A. Paul

Basidiomycota, Agaricomycetes, Agaricales, Tricholomataceae

***Tricholoma* clade /Arvernense**

Tricholoma robustipes Lebeuf, Y. Lamoureux, A. Paul & J. Landry, **sp. nov**. Fig. 22
MycoBank no.: MB 843710

Diagnosis. – Characterized by its yellow to olive yellow pileus with brownish grey to olive brown center; pale yel-

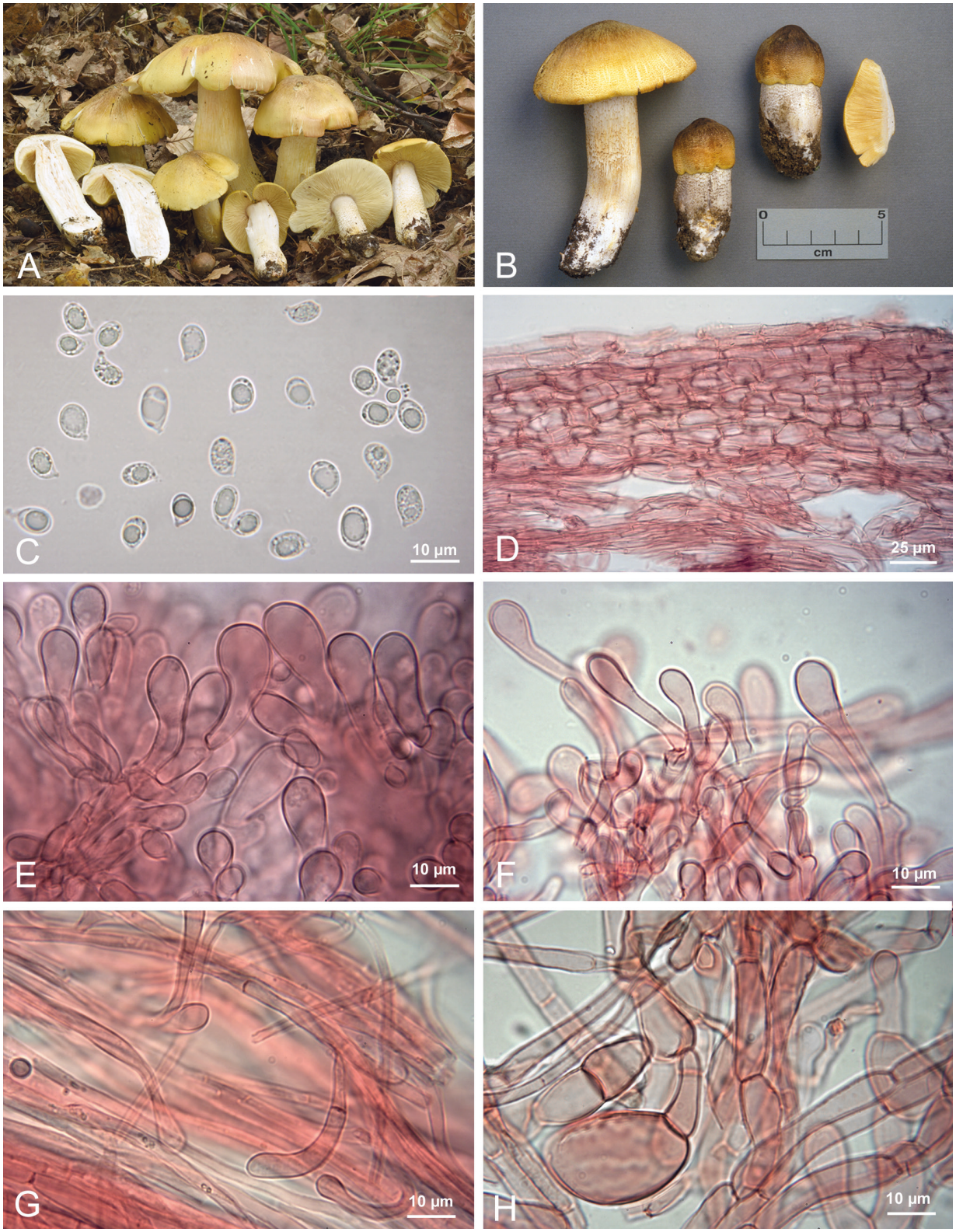

Fig. 22. *Tricholoma robustipes*. **A.** Basidiomata *in situ*, collection DAOM 985003 (holotype). **B.** Basidiomata, collection CMMF001494. **C.** Basidiospores in 3 % KOH. **D.** Pileipellis section in SDS Congo Red. **E–F.** Cheilocystidia. **G.** Caulocystidia. **H.** Stipe scales.

low to white lamellae often with yellow margin; long and robust stipe with white to brown concentric scales on a whitish to pale yellow background; pinkish orange discoloration of all parts with age; numerous clavate to cylindrical cheilocystidia; duplex pileipellis; and occurrence with *Quercus* in northeastern North America. Basidiospores 5.0–9.0 × 4.0–6.5 µm, on average 6.4 × 4.8 µm.

Holotypus. – CANADA. Québec, Saint-Narcisse, Parc de la rivière Batiscan, Barrage sector, 46°33'25.6"N, 72°24'51.9"W, 51 m a.s.l., in a mixed forest of *Quercus rubra*, *Abies balsamea*, *Populus tremuloides* and *Acer* sp., 23 September 2020, *leg*. R. Lebeuf & A. Paul, HRL3316 (DAOM 985003; holotype).

Description. – Pileus 50–170 mm in diameter, parabolic, convex to conico-convex, sometimes flattened at disk, becoming applanate generally with a broad umbo, irregular; surface dry, fibrillose at disk, breaking into small upturned scales towards margin, colored in different shades of yellow to olive yellow (2A6, 3A5, 4A5, 4A7), pale to dark brownish grey to olive brown in a broad zone from center to third or mid-radius, more rarely concolorous at center; margin inflexed then straight, upturned and splitting in age, undate. – Lamellae emarginate, crowded, segmentiform, with numerous forks at all levels, 4–6 mm broad, white to light yellow (4A3–4); margin finely fimbriate under hand lens, often pale to dark yellow, less frequently white. – Stipe 70–200 × 15–40 mm, equal or enlarged towards base, sometimes pointed at extreme base, sometimes deeply buried in the substrate, covered with scattered to numerous small white, yellow, yellowish brown or grey-brown concentric scales on a background that is white or flushed with yellow. – Context white to pale yellow, fibrous. All parts turning pinkish orange in age or when bruised, often starting at stipe. – Odor farinaceous. – Taste farinaceous, mild. – Basidiospores 5.0–8.0(–9.0) × 4.0–6.0(–6.5) µm, av. 6.4 × 4.8 µm, Q = 1.10–1.56(–1.80), Q_{av} = 1.35 [178/6/5], broadly ellipsoid, ellipsoid, rarely subglobose or oblong, inamyloid, smooth. – Basidia 28–45 × 6–8.5 µm, 4-spored, in some collections occasionally 2-spored, narrowly clavate, sometimes ventricose near lamellar edge. – Cheilocystidia 16–36(–52) × 4–13(–17) µm, forming a sterile band, in small groups or entangled in dense tufts, clavate, narrowly clavate, cylindrical, rarely oblong, rarely 1- or 2-septate, the largest ones smooth and thin-walled or finely incrusted with slightly thickened walls (~ 0.5 µm), the smaller ones thin-walled, in KOH hyaline or pale yellow in masses (depending on lamellar edge color), hyaline individually. – Pileipellis duplex: suprapellis a cutis breaking into trichoderm scales, hyphae 2–11 µm, repent, parallel or slightly interwoven, in masses brownish yellow, individually pale yellow, incrusted, with slightly thickened walls (~ 0.5 µm), in places forming erect scales or interspersed with bundles of intertwined darker yellowish brown hyphae; subpellis generally distinct, made of parallel, inflated cells measuring 12–40(–65) × 9–25 µm, smooth, thin-walled, hyaline or pale yellowish brown in masses (intracellular pigment); thromboplerous hyphae rare to abundant. – Stipitipellis a cutis made of 2–6 µm wide hyphae, cylindrical, longitudinal, thin-walled. – Caulocystidia present as recurved end-cells, single, mostly clavate, also cylindrical, 20–65 × 4–9 µm. – Stipe scales made of dense bundles of cylindrical or inflated cells in chains, with thin or thickened walls (up to 1 µm), 15–50 × 4–25 µm, hyaline or with a brown pigment that is mostly diffuse, sometimes in plaques or incrusting. – Clamp connections absent in all examined tissues.

Etymology. – Referring to the long and robust stipe.

Habitat and distribution. – Gregarious to caespitose, more rarely solitary, in hardwood and mixed forests dominated by *Quercus*, particularly *Q. rubra*, in September and October, in calcareous soils. Widely distributed in northeastern North America. Confirmed by ITS sequence in Québec (Canada) and Massachusetts (USA). Reported from Ontario (Canada), Maine, New Hampshire, and Wisconsin (USA) based on pictures posted on MushroomObserver (https://mushroomobserver.org/).

Additional material examined. – *Ibid.* (QFB33132; isotype). Sequences ex-isotype: ON256909 (ITS). – CANADA. Québec, Notre-Dame-de-l'Île-Perrot, in a deciduous forest of *Quercus rubra* and *Fagus grandifolia*., in argillaceous soil, 3 September 2009, *leg*. R. Lebeuf & A. Paul, HRL0295; Sainte-Anne-de-Bellevue, Arboretum Morgan, under *Quercus rubra*, 19 September 2011, *leg*. R. Lebeuf & A. Paul, HRL0923; *ibid*., 27 September 2011, *leg*. R. Lebeuf & A. Paul, HRL0983; Sainte-Ursule, under *Quercus rubra*, 10 September 1994, *leg*. Y. Lamoureux, YL2303 (CMMF002303).

Notes. – The ITS sequence of the isotype is unique, differing from its closest relative, an unnamed sequence from New York (GenBank accession no. MZ206356), at more than 25 positions. In our phylogeny, *T. robustipes* clusters with *T. arvernense* Bon, *T. nigrum*, and *T. pseudoterreum*, described above (Fig. 21). These four species have in common a differentiated subpellis and the presence of distinct cheilocystidia. *Tricholoma arvernense* and *T. pseudoterreum* also have in common the presence of clamp connections in the pileipellis and at the base of basidia. *Tricholoma robustipes* is easily recognized in the field by its robust habit, yellow pileus usually with a brownish grey center, white or

pale-yellow lamellae often with a yellow edge, long stipe sometimes deeply buried in the soil and covered with usually dark concentric scales, and the pinkish orange discoloration of the whole basidioma with age or bruising. It is occasionally observed in hardwood forests of northeastern North America with *Quercus*, particularly *Q. rubra*. When conditions are favorable, large groups of basidiomata can be seen under a single tree.

Tricholoma insigne Ovrebo is another species that is known only from hardwood forests of *Quercus*, *Fagus*, and *Carya* in southeastern Michigan, which develops orange tints on all parts of the basidiomata with age or when bruised. It differs from *T. robustipes* by a more delicate habit (pileus 35–100 mm, stipe 30–80 × 6–17 mm) and different pileal colorations, in tones of reddish grey, grey, or greyish buff owing to the presence of long dark fibrils on a buff, pinkish buff, or reddish orange background. Like *T. robustipes*, *T. insigne* has cheilocystidia and can have a distinct subpellis (Ovrebo 1989). The somewhat similar *T. davisiae* Peck also develops reddish tints with age, but it is less robust, its pileus bears a prominent acute umbo, it is found under conifers, particularly *Pinus banksiana*, and its basidiospores are ellipsoid to oblong, measuring 5.7–9.5 × 4.3–5.2 µm (Ovrebo 1980, 1989). The similar *T. arvernense*, rarely reported in North America (Bessette et al. 2013, Trudell et al. 2022, Landry et al. 2022), has a brownish yellow, orange to olive brown pileus and is found only with conifers (Riva 1988, Christensen & Heilmann-Clausen 2013).

Authors: R. Lebeuf, J. Landry, Y. Lamoureux & A. Paul

Basidiomycota, Agaricomycetes, Agaricales, Tricholomataceae

Tricholoma* section *Rigida

Tricholoma pallens Lebeuf, Y. Lamoureux, A. Paul & J. Landry, **sp. nov.** – Fig. 23
MycoBank no.: MB 843712

Diagnosis. – Differs from the phylogenetically close *Tricholoma olivaceum* by its pileus and stipe color, basidiospore size and shape, presence of numerous cheilocystidia, host tree, and geographical distribution. Basidiospores 5.0–7.5 × 2.8–3.5 µm, on average 5.5 × 3.0 µm, in collections with 4-spored basidia.

Holotypus. – CANADA. Québec, Saint-Stanislas, Parc de la rivière Batiscan, trail La Gélinotte, 46°33'55.5"N, 72°24'14.5"W, 101 m a.s.l., under *Quercus rubra* and *Fagus grandifolia* in sandy soil by the trail, 30 July 2021, *leg.* R. Lebeuf & A. Paul, HRL3381 (DAOM 985004; holotype).

Description. – Pileus (25–)45–120 mm in diameter, hemispherical to convex, becoming planoconvex then applanate with a broad umbo; surface glabrous, subhygrophanous, quickly dry, in young basidiomata yellowish brown (5EF5) at center and olive yellow (4AB4) towards margin, becoming quickly brownish orange (5C4), olivaceous brown to olivaceous grey (4C3) at center and whitish towards margin, often cracking with age or in dry weather; margin inflexed then straight, thin, undate and lobed with age. – Lamellae emarginate, close to subdistant, occasionally forked, segmentiform, usually white, less frequently yellowish white (3A2), 5–11 mm broad. – Stipe 40–70 × (5–)8–20 mm, equal or widening towards base, with extreme base pointed and slightly rooting, flocculose to floccose and white at apex, below smooth to slightly fibrillose, very pale yellowish brown to olive yellow, stuffed then hollow. – Context thick, white, lightweighted. – Odor farinaceous, weakly reminiscent of *T. saponaceum*. – Taste farinaceous, mild to slightly acrid. – Basidiospores 5.0–6.0(–7.5) × 2.8–3.5 µm, av. 5.5 × 3.0 µm in collections with predominantly 4-spored basidia, (5–)5.5–8 × 3–4.5 µm, av. 6.7 × 3.7 µm in collections with predominantly 2-spored basidia, Q = 1.56–2.0, Q_{av} = 1.82 [116/4/4], oblong, smooth, inamyloid. – Basidia 22–30 × 5–6(–7) µm, 2(–3)- or 4-spored, narrowly clavate. – Cheilocystidia 15–40 × 2–7 µm, numerous, irregularly shaped (cylindrical, L-shaped, knobbed, branched, clavate, flexuose, curved), intermixed with basidia. – Pileipellis a cutis; hyphae repent, intricately interwoven, 2–9 µm broad, thin-walled, smooth, pale yellow to brownish yellow in masses, individually hyaline, many transversally sectioned owing to their orientation, with medallion clamps; subpellis not differentiated. – Stipitipellis a cutis made of 1.5–6 µm wide cylindrical hyphae, longitudinal or interwoven, smooth and thin-walled or finely incrusted with slightly thickened walls (up to 0.5 µm broad). – Caulocystidia 26–115 × 5–13 µm, present as recurved endcells on whole stipe surface but more numerous at apex, arranged in fascicles or more rarely single, smooth or finely incrusted, with thin or slightly thickened walls (up to 0.5 µm), in some collections polymorphic and similar to cheilocystidia (cylindrical, flexuose, curved, knobbed, some capitate), in other collections mostly clavate but also cylindrical-capitate, branched or L-shaped. – Clamp connections present in all examined tissues.

Etymology. – Referring to the pale color of basidiomata.

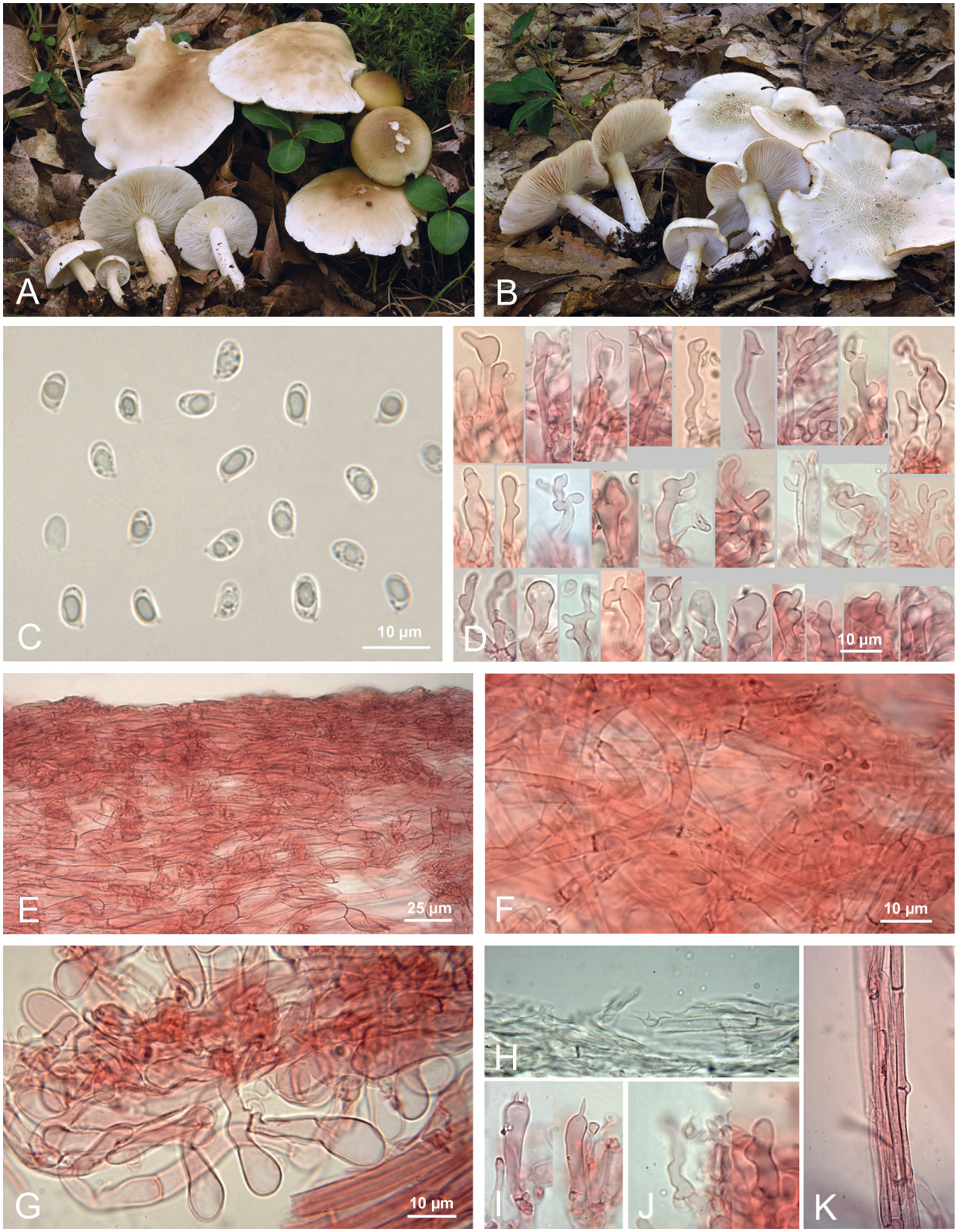

Fig. 23. *Tricholoma pallens*. **A.** Basidiomata *in situ*, collection DAOM 985004 (holotype). **B.** Basidiomata *in situ*, collection QFB33134. **C.** Basidiospores in 3 % KOH. **D.** Cheilocystidia. **E.** Pileipellis section in SDS Congo Red. **F.** Pileipellis view from above. **G.** Caulocystidia. **H–K.** Clamp connections (H) in pileipellis, (I) at the base of basidia, (J) at the base of cheilocystidia, (K) in stipitipellis.

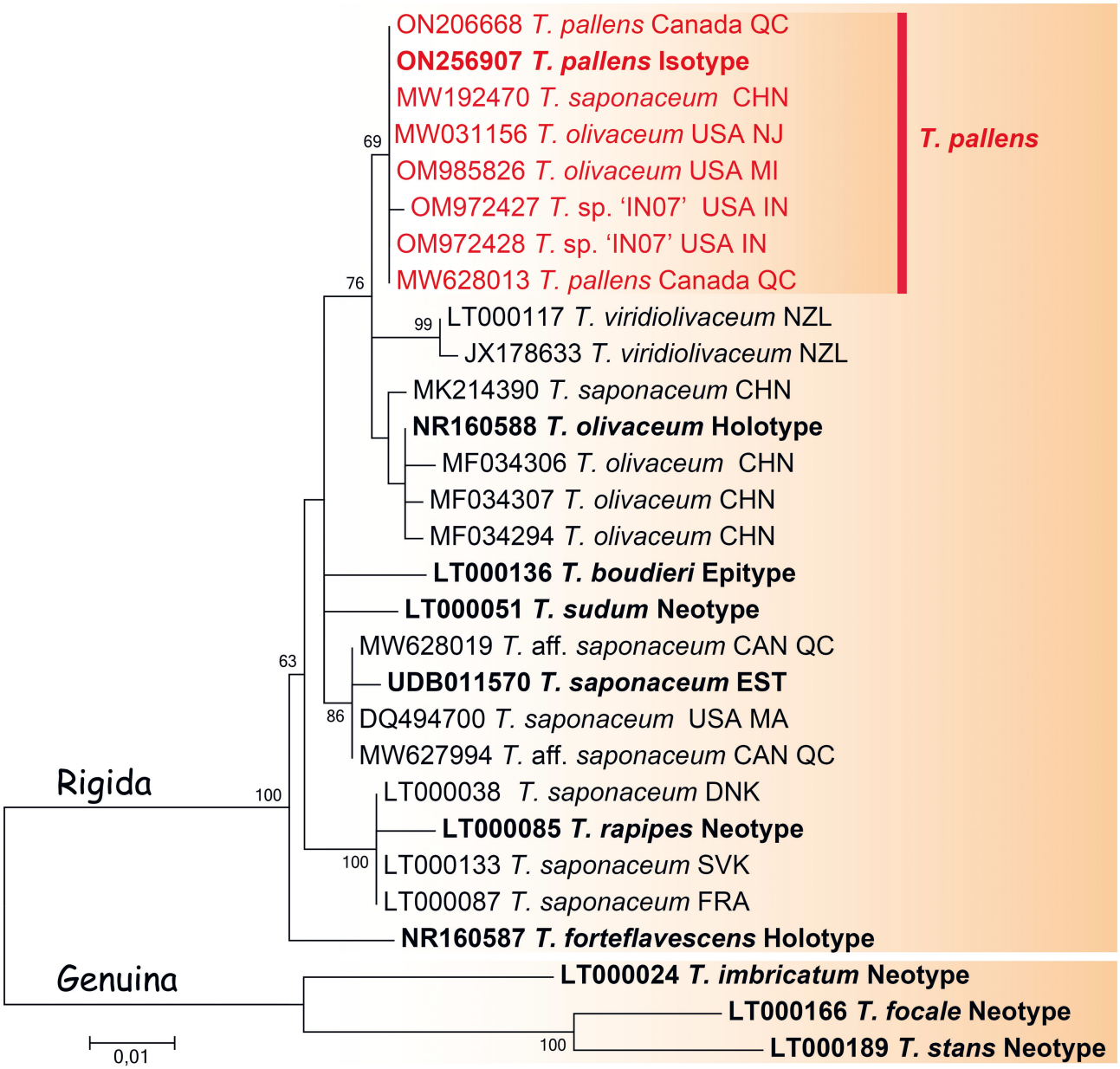

Fig. 24. Phylogeny of selected *Tricholoma* species in sections *Rigida* and *Genuina* reconstructed from an ITS dataset. The tree topology with the highest log likelihood (-lnL = 1737.8554) is shown, resulting from ML inference performed in MEGA7. MLBS values (if ≥60) are shown at the nodes. Section designations following Heilmann-Clausen et al. (2017) and Reschke et al. (2018), ex-type sequences in boldface, new species highlighted in red, bar indicating the expected number of substitutions per site.

Habitat and distribution. – Solitary to gregarious under *Quercus*, *Fagus* and possibly other hardwoods, in calcareous or sandy soil, from mid-July to September. Known from Canada (Québec) and the USA (New Jersey, Indiana, Michigan). Present in China based on an ITS sequence (GenBank accession no. MW192470).

Additional material examined. – *Ibid.* (QFB33134; isotype). Sequences ex-isotype: ON256907 (ITS). – CANADA. Québec, Saint-Stanislas, Parc de la rivière Batiscan, trail Le Portage, in a deciduous forest of *Quercus rubra* and *Fagus grandifolia*, in sandy soil, 20 August 2018, *leg.* R. Lebeuf & A. Paul, HRL2642; *ibid.*, trail Le Lièvre, in a deciduous forest of *F. grandifolia*, *Q. rubra*, and *Populus grandidentata*, in naked soil, 11 August 2022, *leg.* R. Lebeuf & A. Paul, HRL3809; Saint-Narcisse, Parc de la rivière Batiscan, trail Le Buis, at the base of an old *Q. rubra* in a deciduous forest also comprising *F. grandifolia* and *Acer* sp., in naked soil, 8 September 2022, *leg.* R. Lebeuf & A. Paul, HRL4012; Hérouxville, Tavibois, in a mixed forest of *Acer* sp. and planted *Picea* sp.,

adjacent to a small *Q. rubra* 60 cm tall, 14 July 2022, *leg.* R. Lebeuf & A. Paul, HRL3713; Rawdon, in a deciduous forest of *Q. rubra* and *Acer* sp., 8 August 2003, *leg.* Y. Lamoureux, YL3782 (CMMF003782). – USA, New Jersey, Ringwood, Sterling Forest/Tranquility, under *Q. rubra*, *F. grandifolia*, and *Acer* sp., 13 September 2020, *leg.* S. Jakob, iNaturalist ID 59500740 (DAOM 985005).

Notes. – The ITS sequence of the isotype is very similar to several species in section *Rigida*, deviating from its closest relative, *T. olivaceum* Reschke, Popa, Zhu L.Yang & G. Kost, by 3–6 substitutions and indels (Fig. 24). *Tricholoma pallens* is easily recognized in the field by its pileus that is brownish at center, becomes almost white towards margin, and cracks with age or in dry weather; its farinaceous odor weakly reminiscent of unscented soap; and its association with *Quercus*, *Fagus*, and possibly other hardwoods. The single basidioma in collection HRL4012 was old and showed some discoloration: the pileus surface, and to a lesser degree the stipe and the context at stipe base, had taken a pale pinkish buff (5A2) tint, and the pileus margin was orange-brown. We did not observe such a discoloration in our other collections, and did not mention it in the description, as it might not be constant. *Tricholoma olivaceum*, described from China (Reschke et al. 2018), differs morphologically and ecologically in several ways: the pileus is persistently bright olive with a brown to almost black center; the stipe is overlain by dark grey to black fibrils; the basidiospores are ellipsoid, measuring 4.5–6 × 3.5–4 µm; the cheilocystidia are lacking; and it is associated with *Pinus* sp. *Tricholoma saponaceum* (Fr.) P. Kumm., in its broad sense, even though highly variable in color and host trees, shares the same odor, glabrous pileus, and presence of clamp connections. However, it differs in its darker pileal colors and pinkish discoloration at the base of the stipe.

Authors: R. Lebeuf, J. Landry,Y. Lamoureux & A. Paul

Interesting taxonomical notes, new hosts, and geographical records

Ascomycota, Laboulbeniomycetes, Laboulbeniales, Laboulbeniaceae

Camptomyces africanus W. Rossi & M. Leonardi, Phytotaxa 358(2): 94 (2018). – Fig. 25

Material examined. – TANZANIA. Kilimanjaro Region, 14 km NE of Mwanga, North Pare Mountains, Ngofe Hill Forest Reserve, above Vuchama (Sofe) village, 3°35'00.90"S, 37°40'37.56"E, open forest, small and some medium size trees, 1538 m a.s.l., on *Astenus* sp. (Staphylinidae, Paederinae, Paederini), #37205, D. Haelew. 1222 [host labels], 17 November 2010, *leg.* V. Gusarov, slides D. Haelew. 1222a (1 juvenile and 2 mature thalli from sternites), D. Haelew. 1222b (2 juvenile, 1 submature, and 3 mature thalli from sternites), and D. Haelew. 1222c (1 mature thallus from right metatibia); *Ibid.*, on *Astenus* sp., #37204, D. Haelew. 1221 [host labels], 17 November 2010, *leg.* V. Gusarov, slide D. Haelew. 1221a (1 mature thallus from sternites).

Material sequenced. – TANZANIA. Kilimanjaro Region, 14 km NE of Mwanga, North Pare Mountains, Ngofe Hill Forest Reserve, above Vuchama (Sofe) village, 3°35'00.90"S, 37°40'37.56"E, open forest, small and some medium size trees, 1538 m a.s.l., on *Astenus* sp., #37205, D. Haelew. 1222 [host labels], 17 November 2010, *leg.* V. Gusarov, isolate D. Haelew. 1222d (1 mature thallus from sternites), MF314140 (SSU), MF314141 (LSU).

Description. – Thallus (238–)266–294–322(–319) µm from foot to perithecial tip [7], (129–)130–134–138(–140) µm from foot to tip of antheridial neck [5]. – Cell I (58–)61–66–72(–74) × (17–)18–20–22(–23) µm [10], fuscous, uppermost part hyaline, tapering towards the foot, the upper margin distinctly convex. – Cell II (14–)15–18–21(–25) × (19–)20–22–24(–26) µm [10], greyish brown, darker towards cell I, pentagonal, lateral margins slightly convex. – Cell III (15–)16–17–18 × (18–)19–21–23 µm [10], colored darker brown, quadrangular, slightly broader than long. – Antheridium 31–34–37(–41) × (15–)16–18–19(–20) µm [10], about (1.6–)1.9(–2.6) times as long as broad, broadly conical; consisting of three rows of increasingly smaller antheridial cells, extending obliquely upward from the flattened basal cell, and a distinctive, broad, upright efferent neck. – Cell VI hyaline, small, quadrangular, broader than long. – Cell VII 36–42–49(–50) × 19–22–25(–26) µm [3], hyaline, large, horn-shaped, gradually broadening upward. – Perithecium (123–)140–160–180(–182) × (34–)39–48–57 µm [7], yellowish brown, darker in lower part, broadly elliptical, widest below the middle, with indiscernible basal cells, anterior margin curving sigmoidally; elongated neck, slightly bent anteriorly, with subcylindrical margins, tapering to the blunt apex. – Ascospores (24–)25–28–32 × (2.89–)3.11–3.40–3.68(–3.80) µm [8], hyaline, acute-ended, two celled.

Notes. – The family Staphylinidae (rove beetles) is the most diverse family of beetles, with 58,331 species (Solodovnikov et al. 2013). According to Tavares (1979), the family also hosts the highest number of genera of Laboulbeniales: 49. One of these genera is *Camptomyces*. This genus was described to accommodate thalli with "a highly developed type of antheridium […] having a strictly terminal pore without appendages of any kind" (Thaxter 1894). Benjamin (1955) added that the spore apex in species of this genus becomes the terminal pore for discharge of spermatia. *Camptomyces* spe-

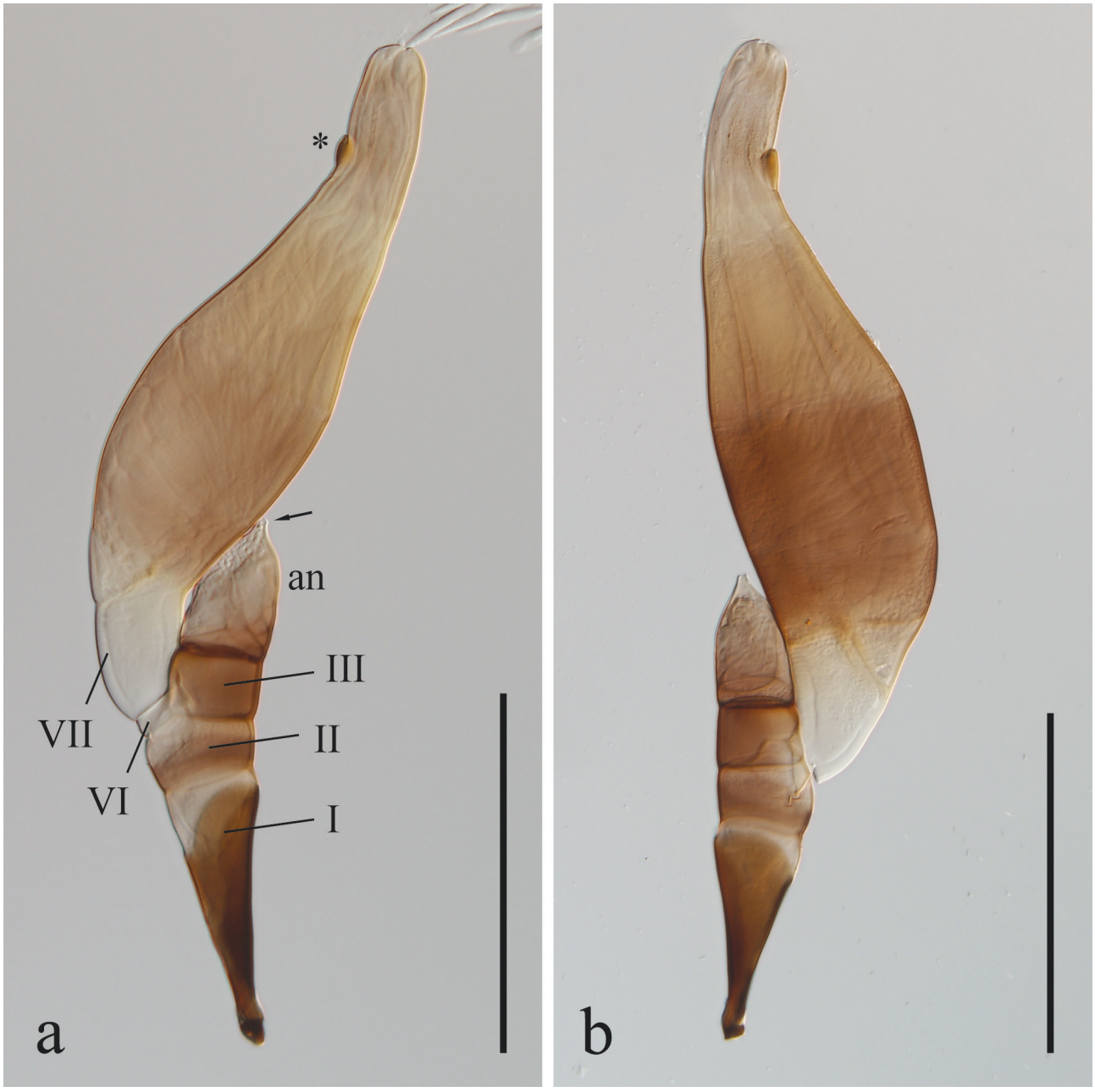

Fig. 25. *Camptomyces africanus*. **A.** Mature thallus, slide D. Haelew. 1221a. Indicated are cells I, II, and III of the receptacle, the compound antheridium (an) with discharge tube (arrow), cells VI and VII, and the remnant of the trichogyne (asterisk). **B.** Mature thallus, slide D. Haelew. 1222a. Scale bars 100 µm.

cies carry a "tongue-like lateral protuberance" below the perithecial apex (Thaxter 1926). All of the mature thalli of *C. africanus* that we observed show this character. This is the remnant of the trichogyne and is usually colored dark brown.

Nine species of *Camptomyces* have thus far been described, all from hosts in the genus *Astenus* Dejean, 1833 (Thaxter 1894, 1896, 1926; Rossi & Cesari Rossi 1980; Rossi & Leonardi 2018). *Camptomyces melanopus* Thaxt. was described from *Sunius prolixus* Erichson, 1844 and *S. longiusculus* Mannerheim, 1831, but these two species are now placed under *Astenus*. Five *Camptomyces* species are known from southeastern Asia (*C. brunneomarginatus* Thaxt., *C. falcatus* Thaxt., *C. recurvatus* Thaxt., *C. subsigmoideus* Thaxt., and *C. sumatrae* Thaxt.),

two species from the American continent (*C. guatemalensis* Thaxt. and *C. melanopus* Thaxt.), one from Europe (*C. europaeus* W. Rossi & Cesari), and one from Africa (*C. africanus* W. Rossi & M. Leonardi). We had presented our Tanzanian material as a new species in 2017 in a manuscript that was ultimately rejected. The *Camptomyces* material specifically was said by reviewers not to be distinguishable from other species such as *C. europaeus*, *C. falcatus*, and *C. sumatrae*—a suggestion we disagree with. Months after this rejection, *C. africanus*, equal in morphology, was described on *Astenus* sp. from Sierra Leone, based on three mature and three immature thalli by Rossi & Leonardi (2018). Here, we report our Tanzanian material as the second country record of *C. africanus*.

Thalli studied here differ slightly from the original description in being more variable in size of the perithecium (123–182 × 34–57 µm vs. 135–140 × 50–52 µm) and the compound antheridium (31–41 µm long vs. 32–35 µm). The ascospores we observed were shorter than those in Rossi & Leonardi (2018): 24–32 µm (mean 29 µm) vs. "about 32 µm". In addition, our thalli were longer than those cited in the protologue (238–319 µm from foot to tip of perithecium vs. 205–215 µm and 129–140 µm from foot to tip of antheridial neck vs. 105–115 µm). Notwithstanding these slight differences in measurements, we see no reason to separate our material from *C. africanus*. This is the first record since the description of the species; *C. africanus* is now known from two collections, one from Sierra Leone (Rossi & Leonardi 2018) and one from Tanzania (this study). It is thus no surprise that we observe some morphological variability with this limited material. Measurements of cells I, II, III, and VII could not be compared since these are lacking in the original description (Rossi & Leonardi 2018).

Camptomyces europaeus differs from *C. africanus* primarily in its receptacle cells: cell I is less elongate compared to *C. africanus*, and cell II is flattened and completely opaque in its lower part. In addition, its cell VI is much larger compared to *C. africanus* (Rossi & Cesari Rossi 1980). *Camptomyces falcatus* differs in its very slender habitus and perithecial basal cells, which are almost as long as the stalk cell (VI). *Camptomyces brunneomarginatus* has a typically darkened cell of the perithecial apex and has very conspicuous ridges at the perithecial margins between the tiers of wall cells. Perithecial ridges or "elevations" (Thaxter 1926) are also present in *C. guatemalensis*, *C. melanopus*, *C. recurvatus*, *C. subsigmoideus*, and *C. sumatrae*. In *C. sumatrae*, the elevations are only slight, but this species also differs from *C. africanus* in its opaque cells I and II, which are separated by an oblique, hyaline septum.

We generated an SSU and LSU sequence of *C. africanus*. These represent the first sequence data for this genus. Phylogenetic reconstructions of SSU–LSU datasets (Blackwell et al. 2020, Haelewaters et al. 2020) resolved this species as sister to *Stigmatomyces* H. Karst. sensu lato (consisting of *Appendiculina* Berl., *Fanniomyces* T. Majewski, *Gloeandromyces* Thaxt., and *Stigmatomyces* sensu stricto. Following the classification system by Tavares (1985), the genus *Camptomyces* belongs to family Laboulbeniaceae, subfamily Peyritschiellioideae, tribe Haplomyceteae, subtribe Haplomycetinae. It has already been established that several subtribes (e.g., Stigmatomycetinae) and tribes (e.g., Laboulbenieae) in their current circumscription are polyphyletic. Isolates of *Cantharomyces* Thaxt. and *Haplomyces* Thaxt. should be obtained to investigate the status of tribe Haplomyceteae.

Authors: D. Haelewaters & M. Gorczak

Basidiomycota, Agaricomycetes, Agaricales, Tricholomataceae

Tricholoma* section *Genuina

Tricholoma fulvimarginatum Ovrebo & Halling, Brittonia 38(3): 260 (1986). – Fig. 26

Material examined. – CANADA. Québec, Saint-Stanislas, Parc de la rivière Batiscan, Trail des Gras, in a mixed forest of *Populus tremuloides*, *Betula* sp. and *Abies balsamea*, 8 October 2018, *leg.* R. Lebeuf & A. Paul, HRL2816 (DAOM 985000; QFB32648); Saint-Stanislas, Parc de la rivière Batiscan, trail Le Portage, in a mixed forest of *Quercus rubra*, *Pinus strobus*, *Abies balsamea*, *Fagus grandifolia*, *Populus tremuloides*, and *Alnus* sp., in sandy soil, by the trail, 2 October 2019, *leg.* R. Lebeuf, HRL3124 (QFB32658; in HRL); Saint-Casimir, chemin Sainte-Anne, in a mixed forest of *Populus* sp., *Betula* sp. and *Picea glauca*, in sandy soil, by the trail, 3 October 2010, *leg.* R. Lebeuf & A. Paul, HRL0634 (QFB32609; in HRL); Gaspé, teaching forest of Cégep de la Gaspésie et des Îles, in a forested area, under *Populus tremuloides* and *Abies balsamea*, in soil, 11 October 2021, *leg.* R. Lebeuf & A. Paul, HRL3617 (QFB33141; in HRL); Saint-Alban, Parc naturel régional de Portneuf, sentier à Ti-Mé, in a mixed forest of *P. tremuloides* and *A. balsamea*, in naked soil, 6 October 2022, *leg.* A. Paul, HRL4108; Saint-Majorique-de-Grantham, at the edge of a mixed forest, under a large group of *Populus* spp., in soil, 27 September 1995, *leg.* Y. Lamoureux, YL2688 (CMMF002688); Sacré-Coeur, under *Populus* sp., *A. balsamea* and *Pinus banksiana*, in soil, 11 October 2019, *leg.* H. Lambert, HL1668 (QFB32593).

Description. – Pileus 40–80(–100) mm in diameter, parabolic, convex, plano-convex, then applanate, sometimes with a low broad umbo, irregular; surface viscid, apricot orange, ochraceous to

Fig. 26. *Tricholoma fulvimarginatum*. **A.** Basidiomata *in situ*, collection DAOM 985000. **B.** Collection CMMF003587. **C.** Collection HRL0634. **D.** Collection HRL3617. **E.** Basidiospores. **F.** Pileipellis section in SDS Congo Red. **G–H.** Caulocystidia.

ochraceous orange (5A6, 5A7, 5AB7, 5B5, 6B5, 6B8), darker when young, paler at margin, with dark brown appressed fibrils or streaked with long innately radiating fibrils; margin inflexed then straight, becoming paler with age. – Lamellae emarginate, close to crowded, segmentiform, 4–9 mm broad, white to orange-white (5A2); edge entire, developing orangish brown spots with age. – Stipe 30–90 × 8–18 mm, equal, more rarely clavate or tapering at base, white and flocculose at apex, below white when very young but soon concolorous with pileus and with brown projecting fibrils. – Context white, brownish orange at extreme stipe base, thick, fibrous, discoloring brownish orange in larval perforations. – Odor farinaceous. – Taste farinaceous, mild. – Basidiospores (4.0–)4.5–6.0(–6.5) × 3.0–4.0(–4.5) µm, av. 5.3 × 3.5 µm, Q = 1.11–1.83, Q_{av} = 1.49 [180/6/6], ellipsoid, oblong, inamyloid, smooth. – Basidia 23–36 × 5–7 µm, 4-spored, narrowly clavate. – Cheilocystidia absent. – Pileipellis an ixocutis 50–250(–400) µm thick; hyphae in matrix repent, interwoven or ascending, 2–8 µm broad, smooth or finely to coarsely incrusted, hyaline individually, pale yellow in mass; underlying hyphae 2.5–7 µm broad, parallel or in bundles, pale yellow in mass, smooth or incrusted, at times coarsely so; subpellis not differentiated. – Stipitipellis a cutis made of cylindrical hyphae 2–13 µm broad, narrow at apex and wider below, longitudinal, superficially entangled, mostly thin-walled, some thick-walled (up to 1 µm), smooth, rarely finely incrusted, hyaline or yellowish brown. – Caulocystidia 12–64 × 4–9 µm, present as recurved end-cells at stipe apex, single or forming small to large fascicles, cylindrical, cylindrical-flexuose, sometimes slightly wider at apex, more rarely clavate, absent lower on stipe – Clamp connections absent in all examined tissues.

Habitat and distribution. – Occasional, in small groups in mixed forests with *Populus* spp., in soil, in late fall (October). Thus far known from the provinces of Québec and Ontario, in Canada, and from the states of Massachusetts and New York, in the USA.

Notes. – *Tricholoma fulvimarginatum* was described by Ovrebo & Halling (1986) from Massachusetts as a member of section *Genuina* growing with *Populus deltoides*. The epithet refers to the color of the lamellar edge, said by Ovrebo & Halling to be "more or less concolorous (Hazel) with pileus throughout development". The species went mostly unnoticed afterwards, as evidenced by the few records found through a search in MyCoPortal (2022): two collections in Canada (Québec and Ontario) from 1986 and one in the USA (New York State) from 2018. In a recent monograph of the genus in North America (Bessette et al. 2013), the species was reported to be occasional in Massachusetts and New York and likely to occur elsewhere in New England and southeastern Canada.

During their survey of *Tricholoma* growing in Québec, Landry et al. (2022) studied many collections of a long-known and occasional species associated with *Populus*, with lamellar edge whitish at first and staining brownish orange with age only. The morphological characters were consistent with the description of *T. fulvimarginatum*, except for the non-marginate lamellae in young stage. Furthermore, the Québec species was found in association with several species of *Populus*, including *P. deltoides*, *P. grandidentata*, and *P. tremuloides*. In some cases, a single *Populus* tree was present in the forested area where the basidiomata were collected and was therefore difficult to see.

Owing to the similarity observed, an ITS sequence of the type specimen of *T. fulvimarginatum* was obtained and proved to be almost identical with the sequences of the Québec collections, the latter differing at most by 1 indel (Fig. 18). Therefore, it appears that *T. fulvimarginatum* is an occasional species with a lamellar edge that can be either whitish or fulvous in young stage. Moreover, it can associate with several species of *Populus*.

Tricholoma fulvimarginatum is well characterized by its rather bright apricot orange, ochraceous to ochraceous orange pileus and stipe, the context discoloring brownish orange when bruised or with age, and its association with *Populus* spp. Among the other orange to orange-brown-capped *Tricholoma* species, *T. aurantium* (Schaeff.) Ricken is the most similar, with its bright orange colors, but it is not associated with *Populus*, and its stipe has a white band at apex and the orange covering breaks into bands with age. *Tricholoma ustaloides* Romagn. and a yet undescribed similar species in northeastern North America occur with *Quercus* and have a bitter pileipellis. *Tricholoma ustale* (Fr.) P. Kumm. is associated with *Fagus* and has indistinct or slightly farinaceous odor and taste. The *Populus*-associated *T. populinum* J.E. Lange differs by its less vividly colored pileus, rather brownish orange to brownish red, and whitish stipe with orangish or brownish fibrils mostly in the lower part. Based on the ITS sequences available in GenBank and UNITE, it is absent from the North American continent. *Tricholoma ammophilum* A.D. Parker, Grubisha & S.A. Trudell, another *Populus*-associated species recently described from the west coast of

North America (Trudell & Parker 2021) and also occurring on the east coast (Landry et al. 2022), differs by its pale brown to reddish brown pileus and white stipe browning with age.

Authors: R. Lebeuf, J. Landry,Y. Lamoureux & A. Paul

Acknowledgements

The editor is thankful for 17 reviewers whose relevant and detailed comments greatly improved the contributions from FUSE 9. R.H. thanks John Pearson and the Iowa Department of Natural Resources for their support for collecting fungi in Iowa State Parks and Preserves, and the Iowa State Preserves Board for permission to collect in preserves. The *Diversispora* authors thank the farmers of the towns Paucarpata and Pamashto (Lamas Province) for providing the facilities to collect soil samples. The *Diversispora* study was supported by the Consejo Nacional de Ciencia, Tecnología e Innovación Tecnológica, within the framework of the project with grant no. 163-2020-FONDECYT. The *Inocybe* study received financial support from the University of the Punjab, Lahore, Pakistan (research grant 2021–2022 to A.N.). The *Mycena* authors thank the Dutch Mycological Society for financial support (Ger Van Zanen legacy) and Lieve Deceuninck for her critical analysis of some basidiomata. The *Phaeotremella* author extends his gratitude to Timothy Y. James for mentorship; Sarah DeLong-Duhon for identifying *Stereum* fungi; Brian P. Looney for advice on studying the micromorphology of jelly fungi; Shaun R. Pennycook for providing expert information on the grammar of scientific nomenclature; Taylor Tai for fieldwork assistance; community scientists Terri Clements and Donna Fulton for contributing tremendously to the documentation of Arizona's funga; the curators, managers, and staff of fungaria that loaned specimens for study; and the Ho-Chunk Nation broadly and Casey J. Brown, Public Relations Officer of the Office of the President, specifically for engaging in joyful dialogue around the naming of *P. dejopia* and for sharing the Ho-Chunk language to commemorate the holotype locality. The *Tricholoma* authors are grateful to Raymond Archambault, curator of CMMF, Sigrid Jakob, and Herman Lambert for lending material to study; Pablo Alvarado for providing a sequence of *T. pallens*; and Mycoquébec for providing sequencing funds for the study on *Tricholoma*. The *Camptomyces* authors are grateful to Vladimir Gusarov (Natural History Museum, University of Oslo, Norway) for sending Laboulbeniales-infected host insects to be studied, Ondřej Koukol for making photographs of Laboulbeniales thalli, and the Pfister Lab at the Harvard University Herbaria for logistical and curatorial support.

References

Abarenkov K., Nilsson R.H., Larsson K.-H., Alexander I., Eberhardt U., Erland S., et al. (2010) The UNITE database for molecular identification of fungi – recent updates and future perspectives. *New Phytologist* **186**(2): 281–285.

Aravindakshan D.M., Manimohan P. (2015) *Mycenas of Kerala*. SporePrint Books, Calicut. India.

Aronsen A., Larsson E. (2015) Studier i släktet *Mycena* (hättor). *Svensk Mykologisk Tidskrift* **36**: 23–29.

Balázs T.K., Błaszkowski J., Chwat G., Góralska A., Gáspár B.K., Lukács A.F., Kovács G.M. (2015) Spore-based study of arbuscular mycorrhizal fungi of semiarid sandy areas in Hungary, with *Diversispora jakucsiae* sp. nov. *Mycological Progress* **14**(1): 1021.

Bengtsson-Palme J., Ryberg M., Hartmann M., Branco S., Wang Z., Godhe A., et al. (2013) Improved software detection and extraction of ITS1 and ITS2 from ribosomal ITS sequences of fungi and other eukaryotes for analysis of environmental sequencing data. *Methods in Ecology and Evolution* **4**: 914–919.

Benjamin R.K. (1955) New genera of Laboulbeniales. *El Aliso* **3**: 183–197.

Benjamin R.K. (1971) Introduction and supplement to Roland Thaxter's contribution towards a monograph of the Laboulbeniaceae. *Bibliotheca Mycologica* **30**: 1–155.

Berbee M.L., Pirseyedi M., Hubbard S. (1999) *Cochliobolus* phylogenetics and the origin of known, highly virulent pathogens inferred from ITS and glyceraldehyde-3-phosphate dehydrogenase gene sequences. *Mycologia* **91**(6): 964–977.

Bessette A.E, Bessette A.R., Roody W.C., Trudell S.A. (2013) *Tricholomas of North America – a mushroom field guide*. University of Texas Press, Austin, TX.

Bidartondo M.I., Bruns T.D. (2002) Fine-level mycorrhizal specificity in the *Monotropoideae* (*Ericaceae*): specificity for fungal species groups. *Molecular Ecology* **11**(3): 557–569.

Bidaud A., Carteret X., Eyssartier G., Moënne-Loccoz P., Reumaux P. (2002) *Atlas des Cortinaires, Pars XII, Sous-genre* Dermocybe *(Fries) Trog, Section* Sericeocybe *(P.D. Orton) Melot*. Éditions Fédération mycologique Dauphiné-Savoie, Lyon, France.

Blackwell M., Haelewaters D., Pfister D.H. (2020) Laboulbeniomycetes: Evolution, natural history, and Thaxter's final word. *Mycologia* **112**(6): 1048–1059.

Błaszkowski J., Blanke V., Renker C., Buscot F. (2004) *Glomus aurantium* and *G. xanthium*, new species in Glomeromycota. *Mycotaxon* **90**(2): 447–467.

Błaszkowski J., Furrazola E., Chwat G., Goralska A., Lukacs A.F., Kovacs G.M. (2015) Three new arbuscular mycorrhizal *Diversispora* species in Glomeromycota. *Mycological Progress* **14**(11): 105.

Błaszkowski J., Niezgoda P., de Paiva J.N., da Silva K.J.G., Theodoro R.C., Jobim K., et al. (2019) *Sieverdingia* gen. nov., *S. tortuosa* comb. nov., and *Diversispora peloponnesiaca* sp. nov. in the Diversisporaceae (Glomeromycota). *Mycological Progress* **18**(11): 1363–1382.

Błaszkowski J., Niezgoda P., Zubek S., Meller E., Milczarski P., Malinowski R., et al. (2022) Three new species of arbuscular mycorrhizal fungi of the genus *Diversispora* from maritime dunes of Poland. *Mycologia* **114**(2): 453–466.

Bouckaert R., Drummond A.J. (2017) bModelTest: Bayesian phylogenetic site model averaging and model comparison. *BMC Ecology and Evolution* **17**(42).

Bouckaert R., Vaughan T.G., Barido-Sottani J., Duchêne S., Fourment M., Gavryushkina A., et al. (2019) BEAST 2.5: An advanced software platform for Bayesian evolutionary analysis. *PLoS Computational Biology* **15**(4): e1006650.

Bougher N.L. (2009) Two intimately co-occurring species of *Mycena* section *Sacchariferae* in south-west Australia. *Mycotaxon* **108**: 159–174.

Brandrud T.E., Dima B., Schmidt-Stohn G., Bellù F. (2014) *Cortinarius* subgenus *Phlegmacium* section *Multiformes* in Europe. *Journal des JEC* **16**: 162–199.

Brandrud T.E., Lindström H., Marklund H., Melot J., Muskos S. (1990–2014) Cortinarius *Flora Photographica*. Cortinarius HB, Östansjö, Sweden.

Breitenbach J., Kränzlin F. (1991) *Champignons de Suisse, Tome 3, Bolets et champignons à lames* (1ère partie). Verlag Mykologia Luzern, Kaznejov, Czech Republic.

Brodegger E., Koncilja M., Krisai-Greilhuber I. (2019) Ein rezenter Fund von *Mycena chloroxantha* var. *appalachienensis* aus dem Botanikzentrum Klagenfurt. Österreichische Zeitschrift für Pilzkunde **27**: 59–64.

Brown S.P., Rigdon-Huss A.R., Jumpponen A. (2014) Analyses of ITS and LSU gene regions provide congruent results on fungal community responses. *Fungal Ecology* **9**: 65–68.

Brun S., Madrid H., Van Den Ende B.G., Andersen B., Marinach-Patrice C., Mazier D., de Hoog G.S. (2013) Multilocus phylogeny and MALDI-TOF analysis of the plant pathogenic species *Alternaria dauci* and relatives. *Fungal Biology* **117**(1): 32–40.

Brundrett M., Melville L., Peterson L. (1994) *Practical methods in mycorrhizal research*. Mycologue Publications, University of Guelph, Guelph, Canada.

Bruns T.D. (1995) Thoughts on the processes that maintain local species diversity of ectomycorrhizal fungi. *Plant Soil* **170**(1): 63–73.

Caligiorne R.B., Licinio P., Dupont J., de Hoog G.S. (2005) Internal transcribed spacer rRNA gene-based phylogenetic reconstruction using algorithms with local and global sequence alignment for black yeasts and their relatives. *Journal of Clinical Microbiology* **43**: 2816–2823.

Capella-Gutiérrez S., Silla-Martínez J.M., Gabaldón T. (2009) TrimAl: A tool for automated alignment trimming in large-scale phylogenetic analyses. *Bioinformatics* **25**: 1972–1973.

Castillo B.T., Nave L.E., Le Moine J.M., James T.Y., Nadelhoffer K.J. (2018) Impacts of experimentally accelerated forest succession on belowground plant and fungal communities. *Soil Biology and Biochemistry* **125**: 44–53.

Chen C.J. (1998) Morphological and molecular studies in the genus *Tremella*. *Bibliotheca Mycologica* **174**: 1–225.

Chernomor O., Von Haeseler A., Minh B.Q. (2016) Terrace aware data structure for phylogenomic inference from supermatrices. *Systematic Biology* **65**(6): 997–1008.

Christensen M., Heilmann-Clausen J. (2013) *The genus Tricholoma – Fungi of Northern Europe* 4. Narayana Press, Odder, Denmark.

Coker W.C. (1920) Notes on the lower Basidiomycetes of North Carolina. *Journal of the Elisha Mitchell Scientific Society* **35**: 113–182.

Cooper A., Desjardin D.E., Perry B.A. (2018) The genus *Mycena* (Basidiomycota, Agaricales, *Mycena*ceae) and allied genera from Republic of São Tomé and Príncipe, West Africa. *Phytotaxa* **383**: 1–47.

Corazon-Guivin M.A., Cerna-Mendoza A., Guerrero-Abad J.C., Vallejos-Tapullima A., Carballar-Hernández S., da Silva G.A., Oehl F. (2019a) *Funneliglomus*, gen. nov., and *Funneliglomus sanmartinensis*, a new arbuscular mycorrhizal fungus from the Amazonia region in Peru. *Sydowia* **71**: 17–24.

Corazon-Guivin M.A, Cerna-Mendoza A., Guerrero-Abad J.C, Vallejos-Tapullima A, Carballar-Hernández S, da Silva G.A, Oehl F. (2019b) *Microkamienskia* gen. nov. and *Microkamienskia peruviana*, a new arbuscular mycorrhizal fungus from Western Amazonia. *Nova Hedwigia* **109**(3–4): 355–368.

Corazon-Guivin M.A., Cerna-Mendoza A., Guerrero-Abad J.C., Vallejos-Tapullima A., Carballar-Hernández S., da Silva G.A., Oehl F. (2019c) *Nanoglomus plukenetiae*, a new fungus from Peru, and a key to small-spored Glomeraceae species, including three new genera in the "*Dominikia* complex/clades". *Mycological Progress* **18**(12): 1395–1409.

Corazon-Guivin M.A, Cerna-Mendoza A., Guerrero-Abad J.C., Vallejos-Tapullima A., da Silva G.A., Oehl F. (2019d) *Acaulospora aspera*, a new fungal species in the Glomeromycetes from rhizosphere soils of the inka nut (*Plukenetia volubilis* L.) in Peru. *Journal of Applied Botany and Food Quality* **92**: 250–257.

Corazon-Guivin M.A.,Vallejos-Tapullima A., de la Sota-Ricaldi A.M., Vallejos-Torres G., Ruíz-Sánchez M.E., Santos V.M., et al. (2022a) *Acaulospora flavopapillosa*, a new fungus in the Glomeromycetes from a coffee plantation in Peru. *Journal of Applied Botany and Food Quality* **95**: 6–16.

Corazon-Guivin M.A., Vallejos-Tapullima A., Rengifo-Del Aguila S., Rondiel N.V., Hernández L.V., Carvajal F.M., Carballar-Hernández S. (2022b) Influence of substrate properties on communities of arbuscular mycorrhizal fungi isolated from agroecosystems in Peru. *Journal of Soil Science and Plant Nutrition* **22**: 4784–4797.

Corazon-Guivin M.A., Vallejos-Tapullima A., Vallejos-Torres G., Tenorio-Cercado M., Mendoza-Caballero W., Marín C., et al. (2022c) *Rhizoglomus cacao*, a new species of the Glomeraceae from the rhizosphere of *Theobroma cacao* in Peru, with an updated identification key for all species attributed to *Rhizoglomus*. *Nova Hedwigia* **115**(1–2): 99–115.

Cortés-Pérez A., Desjardin D.E., Perry B.A., Ramírez-Cruz V., Ramírez-Guillén F.,Villalobos-Arámbula A.R., Rockefeller A. (2019) New species and records of bioluminescent *Mycena* from Mexico. *Mycologia* **111**(2): 319–338.

Dai Y.C. (2011) A revised checklist of corticioid and hydnoid fungi in China for 2010. *Mycoscience* **52**(1): 69–79.

Darriba D., Posada, D., Kozlov, A.M., Stamatakis, A., Morel, B., Flouri, T. (2020). ModelTest-NG: a new and scalable tool for the selection of DNA and protein evolutionary models. *Molecular Biology and Evolution*. **37**(1): 291–294.

de García V., Brizzio S., Russo G., Rosa C.A., Boekhout T., Theelen B., et al. (2010) *Cryptococcus spencermartinsiae* sp. nov., a basidiomycetous yeast isolated from glacial waters and apple fruits. *International Journal of Systematic and Evolutionary Microbiology* **60**(3): 707–711.

Degawa Y., Endoh R., Masumoto H.,Yoshihashi Y., Ohkuma M., Degawa Y. (2022) Taxonomic study of polymorphic basidiomycetous fungi *Sirobasidium* and *Sirotrema*: *Sirobasidium apiculatum* sp. nov., *Phaeotremella translucens* comb. nov. and rediscovery of *Sirobasidium japonicum* in Japan. *Antonie van Leeuwenhoek* **115**: 1421–1436.

DeLong-Duhon S.G., Bagley R.K. (2020) Phylogeny, morphology, and ecology resurrect previously synonymized species of North American *Stereum*. *BioRxiv*. doi: 10.1101/2020.10.16.342840

Desjardin D.E. (1995) A preliminary accounting of the worldwide members of *Mycena* sect. *Sacchariferae*. *Bibliotheca Mycologica* **159**: 1–89.

Desjardin D.E., Capelari M., Stevani C. (2007) Bioluminescent *Mycena* species from São Paulo, Brazil. *Mycologia* **99**(2): 317–331.

Dima B., Liimatainen K., Niskanen T., Bojantchev D., Harrower E., Papp V., et al. (2021) Type studies and fourteen new North American species of *Cortinarius* section *Anomali* reveal high continental species diversity. *Mycological Progress* **20**: 1399–1439.

Dima B., Lindström H., Liimatainen K., Olson Å., Soop K., Kytövuori I., et al. (2016) Typification of Friesian names in *Cortinarius* sections *Anomali*, *Spilomei*, and *Bolares*, and

description of two new species from northern Europe. *Mycological Progress* **15**: 903–919.
Dirks, A.C., Jackson, R.D. (2020) Community structure of arbuscular mycorrhizal fungi in soils of switchgrass harvested for bioenergy. *Applied and Environmental Microbiology* **86**(19): e00880-20.
Drummond A.J., Rambaut A. (2007) BEAST: Bayesian evolutionary analysis by sampling trees. *BMC Evolutionary Biology* **7**(1): 214.
Edgar R.C. (2004) MUSCLE: multiple sequence alignment with high accuracy and high throughput. *Nucleic Acids Research* 32(5): 1792–1797.
Esteve-Raventós F., Niskanen T., Platas G., Liimatainen K., Ortega A. (2013) *Cortinarius pseudofallax* (Cortinariaceae, Agaricales), the first records from the Iberian Peninsula and Fennoscandia, and taxonomic notes on the *C. parvannulatus/cedriolens* group. *Mycological Progress* **13**: 393–398.
Estrada B., Palenzuela J., Barea J.M., Ruiz-Lozano J.M., da Silva G.A., Oehl F. (2011) *Diversispora clara* (Glomeromycetes)–a new species from saline dunes in the Natural Park Cabo de Gata (Spain). *Mycotaxon* **118**(1): 73–81.
Fell J.W., Boekhout T., Fonseca A., Scorzetti G., Statzell-Tallman A. (2000). Biodiversity and systematics of basidiomycetous yeasts as determined by large-subunit rDNA D1/D2 domain sequence analysis. *International Journal of Systematic and Evolutionary Microbiology* **50**(3): 1351–1371.
Flouri T., Izquierdo-Carrasco F., Darriba D., Aberer A.J., Nguyen L.T, Minh B.Q., et al. (2014) The phylogenetic likelihood library. *Systematic Biology* **64**(2): 356–362.
Gamper H.A., Walker C., Schüßler A. (2009) *Diversispora celata* sp. nov: molecular ecology and phylotaxonomy of an inconspicuous arbuscular mycorrhizal fungus. *New Phytologist* **182**(2): 495–506.
Gao J., Xie R., Wang N., Zhang J., Sun X., Wang H., et al. (2022) Rapid identification of *Amanita citrinoannulata* poisoning using colorimetric and real-time fluorescence and loop-mediated isothermal amplification (LAMP) based on the nuclear ITS region. *Food Chemistry: Molecular Sciences* **4**: 100082.
Gardes M., Bruns T.D. (1993) ITS primers with enhanced specificity for Basidiomycetes – application to the identification of mycorrhizae and rusts. *Molecular Ecology* **2**(2): 113–118.
Gouy M., Guindon S., Gascuel O. (2010) SeaView version 4: A multiplatform graphical user interface for sequence alignment and phylogenetic tree building. *Molecular Biology and Evolution* **27**(2): 221–224.
Gubitz C. (2012) Eine mykofloristische Bestandsaufnahme in den Gewächshäusern des Ökologisch-Botanischen Gartens der Universität Bayreuth – Teil 2. *Zeitschrift für Mycologie* **78**: 9-52.
Guillén A., Serrano-Tamay F.J., Peris J.B., Arrillaga I. (2020) *Diversispora valentina* (Diversisporaceae), a new species of arbuscular mycorrhizal fungi from the Mediterranean sand dunes of Spain. *Phytotaxa* **468**(1): 62–74.
Guindon S., Gascuel O. (2003) A simple, fast, and accurate algorithm to estimate large phylogenies by maximum likelihood. *Systematic Biology* **52**(5): 696–704.
Haelewaters D., De Kesel A., Pfister D.H. (2018) Integrative taxonomy reveals hidden species within a common fungal parasite of ladybirds. *Scientific Reports* **8**(1): 15966.
Haelewaters D., Dima B., Abdel-Hafiz B.I.I., Abdel-Wahab M.A., Abul-Ezz S.R., Acar I., et al. (2020) Fungal Systematics and Evolution 6. *Sydowia* **72**: 231–356.
Haelewaters D., Gorczak M., Pfliegler W.P., Tartally A., Tischer M., Wrzosek M., Pfister D.H. (2015) Bringing Laboulbeniales to the 21st century: enhanced techniques for extraction and PCR amplification of DNA from minute ectoparasitic fungi. *IMA Fungus* **6**(2): 363–372.
Haelewaters D., Pfliegler W.P., Gorczak M., Pfister D.H. (2019) Birth of an order: comprehensive molecular phylogenetic study reveals that *Herpomyces* (Fungi, Laboulbeniomycetes) is not part of Laboulbeniales. *Molecular Phylogenetics and Evolution* **133**: 286–301.
Haelewaters D., Schoutteten N., Medina-van Berkum P., Martin T.E., Verbeken A., Aime M.C. (2021) Pioneering a fungal inventory at Cusuco National Park, Honduras. *Journal of Mesoamerican Biology* **1**(1): 111–131.
Hall T.A. (1999) BioEdit: a user-friendly biological sequence alignment editor and analysis program for Windows 95/98/NT. *Nucleic Acids Symposium Series* **41**: 95–98.
Harder C.B., Læssøe T., Frøslev T.G., Ekelund F., Rosendahl S., Kjøller R. (2013) A three-gene phylogeny of the *Mycena pura* complex reveals 11 phylogenetic species and shows ITS to be unreliable for species identification. *Fungal Biology* **117**: 764–775.
Heilmann-Clausen J., Christensen M., Frøslev T.G., Kjøller R. (2017) Taxonomy of *Tricholoma* in northern Europe based on ITS sequence data and morphological characters. *Persoonia* **38**: 38–57.
Hernández-Restrepo M., Madrid H., Tan Y.P., da Cunha K.C., Gené J., Guarro J., Crous P.W. (2018) Multi-locus phylogeny and taxonomy of *Exserohilum*. *Persoonia* **41**(1): 71–108.
Hewitt E.J. (1966) *Sand and water culture methods used in the study of plant nutrition*. Farnhan Royal, Commonwealth Agricultural Bureau, Farnham, England.
Hoang D.T., Chernomor O., von Haeseler A., Minh B.Q., Vinh L.S. (2018) UFBoot2: Improving the ultrafast bootstrap approximation. *Molecular Biology and Evolution* **35**(2): 518–522.
Hopple J.S. Jr. (1994) *Phylogenetic investigations in the genus Coprinus based on morphological and molecular characters*. Doctoral thesis. Duke University, Durham, NC.
Horak E., Matheny P.B., Desjardin D.E., Soytong K. (2015) The genus *Inocybe* (Inocybaceae, Agaricales, Basidiomycota) in Thailand and Malaysia. *Phytotaxa* **230**(3): 201–238.
Jabeen S., Khalid A.N. (2020) *Pseudosperma flavorimosum* sp. nov. from Pakistan. *Mycotaxon* **135**(1): 183–193.
James T.Y., Stenlid J., Olson Å., Johannesson H. (2008) Evolutionary significance of imbalanced nuclear ratios within heterokaryons of the basidiomycete fungus *Heterobasidion parviporum*. *Evolution* **62**(9): 2279–2296.
Jia F., Lo N., Ho S.Y.W. (2014) The impact of modelling rate heterogeneity among sites on phylogenetic estimates of intraspecific evolutionary rates and timescales. *PLoS One* **9**(5): e95722.
Jobim K., Błaszkowski J., Niezgoda P., Kozłowska A., Zubek S., Mleczko P., Goto B.T. (2019) New sporocarpic taxa in the phylum Glomeromycota: *Sclerocarpum amazonicum* gen. et sp. nov. in the family Glomeraceae (Glomerales) and *Diversispora sporocarpia* sp. nov. in the Diversisporaceae (Diversisporales). *Mycological Progress* **18**(3): 369–384.
Kalyaanamoorthy S., Minh B.Q., Wong T.K., von Haeseler A., Jermiin L.S. (2017) ModelFinder: fast model selection for accurate phylogenetic estimates. *Nature Methods* **14**(6): 587–589.
Katoh K., Standley D.M. (2013) MAFFT multiple sequence alignment software version 7: improvements in perfor-

mance and usability. *Molecular Biology and Evolution* **30**: 772–780.
Kennedy L.J., Stutz J.C., Morton, J.B. (1999). *Glomus eburneum* and *G. luteum*, two new species of arbuscular mycorrhizal fungi, with emendation of *G. spurcum*. *Mycologia* **91**(6): 1083–1093.
Khan M.B., Naseer A., Aqdus F., Ishaq M., Fiaz M., Khalid A.N. (2022) *Inocybe quercicola* sp. nov. (Agaricales, Inocybaceae), from Pakistan. *Microbial Biosystems* **6**(2): 22–29.
Kibby G. (2010) *The genus Tricholoma in Britain*. Geoffrey Kibby (privately published). https://www.nhbs.com/the-genus-tricholoma-in-britain-book (accessed 25 May 2023)
Kornerup A., Wanscher J.H. (1978) *Methuen handbook of colour, 3rd ed.* Eyre Methuen, London, UK.
Koske R.E., Tessier B. (1983) A convenient, permanent slide mounting medium. *Mycological Society of America Newsletter* **34**: 59.
Kozlov A.M., Darriba D., Flouri T., Morel B., Stamatakis A. (2019) RAxML-NG: A fast, scalable, and user-friendly tool for maximum likelihood phylogenetic inference. *Bioinformatics* **35**: 4453–4455.
Krüger M., Stockinger H., Krüger C., Schüßler A. (2009) DNA-based species level detection of Glomeromycota: one PCR primer set for all arbuscular mycorrhizal fungi. *New Phytologist* **183**(1): 212–223.
Kumar S., Stecher G., Li M., Knyaz C., Tamura K. (2018) MEGA X: Molecular Evolutionary Genetics Analysis across computing platforms. *Molecular Biology and Evolution* **35**(6): 1547–1549.
Kumar S., Stecher G., Tamura K. (2016) MEGA7: Molecular Evolutionary Genetics Analysis version 7.0 for bigger datasets. *Molecular Biology and Evolution* **33**(7): 1870–1874.
Kytövuori I., Niskanen T., Liimatainen K., Lindström H. (2005) *Cortinarius sordidemaculatus* and two new related species, *C. anisatus* and *C. neofurvolaesus*, in Fennoscandia (Basidiomycota, Agaricales). *Karstenia* **45**: 33–49.
Landry J., Lamoureux Y., Lebeuf R. (2022) *Répertoire des tricholomes du Québec, 1re édition*. Mycoquébec, Québec, Canada.
Landry J., Lamoureux Y., Lebeuf R., Paul A., Lambert H., Labbé R. (2021) *Répertoire des cortinaires du Québec, 1re édition*. Mycoquébec, Québec, Canada.
Larkin M.A., Blackshields G., Brown N.P., Chenna R., McGettigan P.A., McWilliam H., et al. (2007) Clustal W and Clustal X version 2.0. *Bioinformatics* **23**(21): 2947–2948.
Lebeuf R., Alexandrova A.V., Cerna-Mendoza A., Corazon-Guivin M.A., da Silva, G.A., de la Sota-Ricaldi A.M., et al. (2022) Fungal Systematics and Evolution: FUSE 8. *Sydowia* **74**: 193–249.
Li A.H., Yuan F.X., Groenewald M., Bensch K., Yurkov A.M., Li K., et al. (2020) Diversity and phylogeny of basidiomycetous yeasts from plant leaves and soil: Proposal of two new orders, three new families, eight new genera and one hundred and seven new species. *Studies in Mycology* **96**: 17–140.
Li A.H., Zhou Y., Jia B.S., Liu Z.X., Sampaio J.P., Zhou Y.G. (2019) *Heterocephalacria sinensis* sp. nov., *Phaeotremella lacus* sp. nov. and *Solicoccozyma aquatica* sp. nov., three novel basidiomycetous yeast species isolated from crater lakes. *International Journal of Systematic and Evolutionary Microbiology* **69**(12): 3728–3739.
Liimatainen K. (2017) Nomenclatural novelties. *Index Fungorum* **344**: 1–5.
Liimatainen K., Carteret X., Dima B., Kytövuori I., Bidaud A., Reumaux P., et al. (2017) *Cortinarius* section *Bicolores* and section *Saturnini* (Basidiomycota, Agaricales), a morphogenetic overview of European and North American species. *Persoonia* **39**: 175–200.
Liimatainen K., Kim J.T., Pokorny L., Kirk P.M., Dentinger B., Niskanen T. (2022) Taming the beast: a revised classification of Cortinariaceae based on genomic data. *Fungal Diversity* **112**: 89–170.
Liimatainen K., Niskanen, T. (2021) Nomenclatural novelties. *Index Fungorum* **487**: 1–7.
Liimatainen K., Niskanen T., Dima B., Ammirati J.F., Kirk P.M., Kytövuori I. (2020) Mission impossible completed: unlocking the nomenclature of the largest and most complicated subgenus of *Cortinarius*, *Telamonia*. *Fungal Diversity* **104**: 291–331.
Liimatainen K., Niskanen T., Dima B., Kytövuori I., Ammirati J.F., Frøslev T.G. (2014) The largest type study of Agaricales species to date: bringing identification and nomenclature of *Phlegmacium* (*Cortinarius*) into the DNA era. *Persoonia* **33**: 98–140.
Liu X.Z., Wang Q.M., Göker M., Groenewald M., Kachalkin A.V., Lumbsch H.T., et al. (2015) Towards an integrated phylogenetic classification of the Tremellomycetes. *Studies in Mycology* **81**: 85–147.
Lloyd C.G. (1923) Mycological Notes No. 70. *Mycological Writings* **7**: 1219–1236.
Lodge D.J., Padamsee M., Matheny P.B., Aime M.C., Cantrell S.A., Boertmann D., et al. (2014) Molecular phylogeny, morphology, pigment chemistry and ecology in Hygrophoraceae (Agaricales). *Fungal Diversity* **64**: 1–99.
Löytynoja A., Goldman N. (2005) An algorithm for progressive multiple alignment of sequences with insertions. *Proceedings of the National Academy of Sciences* **102**(30): 10557–10562.
Löytynoja A., Goldman N. (2008) Phylogeny-aware gap placement prevents errors in sequence alignment and evolutionary analysis. *Science* **320**(5883): 1632–1635.
Löytynoja A., Vilella A.J., Goldman N. (2012) Accurate extension of multiple sequence alignments using a phylogeny-aware graph algorithm. *Bioinformatics* **28**(13): 1684–1691.
Maas Geesteranus R.A., de Meijer A.A.R. (1997) Mycenae Paranaenses. *Verhandelingen Koninklijke Nederlandse Akademie van Wetenschappen Afdeling Natuurkunde* **97**: 1–164.
Maas Geesteranus R.A., de Meijer A.A.R. (1998) Further Mycenas from the state of Paraná, Brazil. *Persoonia* **17**: 29–46.
Madrid H., da Cunha K.C., Gené J., Dijksterhuis J., Cano J., Sutton D.A., et al. (2014) Novel *Curvularia* species from clinical specimens. *Persoonia* **33**(1): 48–60.
Malysheva V.F., Malysheva E.F., Bulakh E.M. (2015) The genus *Tremella* (Tremellales, Basidiomycota) in Russia with description of two new species and proposal of one nomenclatural combination. *Phytotaxa* **238**(1): 40–70.
Manamgoda D.S., Cai L., Bahkali A.H., Chukeatirote E., Hyde K.D. (2011) *Cochliobolus*: an overview and current status of the species. *Fungal Diversity* **51**(1): 3–42.
Manamgoda D.S., Cai L., McKenzie E.H.C., Crous P.W., Madrid H., Chukeatirote E., Shivas R.G., Tan Y.P., Hyde K.D. (2012) A phylogenetic and taxonomic re-evaluation of the *Bipolaris–Cochliobolus–Curvularia* complex. *Fungal Diversity* **56**(1): 131–144.
Manamgoda D.S., Rossman A.Y., Castlebury L.A., Crous P.W., Madrid H., Chukeatirote E., Hyde K.D. (2014) The genus *Bipolaris*. *Studies in Mycology* **79**(1): 221–288.
Marin-Felix Y., Groenewald J.Z., Cai L., Chen Q., Marincowitz S., I. Barnes I. & al. (2017) Genera of phytopathogenic fungi: GOPHY 1. Studies in Mycology **86**: 99–216.

Matheny P.B., Bougher N.L. (2017) *Fungi of Australia: Inocybaceae*. CSIRO Publishing, Clayton, Australia.

Matheny P.B., Curtis J.M., Hofstetter V., Aime M.C., Moncalvo J.M., Ge Z.W., et al. (2006) Major clades of Agaricales: a multilocus phylogenetic overview. *Mycologia* **98**(6): 982–995.

Middelhoven W.J. (2006) Polysaccharides and phenolic compounds as substrate for yeasts isolated from rotten wood and description of *Cryptococcus fagi* sp. nov. *Antonie van Leeuwenhoek* **90**: 57–67.

Miller M.A., Pfeiffer W., Schwartz T. (2010) Creating the CIPRES Science Gateway for inference of large phylogenetic trees. In: *2010 Proceedings of the Gateway Computing Environments Workshop* (GCE), New Orleans, LA: 1–8.

Milne I., Wright F., Rowe G., Marshal D.F., Husmeier D., McGuire G. (2004) TOPALi: Software for automatic identification of recombinant sequences within DNA multiple alignments. *Bioinformatics* **20**(11): 1806–1807.

Moncalvo J.M., Lutzoni F.M., Rehner S.A., Johnson J., Vilgalys R. (2000) Phylogenetic relationships of agaric fungi based on nuclear large subunit ribosomal DNA sequences. *Systematic Biology* **49**(2): 278–305.

Mosse B. (1962) Establishment of vesicular-arbuscular mycorrhiza under aseptic conditions. *Journal of Genetic Microbiology* **27**(3): 509–520.

MyCoPortal (2022) Mycology Collections Portal. Specimens & Observations. https://www.mycoportal.org/portal/collections/index.php (accessed 27 April 2023)

Na Q., Bau T. (2019a) *Mycena* sect. *Sacchariferae*: three new species with basal discs from China. *Mycological Progress* **18**: 483–493.

Na Q., Bau T. (2019b) Recognition of *Mycena* sect. *Amparoina* sect. nov. (Mycenaceae, Agaricales), including four new species and revision of the limits of sect. *Sacchariferae*. *MycoKeys* **52**: 103–124.

Na Q., Bau T. (2020) Ten new records of *Mycena* from China. *Mycosystema* **39**: 1783–1808.

Naseer A., Ghani S., Niazi A.R., Khalid A.N. (2019) *Inocybe caroticolor* from oak forests of Pakistan. *Mycotaxon* **134**(2): 241–251.

Nguyen L., Schmidt H.A., von Haeseler A., Minh B.Q. (2015) IQ-TREE: A fast and effective stochastic algorithm for estimating maximum likelihood phylogenies. *Molecular Biology and Evolution* **32**(1): 268–274.

Niskanen T. (2020) Nomenclatural novelties. *Index Fungorum* **438**: 1–8.

Niskanen T., Kytövuori I., Liimatainen K. (2009) *Cortinarius* sect. *Brunnei* (Basidiomycota, Agaricales) in North Europe. *Mycological Research* **113**(2): 182–206.

Niskanen T., Liimatainen K., Ammirati, J.F. (2013) Five new *Telamonia* species (Cortinarius, Agaricales) from western North America. *Botany* **91**(7): 478–485.

Niskanen T., Liimatainen K., Kytövuori I. (2006) Taxonomy, ecology and distribution of *Cortinarius rubrovioleipes* E. Bendiksen & K. Bendiksen and *C. hinnuleoarmillatus* Reumaux (Basidiomycota, Agaricales) in Fennoscandia. *Karstenia* **46**: 1–12.

Niskanen T., Liimatainen K., Kytövuori I., Ammirati J.F. (2012) New *Cortinarius* species from conifer-dominated forests of North America and Europe. *Botany* **90**(8): 743–754.

Oehl, F., da Silva, G.A., Sánchez-Castro, I., Goto, B.T., Maia, L.C., Vieira, H.E.E., et al. (2011) Revision of Glomeromycetes with entrophosporoid and glomoid spore formation with three new genera. *Mycotaxon* **117**(1): 297–316.

Ogden T.H., Rosenberg M.S. (2006) Multiple sequence alignment accuracy and phylogenetic inference. *Systematic Biology* **55**(2): 314–328.

Olsen, S.R., Cole, C.V., Watanabe, F.S., Dean, L.A. (1954) Estimation of available phosphorus in soils by extraction with sodium bicarbonate. *Circular* **939**: 1–19.

Osmundson T.W., Robert V.A., Schoch C.L., Baker L.J., Smith A., Robich G., et al. (2013) Filling gaps in biodiversity knowledge for macrofungi: contributions and assessment of an herbarium collection DNA barcode sequencing project. *PLoS One* **8**(4): e62419.

Ovrebo C.L. (1980) *A taxonomic study of the genus Tricholoma (Agaricales) in the Great Lakes region*. Doctoral thesis. University of Toronto, Toronto, Canada.

Ovrebo C.L. (1989) *Tricholoma*, subgenus *Tricholoma*, section *Albidogrisea*: North American species found principally in the Great Lakes region. *Canadian Journal of Botany* **67**(11): 3134–3152.

Ovrebo C.L., Halling R.E. (1986) *Tricholoma fulvimarginatum* (Tricholomataceae): a new species from North America associated with cottonwood. *Brittonia* **38**: 260–263.

Ovrebo C.L., Halling R.E., Hughes K.W., Kuo M. (2021) New species and records of *Tricholoma* (Agaricales: Tricholomataceae) sections *Genuina* and *Megatricholoma* from Costa Rica and United States. *Journal of the Botanical Research Institute of Texas* **15**(2): 545–557.

Pickles B.J., Genney D.R., Anderson I.C., Alexander I.J. (2012) Spatial analysis of ectomycorrhizal fungi reveals that root tip communities are structured by competitive interactions. *Molecular Ecology* **21**(20): 5110–5123.

Rehner S.A., Buckley E. (2005) A *Beauveria* phylogeny inferred from nuclear ITS and EF1-α sequences: Evidence for cryptic diversification and links to *Cordyceps* teleomorphs. *Mycologia* **97**(1): 84–98.

Reschke K., Popa F., Yang Z.L., Kost G. (2018) Diversity and taxonomy of *Tricholoma* species from Yunnan, China, and notes on species from Europe and North America. *Mycologia* **110**(6): 1081–1109.

Riva A. (1988) Tricholoma *(Fr.) Staude*. *Fungi Europaei 3*. Libreria editrice Giovanna Biella, Saronno, Italy.

Roberts P. (1999) British *Tremella* species II: *T. encephala*, *T. steidleri* and *T. foliacea*. *Mycologist* **3**(13): 127–131.

Robich G. (2007) Mycena *d'Europa*. Associazione Micologica Bresadola, Trento, Italy.

Ronquist F., Huelsenbeck J.P. (2003) MrBayes 3: Bayesian phylogenetic inference under mixed models. *Bioinformatics* **19**(12): 1572–1574.

Rossi W., Cesari Rossi M.G. (1980) Nuovo contributo alla conoscenza delle Laboulbeniali (Ascomycetes) parasite di Stafilinidi italiani (Insecta, Coleoptera). *Giornale Botanico Italiano* **114**:187–192.

Rossi W., Leonardi M. (2018) New species and new records of Laboulbeniales (Ascomycota) from Sierra Leone. *Phytotaxa* **358**(2): 91–116.

Saba M., Haelewaters D., Pfister D.H., Khalid A.N. (2020) New species of *Pseudosperma* (Agaricales, Inocybaceae) from pine-dominated forests of western Himalayas. *Mycokeys* **69**: 1–31.

Saba M., Khalid A.N. (2020) *Mallocybe velutina* (Agaricales, Inocybaceae), a new species from Pakistan. *Mycoscience* **61**(6): 348–352.

Sánchez-Garcia M., Matheny P.B., Palfner G., Lodge J.D. (2014) Deconstructing the *Tricholomataceae* (Agaricales) and introduction of the new genera *Albomagister*, *Cor-*

neriella, *Pogonoloma* and *Pseudotricholoma*. *Taxon* **63**: 993–1007.
Sánchez-García M., Matheny P.B. (2016) Is the switch to an ectomycorrhizal state an evolutionary key innovation in mushroom-forming fungi? A case study in the Tricholomatineae (Agaricales). *Evolution* **71**(1): 51–65.
Schüßler A., Krüger M., Walker C. (2011) Revealing natural relationships among arbuscular mycorrhizal fungi: culture line BEG47 represents *Diversispora epigaea*, not *Glomus versiforme*. *PLoS One* **6**(8): e23333.
Scorzetti G., Fell J.W., Fonseca A., Statzell-Tallman A. (2002) Systematics of basidiomycetous yeasts: A comparison of large subunit D1/D2 and internal transcribed spacer rDNA regions. *FEMS Yeast Research* **2**(4): 495–517.
Shanks K.M. (1996) New species of *Tricholoma* from California and Oregon. *Mycologia* **88**(3): 497–508.
Singer R. (1976) Amparoinaceae and Montagneaceae. *Revue de Mycologie* **40**: 57–64.
Smith A.S. (1942) New and unusual agarics from Michigan. III. *Papers of the Michigan Academy of Science, Arts, and Letters* **27**: 57–74.
Solodovnikov A., Yue Y., Tarasov S., Ren D. (2013) Extinct and extant rove beetles meet in the matrix: Early Cretaceous fossils shed light on the evolution of a hyperdiverse insect lineage (Coleoptera: Staphylinidae: Staphylininae). *Cladistics* **29**(4): 360–403.
Song J., Liang J.F., Mehrabi-Koushki M., Krisai-Greilhuber I., Ali B., Bhatt, V.K., et al. (2019) Fungal Systematics and Evolution: FUSE 5. *Sydowia* **71**: 141–245.
Spain J.L. (1990) Arguments for diagnoses based on unaltered wall structures. *Mycotaxon* **38**: 71–76.
Spirin V., Malysheva V., Yurkov A., Miettinen O., Larsson K.H. (2018) Studies in the *Phaeotremella foliacea* group (Tremellomycetes, Basidiomycota). *Mycological Progress* **17**: 451–466.
Stamatakis A. (2006) RAxML-VI-HPC: maximum likelihood-based phylogenetic analyses with thousands of taxa and mixed models. *Bioinformatics* **22**: 2688–2690.
Stamatakis A. (2014) RAxML version 8: a tool for phylogenetic analysis and post-analysis of large phylogenies. *Bioinformatics* **30**: 1312–1313.
Stockinger H., Krüger M., Schüßler A. (2010) DNA barcoding of arbuscular mycorrhizal fungi. *New Phytologist* **187**(2): 461–474.
Stucky B.J. (2012) SeqTrace: A graphical tool for rapidly processing DNA sequencing chromatograms. *Journal of Biomolecular Techniques* **23**(3): 90–93.
Suárez-Santiago V.N., Ortega A., Peintner U., López-Flores I. (2009) Study on *Cortinarius* subgenus *Telamonia* section *Hydrocybe* in Europe, with especial emphasis on Mediterranean taxa. *Mycological Research* **113**(10): 1070–1090.
Sun Y., Wang G.S., Li A.H., Wangmu, Chui X.Q., Jiang J.H., Wang Q.M. (2020) *Phaeotremella camelliae* sp. nov. (Phaeotremellaceae, Tremellales), a novel yeast isolated from tea-oil fruits in Jiangxi Province, China. *Current Microbiology* **77**: 3168–3173.
Symanczik, S., Al-Yahya'ei, M.N., Kozłowska, A., Ryszka, P., Błaszkowski, J. (2018) A new genus, *Desertispora*, and a new species, *Diversispora sabulosa*, in the family Diversisporaceae (order Diversisporales, subphylum Glomeromycotina). *Mycological Progress* **17**: 437–449.
Tamura K., Nei M. (1993) Estimation of the number of nucleotide substitutions in the control region of mitochondrial DNA in humans and chimpanzees. *Molecular Biology and Evolution* **10**(3): 512–526.
Tan Y.P., Crous P.W., Shivas R.G. (2016) Eight novel *Bipolaris* species identified from John Alcorn's collections at the Queensland Plant Pathology Herbarium (BRIP). *Mycological Progress* **15**(10–11): 1203–1214.
Tan Y.P., Madrid H., Crous P.W., Shivas R.G. (2014) *Johnalcornia* gen. et comb. nov., and nine new combinations in *Curvularia* based on molecular phylogenetic analysis. *Australasian Plant Pathology* **43**(6): 589–603.
Tavares I.I. (1979) The Laboulbeniales and their arthropod hosts. In: *Insect-fungus symbiosis, nutrition, mutualism, and commensalism* (Batra L.R., ed.), Wiley, New York, NY: 229–258.
Tavares I.I. (1985) *Laboulbeniales (Fungi, Ascomycetes)*. Mycologia Memoirs 9. Cramer, Vaduz.
Teasdale S.E., Beulke A.K., Guy P.L., Orlovich D.A. (2013) Environmental barcoding of the ectomycorrhizal fungus *Cortinarius*. *Fungal Diversity* **58**: 299–310.
Thaxter R. (1894) New genera and species of Laboulbeniaceae, with a synopsis of the known species. *Proceedings of the American Academy of Arts and Sciences* **29**: 92–111.
Thaxter R. (1896) Contribution towards a monograph of the Laboulbeniaceae. *Memoirs of the American Academy of Arts and Sciences* **12**(3):187–429.
Thaxter R. (1926) Contribution towards a monograph of the Laboulbeniaceae. Part IV. *Memoirs of the American Academy of Arts and Sciences* **15**(4): 427–580, Plates I–XXIV.
Thiers B. (continuously updated) Index Herbariorum: A global directory of public herbaria and associated staff. New York Botanic Garden's Virtual Herbarium. http://sweetgum.nybg.org/ih/ (accessed 1 April 2022).
Tóth A., Hausknecht A., Krisai-Greilhuber I., Papp T., Vágvölgyi C., Nagy L.G. (2013) Iteratively refined guide trees help improving alignment and phylogenetic inference in the mushroom family *Bolbitiaceae*. *PLoS One* **8**(2): e56143.
Traba-Velay J.M., Couceiro A., Villarreal M., Naveira H., Vila-Sanjurjo A. (2021) *Tres especies nuevas de* Mycena *sección* Amparoina *de la Península Ibérica*. I Congreso Andaluz de Micologia, Granada, Spain.
Trudell S.A., Matheny P.B., Parker A.D, Gordon M., Dougil D.B., Cline E.T. (2022) Pacific Northwest Tricholomas: are we using the right names? https://svims.club/wp-content/uploads/2022/03/Trudell-et-alTricholomas-Right-Names-2022.pdf (accessed 28 April 2023)
Trudell S.A., Parker A.D. (2021) Nomenclatural novelties. *Index Fungorum* **502**: 1–6.
Vellinga E.C. 1988. Glossary. In: *Flora Agaricina Neerlandica 1* (eds. Bas C., Kuyper T.W., Noordeloos M.E., Vellinga E.C.). Balkema, Rotterdam, The Netherlands: 54–64.
Vilgalys R., Hester M. (1990) Rapid genetic identification and mapping of enzymatically amplified ribosomal DNA from several *Cryptococcus* species. *Journal of Bacteriology* **172**: 4238–4246.
Vu D., Groenewald M., Szöke S., Cardinali G., Eberhardt U., Stielow B., et al. (2016) DNA barcoding analysis of more than 9 000 yeast isolates contributes to quantitative thresholds for yeast species and genera delimitation. *Studies in Mycology* **85**: 91–105.
Wächter D., Melzer A. (2020) Proposal for a subdivision of the family *Psathyrellaceae* based on a taxon-rich phylogenetic analysis with iterative multigene guide tree. *Mycological Progress* **19**: 1151–1265.
Wedin M., Zamora J.C., Millanes A.M. (2016) *Phaeotremella foliacea* comb. nov. (Tremellales, Tremellomycetes, Agaricomycotina). *Mycosphere* **7**: 295–296.

Werle E., Schneider C., Renner M., Volker M., Fiehn W. (1994) Convenient single-step, one tube purification of PCR products for direct sequencing. *Nucleic Acids Research* **22**(20): 4354–4355.

White T.J., Bruns T., Lee S., Taylor J. (1990) Amplification and direct sequencing of fungal ribosomal RNA genes for phylogenetics. In: *PCR protocols: a guide to methods and applications* (eds. Innis M.A., Gelfand D.H., Sninsky J.J., White T.J.). Academic Press, New York, NY: 315–322.

Wrzosek M. (2000) *Taksonomia i filogeneza Mucorales (Zygomycetes) w świetle analiz morfometrycznych oraz wybranych markerów molekularnych*. [*Taxonomy and phylogeny of Mucorales (Zygomycetes) in the light of morphometrical and selected molecular markers analyses*]. Doctoral thesis. University of Warsaw, Warsaw, Poland.

Yuan H.S., Lu X., Dai Y.C., Hyde K.D., Kan Y.H., Kušan I., et al. (2020) Fungal diversity notes 1277–1386: Taxonomic and phylogenetic contributions to fungal taxa. *Fungal Diversity* **104**: 1–266.

(Manuscript accepted 12 March 2023; Corresponding Editor: D. Haelewaters)